Non-canonical action of thyroid hormone receptors α and β

Inaugural-Dissertation

zur

Erlangung des Doktorgrades

doctor rerum naturalium

(Dr. rer. nat.)

der Fakultät für

Biologie

an der

Universität Duisburg-Essen

vorgelegt von

Georg Sebastian Hönes

aus Dorsten

April 2017

Die der vorliegenden Arbeit zugrundeliegenden Experimente wurden in der Klinik für Endokrinologie, Diabetologie und Stoffwechsel am Universitätsklinikum Essen durchgeführt.

1. Gutachter: PD Dr. Lars C. Möller
2. Gutachterin: Prof. Dr. Andrea Vortkamp
3. Gutachter: Prof. Dr. Lutz Schomburg

Vorsitzende des Prüfungsausschusses: Prof. Dr. Perihan Nalbant

Tag der mündlichen Prüfung: 07.09.17

Contents

Zusammenfassung

Schilddrüsenhormone (Thyroidhormone, TH) spielen eine bedeutende Rolle bei der Organentwicklung, dem Wachstum, der Regulierung der Körpertemperatur und der Herzfrequenz, sowie bei der Steuerung bestimmter metabolischer Prozesse. TH vermitteln ihre Wirkung über die Schilddrüsenhormonrezeptoren (TR) α und β, welche an TH-Response-Elemente (TREs) in regulatorischen Sequenzen von Zielgenen binden. Dieser nukleäre Signalweg ist als kanonische Wirkungsweise von TH etabliert. Seit wenigen Jahren ist bekannt, dass TRs auch intrazelluläre Signalkaskaden aktivieren können. Ob diese sogenannte nicht-kanonische Wirkweise der TRs eine physiologische Relevanz besitzt, ist bis heute ungeklärt. Dies liegt hauptsächlich daran, dass ein geeignetes Mausmodell zur spezifischen Untersuchung der nicht-kanonischen Funktion *in vivo*, nicht existiert.

Um dies zu klären, wurden zwei Knock-In Mausmodelle ($TR\alpha^{GS}$ und $TR\beta^{GS}$) mit Mutationen in der DNA-Bindedomäne der TRs generiert. Hierdurch wird die Bindung der TRs an die TREs aufgehoben. Folglich geht die kanonische Wirkung verloren, aber die nicht-kanonische bleibt erhalten. Ein phänotypischer Vergleich der TR^{GS}-Mäuse mit Wildtyp- und TR-knockout Mäusen belegte die physiologische Relevanz der nicht-kanonischen TR-Wirkung. Trotz des Verlustes der DNA-Bindung waren einige wichtige physiologische TH-Effekte erhalten: Die Herzfrequenz, die Körpertemperatur, der Blutzucker und auch die Triglyzeride waren alle über den nicht-kanonischen Signalweg reguliert. Im Gegensatz dazu führte der Verlust der DNA-Bindung des TRβ zu einer gestörten Hypothalamus-Hypophysen-Schilddrüsen-Achse mit Ausbildung einer Hormonresistenz, während eine Mutation in der DNA-Bindedomäne des TRα zu einer stark verzögerten Knochenentwicklung führte.

Diese Ergebnisse belegen, dass sich die $TR\alpha^{GS}$- und $TR\beta^{GS}$-Mausmodelle zur Untersuchung der nicht-kanonischen TR-Wirkung eignen. Darüber hinaus demonstriert die vorliegende Arbeit, dass sich die kanonische und nicht-kanonische Wirkweise klar trennen lassen und dass letztere ebenfalls an der Vermittlung wichtiger physiologischer TH-Effekte beteiligt ist. Diese neuen Erkenntnisse leiten einen Paradigmenwechsel ein, da die TR/TH-vermittelten Effekte nicht nur von der Regulierung bestimmter Gene abhängig sind.

Abstract

Thyroid hormones (THs) are crucial to maintain a diverse set of physiological functions like organ development, growth, regulation of body temperature, heart rate and certain metabolic processes. TH effects are mediated via the TH receptors (TRs) α and β. TRs act by binding to TH response elements (TREs) on regulatory sequences of target genes. This nuclear signaling is established as the canonical pathway for TH action. In addition, however, TRs can activate intracellular second messenger signaling pathways. Whether such non-canonical TR signaling is physiologically relevant *in vivo* is unknown, mainly, because a suitable mouse model to study canonical and non-canonical TR action separately *in vivo* did not exist.

To address this issue, two knock-in mouse models ($TR\alpha^{GS}$ and $TR\beta^{GS}$) with a mutation in the TR DNA-binding domain were generated. This mutation abrogates binding to TREs and leads to a complete loss of canonical TH actions. Phenotypical comparison of wild-type, TR-knockout and the mutant TR^{GS} mice revealed the physiological relevance of non-canonical TR signaling. Strikingly, several important physiological TH effects were preserved despite disrupted DNA binding: heart rate, body temperature, blood glucose and triglycerides were all regulated by non-canonical TR signaling. In contrast, TRE-binding defective TRβ leads to disruption of the hypothalamic-pituitary-thyroid axis with resistance to TH, while mutation of TRα causes a severe delay in skeletal development, demonstrating these effects are TRE-mediated and tissue-specific.

These results show that the $TR\alpha^{GS}$ and $TR\beta^{GS}$ mutant mice are suitable models to study non-canonical TR signaling *in vivo*. Moreover, the present thesis demonstrates that non-canonical TR signaling exerts important physiological effects, which are clearly separated from canonical actions. Consequently, these data challenge the current paradigm that TH actions are mediated exclusively through regulation of gene transcription at the nuclear level.

Introduction

The thyroid gland and thyroid hormone synthesis

Synthesis and secretion of thyroid hormones

Thyroid hormone (TH) plays an essential role in organ development and homeostatic regulation. The THs T4 (3,5,3',5'-tetraiodothyroxine; thyroxine) and T3 (3,5,3'-triiodothyronine, thyronine) are exclusively synthesized by the thyroid gland. This endocrine organ consists of two lobes connected by a cellular belt (*isthmus glandularis*) located at the anterior side of the trachea (Figure 1). TH synthesis takes place in the lumen of the thyroid follicles which are formed by cuboidal thyrocytes.

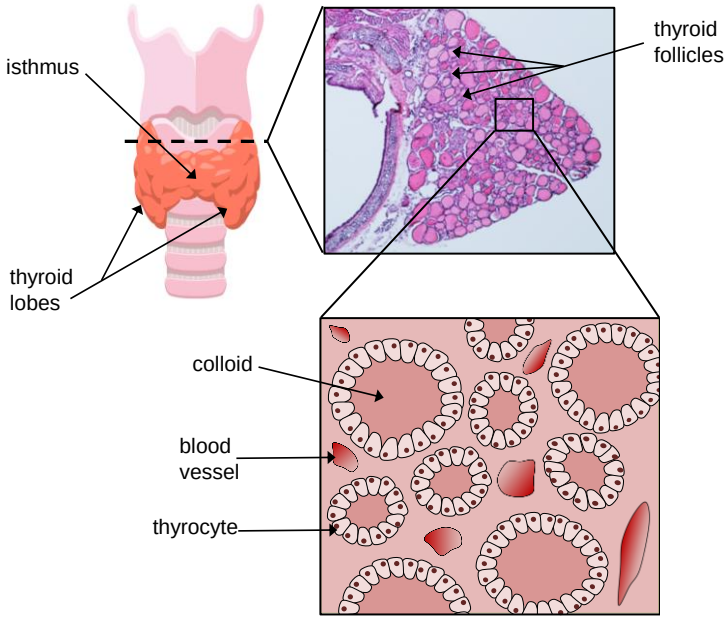

Figure 1: Location and histology of the thyroid gland. *The thyroid gland is located anterior at the trachea. The lobes consist of thyroid follicles which are formed by thyrocytes.*

The thyroid follicular cells take up iodide (I^-) against the concentration gradient from the basal side through a sodium/iodine symporter (NIS). Thus, the intracellular I^- concentration in the thyroid follicular cells can be up to 50-fold compared to the I^- concentration in blood. This process is called *the iodine trap*. Pendrin, a chloride/iodine transporter and anoctamin (a Ca^+-dependent chloride channel with affinity for I^-) are both located at the apical membrane and facilitate I^- efflux into the follicular lumen (Silveira & Kopp, 2015; Twyffels *et al.*, 2014; Yoshida *et al.*, 2002).

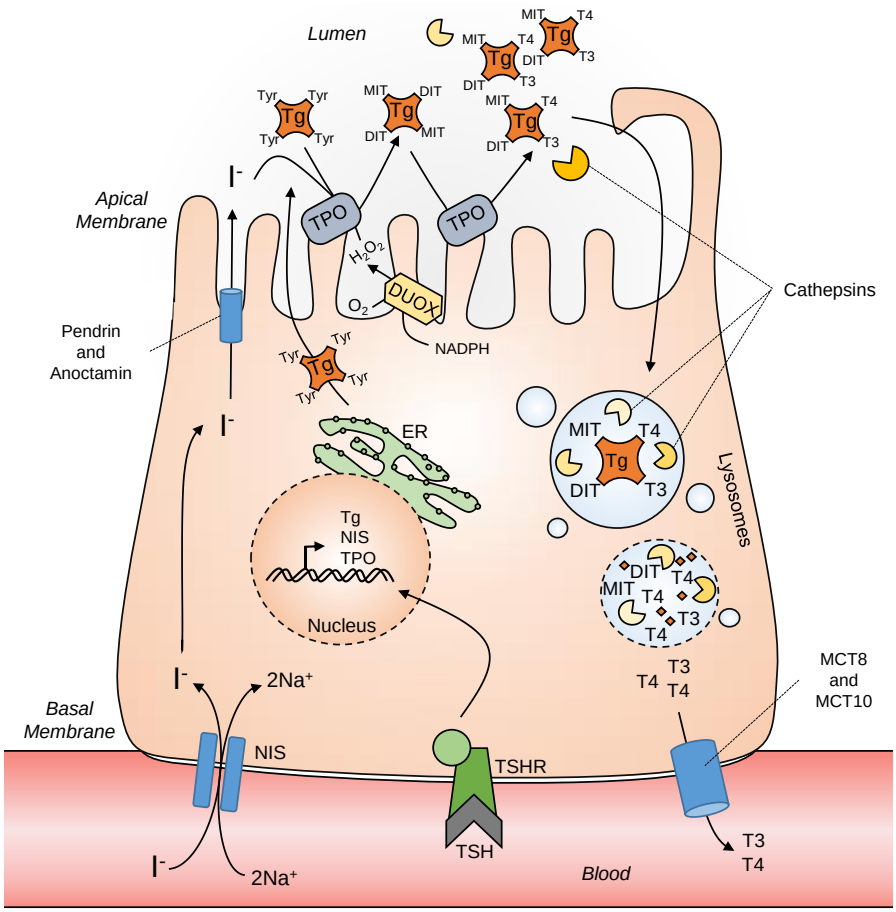

Figure 2: Thyroid hormone synthesis and secretion. *The thyrocyte takes up iodide (I^-) from the blood and concentrates it intracellularly via the iodine/sodium symporter NIS. Pendrin and anoctamin transport I^- across the apical membrane into the lumen. Stimulation of the TSH receptor (TSHR, located at the basal membrane) via TSH (thyroid-stimulating hormone) results in an increased expression of NIS, thyroid peroxidase (TPO) and thyroglobulin (Tg). Latter contains several tyrosyl residues (Tyr). Thus, Tg functions as a protein matrix for TH synthesis and is exported into the lumen. TPO iodinates the tyrosyl residues to form monoiodotyrosine (MIT) and diiodotyrosine (DIT), using H_2O_2 as a cofactor. H_2O_2 is provided by the dual oxidase (DUOX) via reduction of O_2. Coupling of MIT and DIT to T3 and T4 is catalyzed by TPO. Tg with bound TH is endocytosed and degraded by cathepsins in lysosomes to releases TH. THs are secreted into blood via monocarboxylate transporter 8 (MCT8) and MCT10 at the basal membrane. (Additional abbreviations: ER, endoplasmatic reticulum; NADPH, reduced form of nicotinamide dinucleotide phosphate; $NADP^+$, oxidized form of nicotinamide dinucleotide phosphate)*

The follicular cells also synthesize thyroglobulin (Tg), a 660 kDa dimeric protein with several tyrosyl residues which provide a polypeptide matrix for the biosynthesis of THs (Figure 2). After secretion of Tg into the lumen the thyroid peroxidase (TPO), an enzyme complex bound to the luminal side of the apical membrane, iodinates the tyrosyl residues to form monoiodotyrosine (MIT) and diiodotyrosine (DIT) (Xiao, Dorris, Rawitch, & Taurog, 1996). In a second step TPO couples two DIT molecules to form T4 and one MIT with one DIT to form T3 which are still bound to Tg. For these reactions TPO needs hydrogen peroxide (H_2O_2), which is formed in an

NADPH-dependent manner by DUOX1 and DUOX2 (dual oxidase). DUOX1 and DUOX2 are also located at the apical membrane (Carvalho & Dupuy, 2013). The prohormone Tg with bound T4 and T3 is cross-linked and accumulates as colloid in the follicular lumen (Miot, Dupuy, Dumont, & Rousset, 2000; Tokuyama, Yoshinari, Rawitch, & Taurog, 1987).

Solubilization and internalization of accumulated, insoluble Tg is initiated via the cysteine proteases cathepsin B, K, L and S (Jordans *et al.*, 2009). Solubilized Tg is taken up by the follicular cells via vesicle-mediated endocytosis and is transported to lysosomal compartments for proteolytic cleavage through hydrolyzation by cathepsins to release T4 and T3 (Friedrichs *et al.*, 2003) (Figure 2). The free TH molecules T4 and T3 are secreted into blood via the TH-transporters mono carboxylate transporter 8 (MCT8) and MCT10 located at the basal membrane (Di Cosmo *et al.*, 2010; Trajkovic-Arsic *et al.*, 2010). The T4/T3 secretion ratio is about 10/1 and 100 µg of T4 and 10 µg of T3 are secreted per day (Nussey & Whitehead, 2001).

The hypothalamic-pituitary-thyroid axis

TH synthesis and secretion is regulated via the hypothalamic-pituitary-thyroid (HPT) axis which allows keeping TH concentration in blood within a narrow range (Figure 3). Thyrotropin-releasing hormone (TRH) is expressed in neurons of the paraventricular nucleus of the hypothalamus. TRH travels along the hypophyseal portal system to the anterior pituitary gland where it stimulates thyrotropic cells to release thyroid-stimulating hormone (TSH; thyrotropin) (Ortiga-Carvalho, Chiamolera, Pazos-Moura, & Wondisford, 2016). TSH is a heterodimeric glycoprotein consisting of two subunits, α and β. The β subunit determines the specificity to the TSH-receptor (TSHR). The TSHR belongs to the family of G_s-protein coupled integral membrane proteins and is mainly expressed by thyroid epithelial cells. Activation of TSHR by TSH increases expression of NIS, Tg, TPO and leads to a raise in H_2O_2 production (Figure 2) (Miot *et al.*, 2000). Consequently, TH synthesis and secretion is increased (Nussey & Whitehead, 2001). The higher active state of the thyrocyte is reflected by a change from a cubic to a prismatic appearance (Friedrichs *et al.*, 2003). The increased TH concentration in blood negatively affects TRH expression and secretion in the hypothalamus, as well as TSH expression in the pituitary and

therefore functions as a negative feedback loop (Shibusawa, Hashimoto, *et al.*, 2003; Weiss *et al.*, 1997).

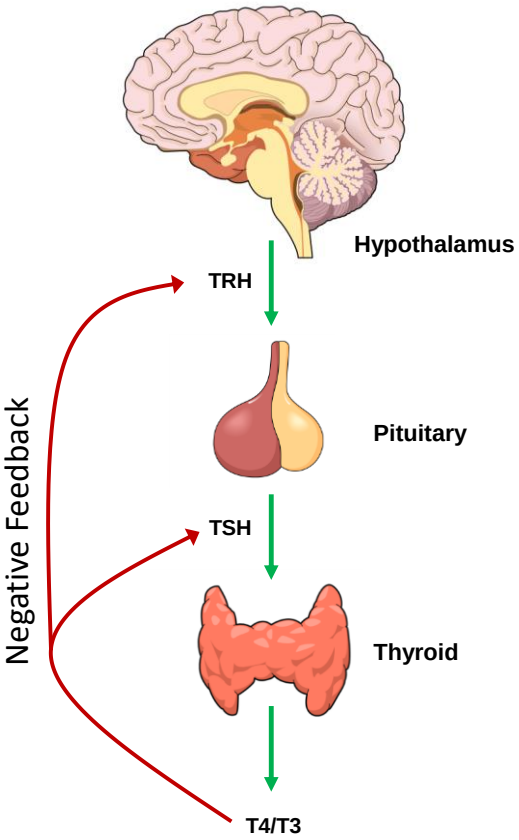

Figure 3: Regulation of thyroid hormone synthesis and secretion via the hypothalamic-pituitary-thyroid axis. *Thyrotropin-releasing hormone (TRH) is synthesized and secreted by the paraventricular nucleus of the hypothalamus. At the pituitary level, TRH stimulates thyrotropin (TSH) expression and secretion. TSH binds to and activates the TSHR (TSH receptor) on thyrocytes which leads to an increase in TH synthesis and secretion. In turn, T3 inhibits TRH and TSH expression and secretion, acting as a negative feedback loop. (green arrows indicate stimulation; red arrows indicate inhibition)*

Thyroid hormone transport, cellular uptake and activation

TH transport and cellular uptake

Once secreted into blood THs bind to carrier proteins like albumin, transthyretin and primarily thyroxin-binding globulin (TBG, also known as serine protease inhibitor, SERPIN A7). THs are mainly found in a protein-bound state and only less than 0.5% of THs are free and thus immediately available for the cells (Sarne, 1988). Binding to TBG and other carrier proteins inhibits rapid clearance of TH from the blood and helps to keep the TH pool stable. In case of hypothyroidism a decrease in TH serum

concentration leads to an increased TBG expression in liver, which in turn helps to defend an euthyroid TH status (Vranckx, Savu, Maya, & Nunez, 1990).

Only the vanishingly low amount of 0.5% free TH is available for cells to be taken up. For a long time it was thought, that the hydrophobic THs would be able to pass the cellular membrane directly by passive diffusion. This so called "*free hormone hypothesis*" was formulated by Robbins and Rall in 1960 (Robbins & Rall, 1960). In the late 70´s it was shown by two independent groups that cellular TH transport across the membrane is energy-dependent and thus cannot occur via passive diffusion (Krenning, Docter, Bernard, Visser, & Hennemann, 1978; Rao, Eckel, Rao, & Breuer, 1976). Today several active TH transporters are identified. The best characterized transporters are MCT8 and MCT10 belonging to the family of mono carboxylate transporters. Additionally, organic anion transporting-polypeptide 1c1 was shown to transport TH in mice and L-type amino acid transporter 2 was also identified to be able to transport TH and TH metabolites, respectively (Kinne *et al.*, 2015; Pizzagalli *et al.*, 2002).

Deiodinase-dependent TH metabolism

Although the thyroid gland primarily secretes T4, T3 is the more biologically active form. The conversion from T4 to T3 requires deiodination of the 5'-iodine. About 80% of the daily extrathyroidal T3 production takes place in peripheral tissue (Schimmel & Utiger, 1977). The biochemical reaction of deiodination is carried out by selenoenzymes called deiodinase (DIO)1, DIO2 and DIO3. Deiodinases are differently expressed among tissues, exhibit a diverse substrate spectrum and differ in their mode of deiodination (Figure 4). In mice, Dio1 is mainly expressed in liver, kidney and intestine and moreover is the only deiodinase that can function as an outer- and an inner-ring deiodinase. By contrast, Dio2 is mainly expressed in CNS (central nervous system), pituitary and brown adipose tissue (BAT) and is a strict outer-ring deiodinase. During fetal life expression of Dio3 reaches a maximum, suggesting a pivotal role of Dio3 in organ development. Dio3 is solely able to deiodinate the inner-ring, at position 5 and therefore inactivates T4 or T3 to reverse T3 (rT3) or 3,3'-diiodothyronine, respectively (Bates, St Germain, & Galton, 1999; Bianco & Kim, 2006; Bianco, Salvatore, Gereben, Berry, & Larsen, 2002).

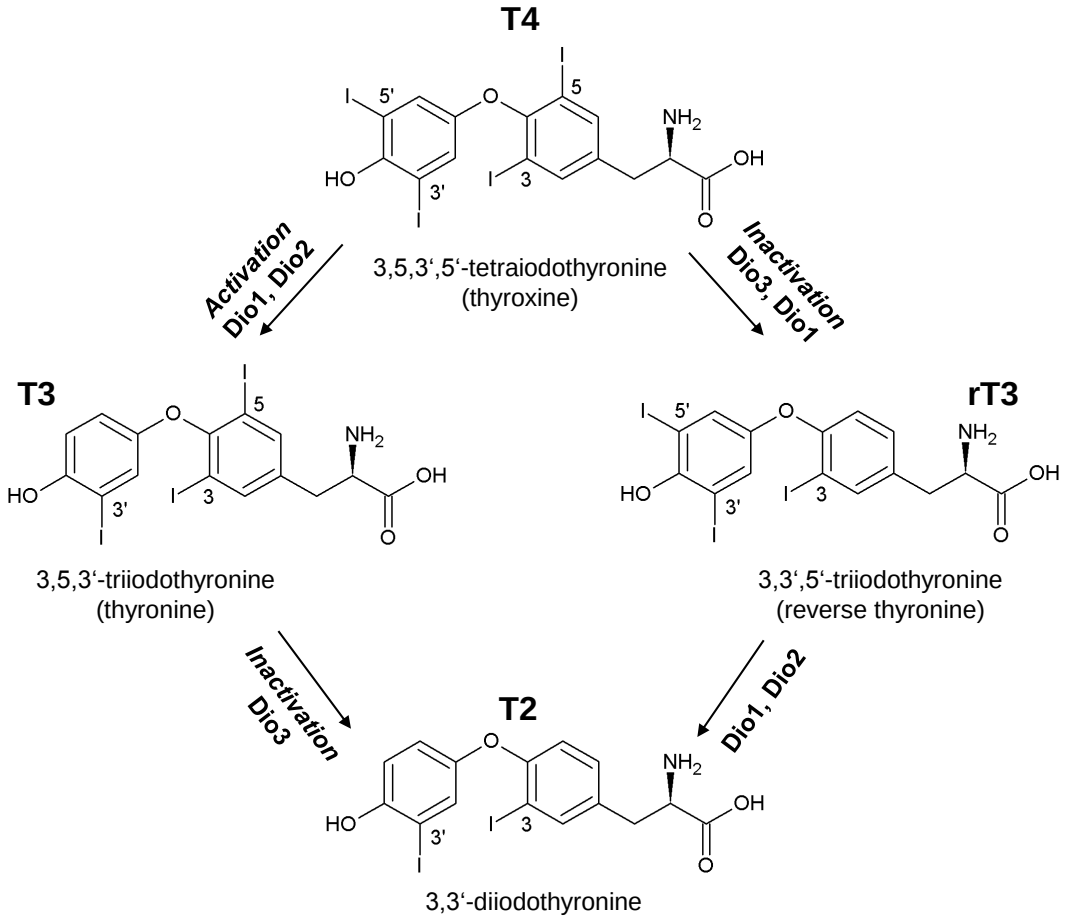

Figure 4: Activation and inactivation of thyroid hormones through deiodinases. *Outer-ring deiodination of T4 by Dio1 or Dio2 (deiodinase 1 and 2) results in the formation of the active form of TH, T3. Throxine can also be deiodinated at its inner-ring via Dio1 or Dio3. Inner-ring deiodination of T4 results in the formation of reverse T3 (rT3), a biologically inactive TH metabolite. As a strict inner-ring deiodinase, Dio3 is able to inactivate T3 and generate 3,3’-diiodothyronine (T2). rT3 can also be further deiodinated to T2 via Dio1 or Dio2.*

The thyroid hormone receptors α and β

Discovery of thyroid hormone receptors

Since the work of Tata *et al.* in 1963 and 1966, it was suggested that TH can regulate the expression of certain target genes (Tata *et al.*, 1963; Tata & Widnell, 1966). However, it took about 20 years until the groups of Vennström and Evans simultaneously discovered that the human homologs of the avian erythroblastosis virus gene loci *v-erbA* and *v-erbB* are receptors for TH (Jansson, 1983; Sap *et al.*, 1986; Vennstrom & Bishop, 1982; Weinberger *et al.*, 1986). The following years of research revealed that these thyroid hormone receptors (TRs) belong to the

superfamily of nuclear receptors, like the estrogen receptor and steroid receptors (Beato, Herrlich, & Schutz, 1995). This marked the beginning of TR research.

Molecular structure and characteristics of thyroid hormone receptor isoforms

The isoforms TRα and TRβ are encoded by the two gene loci *THRA* and *THRB* on chromosome 17 and 3, respectively. A very diverse set of TR isoforms (TRα1, TRα2, TRαΔ1, TRαΔ2, TRα p30, TRα p43, TRβ1, TRβ2, TRβ3, TRβΔ3 and TRβ4) is generated via alternative splicing, translation and by alternative transcription of the two genes. These TR isoforms differ in length at both their amino and carboxy termini and exhibit different physiological functions (Chassande *et al.*, 1997; Hollenberg, Monden, & Wondisford, 1995; Lazar, 1993; Tagami *et al.*, 2010; Williams, 2000).

Both genes, *THRA* and *THRB,* are highly homologous resulting in two receptor isoforms with high concordance regarding their amino acid sequence and domain structure, respectively (Figure 5). As they belong to the family of nuclear receptors, TRs share a similar domain structure with other nuclear receptors (Pawlak, Lefebvre, & Staels, 2012). An N-terminal domain (A/B domain) with co-activator binding sites (AF1 domain) is followed by a DNA-binding domain (DBD). The DBD consists of two zinc-finger motifs for recognizing and binding to specific regulatory DNA sequences – thyroid hormone response elements (TREs). Additional to DNA binding, the DBD also mediates hetero-dimerization. A less conserved region connects the DBD with the ligand-binding domain (LBD). This so-called hinge region is involved in nuclear localization of the receptor as it exhibits a 26 amino acids long nuclear localization sequence (NLS) (Baumann, Maruvada, Hager, & Yen, 2001; Maruvada, Baumann, Hager, & Yen, 2003). Beside a NLS the receptors also contain nuclear export signals (NES) within the N-terminal AF1 domain and within the C-terminal LBD (Mavinakere, Powers, Subramanian, Roggero, & Allison, 2012). These motifs enable the receptors to shuttle between the nucleus and cytoplasm, whereas in steady-state the majority of TR is located in the nucleus (Baumann *et al.*, 2001). T3, the active TH, binds to the LBD with high affinity and is buried inside a hydrophobic pocket formed by α-helices of the LBD (Apriletti *et al.*, 1998). T3 binding to TRs induces a conformational change especially of the carboxy-terminal helix 12. This helix contains the activation function 2 (AF2) domain. The amino acid sequence of the AF2 domain of TRα and TRβ is highly conserved between these two isoforms and mediates important interaction

with coactivators such as SRC-1 (steroid receptor coactivator-1). It is worth mentioning, that all domains despite of their name can have multiple functions (Yen, 2001).

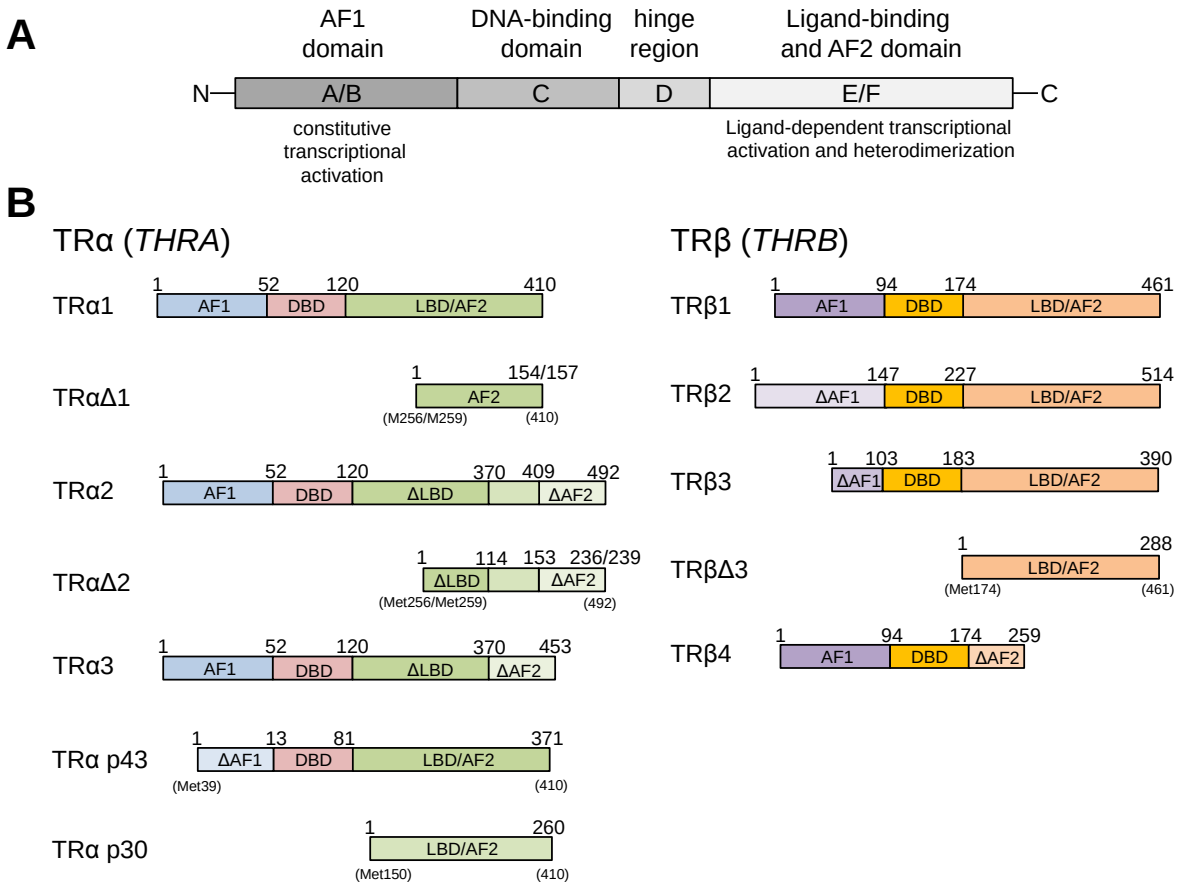

Figure 5: General and isoform-specific structure of thyroid hormone receptors. *(**A**) General domain structure of nuclear receptors. (**B**) Domain structure of TRα isoforms (left) and TRβ isoforms (right). (N = N-terminus; C = C-terminus; DBD = DNA-binding domain; LBD = ligand-binding domain; AF1/2 = protein interaction domain; ΔLBD = LBD incapable of T3 binding; ΔAF1/2 = truncated or altered AF1/2 domain; internal methionines (Met) used as alternative translational start sites, as well as the corresponding last amino acid in full-length isoform are written in brackets)*

Tissue-specific expression and distribution of TR isoforms

There is an isoform-specific expression, regulated developmentally and in a tissue-specific manner (Forrest, Sjoberg, & Vennstrom, 1990). Noteworthy, expression of mRNA does not always correlate with protein concentration (Schwartz, Lazar, & Oppenheimer, 1994). Even though TRs are virtually expressed in all tissues, there is a distinct tissue-specific expression of TR isoforms, which contributes to the isoform related tissue-specific action mediated by TRs (Bookout *et al.*, 2006). TRβ1 is the

predominantly expressed isoform in liver, whereas in cardiomyocytes 70% of the expressed TR is TRα1 and TRβ1 accounts for only 30%. It was shown that TRβ2 is abundantly expressed in pituitary, but it was less verifiable in other tissues (Schwartz *et al.*, 1994). However, the established view in TR isoform-specific tissue distribution locates TRα expression mainly in heart, brain (e.g. cortex), skeletal muscle, bone, spleen, pancreas, adipose tissue, kidney and gut, whereas TRβ expression was found in liver, brain (e.g. hippocampus, pituitary), bone, pancreas, adipose tissue and kidney.

The isoforms TRα2, TRαΔ1, TRαΔ2, TRβΔ3 and TRβ4 exhibit altered or truncated C-termini (Figure 5) and hence are not able to bind T3. Thus, these isoforms are expected to act in a dominant negative fashion, competing for cofactors and TREs with the full-length TRs (Chassande *et al.*, 1997; Moriyama *et al.*, 2016; Plateroti *et al.*, 2001; Williams, 2000). As mentioned above, TR isoforms are very diverse regarding their length and thus also exhibit a different domain composition. In turn, these differences affect localization of TRs, as well as physiological functions. For example, the 43 kDa TRα isoform (TRα p43) is located in the mitochondrial matrix, even though bearing a NLS. TRα p43 exhibits a functional DBD, hence functioning as a mitochondrial transcription factor (Wrutniak-Cabello, Casas, & Cabello, 2001). In 2014, Kalyanaraman *et al.* demonstrated that methionine at position 150 (Met^{150}) serves as an internal translation initiation site to produce a 30 kDa TRα (TRα p30), which is neither located in the nucleus nor in mitochondria but binds to the inner site of the plasma membrane (Kalyanaraman *et al.*, 2014). Three methionine residues (Met^{120}, Met^{122} and Met^{150}) are highly evolutionary conserved in TRα but absent in TRβ, probably explaining why the set of isoforms of TRα is more variable than that of TRβ.

TR mediated physiological actions

Isoform-specific TR actions –lessons from mouse studies

The knowledge about TRs affecting physiological functions was gained through studies on TR knockout (KO) or mutant mice throughout the years. Using isoform-specific TR^{KO} mouse models enabled attribution of known physiological TH effects to either TRα or TRβ (Gauthier *et al.*, 1999).

It was shown that TRα mainly affects early *postnatal* development, cardiac function and bone development. A complete KO of all functional products of the *Thra* gene locus ($TR\alpha^{0/0}$ mouse model) resulted in a delayed *postnatal* development which showed up with a delayed growth and gain of body weight, as well as a delayed bone maturation (Gauthier *et al.*, 2001). Further studies on $TR\alpha^{KO}$ mouse models revealed a participation of TRα on regulating heart rate (HR). Mice lacking TRα have a reduced HR of about 20% and a decreased expression of pacemaker channels *Hcn2* and *Hcn4* (Wikstrom *et al.*, 1998; Gloss *et al.*, 2001). Additionally, TRα-dependent cardio protective effects against ischemia-reperfusion have been reported (Pantos & Mourouzis, 2014; Pantos *et al.*, 2011). Further phenotyping of $TR\alpha^{KO}$ mice revealed a decrease in body temperature of about 0.5 °C in comparison to WT mice. Thus, attributing TRα signaling to the TH-mediated regulation of body temperature. In several brain areas like cortex and striatum TRα1 is the predominant receptor for regulation of TH-dependent gene expression (Gil-Ibanez, Bernal, & Morte, 2014; Gil-Ibanez, Morte, & Bernal, 2013). All in all, the complex and organ spanning functions of TRα imply that dominant negative mutations, which result in resistance to thyroid hormone through TRα (RTHα), are associated with a severe phenotype, not only affecting growth but also affecting brain development, heart rate and body temperature (Bochukova *et al.*, 2012; Zavacki & Larsen, 2013).

TRβ is known to maintain the negative feedback loop of the HPT axis. It was shown that the TRβ2 isoform regulates TSH expression in the pituitary in a DNA-binding dependent manner (Shibusawa, Hashimoto, *et al.*, 2003). A lack of TRβ2 leads to an increased expression and secretion of TSH which results in an enlargement of the thyroid gland and increased TH synthesis (Forrest, Hanebuth, *et al.*, 1996; Weiss *et al.*, 1997). But also development and function of cochlear and retina, parts of the sensory system, are regulated by TRβ (Forrest, Erway, Ng, Altschuler, & Curran, 1996; Jones, Srinivas, Ng, & Forrest, 2003). TRβ malfunction is associated with deafness and altered retinal cone photoreceptor differentiation (Jones *et al.*, 2003). In liver, TRβ regulates several metabolic functions like lipid and cholesterol metabolism (Feng, Jiang, Meltzer, & Yen, 2000; Flores-Morales *et al.*, 2002; Gullberg, Rudling, Forrest, Angelin, & Vennstrom, 2000; Perra *et al.*, 2008; Pramfalk, Pedrelli, & Parini, 2011). Anti-apoptotic and proliferative effects of TRβ on hepatocytes and pancreatic acinar cells were proven in *in vivo* studies (Columbano *et al.*, 2008; Kowalik *et al.*,

2010; Ledda-Columbano, Perra, Pibiri, Molotzu, & Columbano, 2005; Lopez-Fontal *et al.*, 2010).

DBD and binding to thyroid hormone response elements

The DBD is formed by two α-helices and two zinc-finger binding motifs, each coordinated by four conserved cysteine residues. The P-box, an amino acid sequence located between and just distal to the third and fourth cysteines in the N-terminal helix of the first zinc-finger, interacts directly with the DNA at the major groove. The amino acid sequence of the P-box of TRs is identical to that of estrogen receptor (ER), retinoid acid receptor (RAR), retinoid x receptor (RXR), vitamin D receptor (VDR), as well as a couple of other nuclear receptors with unknown ligands (orphan receptors) (Lazar, 1993). The most important amino acids for DNA sequence recognition and binding by TRs are glutamic acid and two glycine residues (briefly EGG) within the P-box (Figure 6). It was shown for TRs and for ER that mutation of the first two amino acids of the EGG motif is sufficient to terminate DNA binding (Nelson, Hendy, Faris, & Romaniuk, 1994).

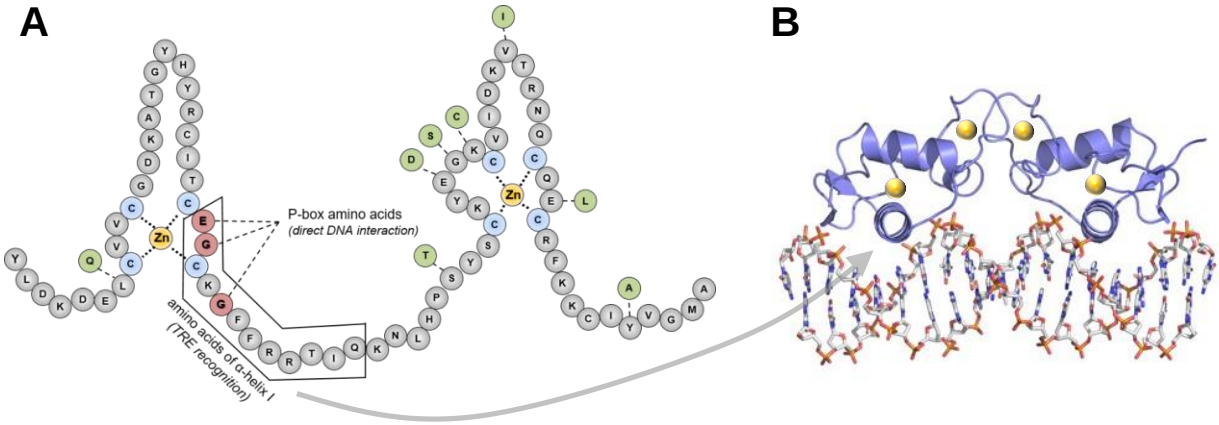

Figure 6: DNA-binding domain of TRα and TRβ and DNA TRE recognition. *(**A**) DNA-binding domain (DBD) of TRα and TRβ. Corresponding amino acid residues of TRα are marked in green. Cystein residues (C) and zinc (Zn) are highlighted in light blue and yellow, respectively. Amino acids of DNA recognition helix are framed and P-box amino acids are labelled in red. The arrow indicates location of recognition helix in the major groove. (**B**) 3D-sturcture of nuclear receptor DBD interaction with DNA in the major groove. Zn atoms are yellow. Figure (B) modified after Schwabe et al. (Schwabe, Chapman, Finch, & Rhodes, 1993).*

This EGG motif recognizes a six base pair DNA consensus sequence (G/A)GGT(C/G)A. TRs are able to bind DNA as monomers, homodimers and heterodimers. To the latter, the hexamer AGGTCA only forms one half-site of the TRE. Consequently, a second hexamer is needed for the binding partner. For TREs the two half-sites can be arranged as direct repeats (DRs), palindromes (PALs), inverted palindromes (IPs) and everted repeats (Williams, Zavacki, Harney, & Brent, 1994). The spacing between the half-sites is important for successful binding of TRs. Thus, it was shown that there is an optimal spacing existing for each TRE subtype, for example 4 nucleotides for a DR (DR4) and 6 for an inverted palindrome (IP6) (Chen & Young, 2010; Yen, 2001).

Canonical TR action –Transcriptional regulation of TH target genes

TRs are ligand dependent transcription factors and regulate the expression of TH target genes. This is considered the canonical action of TRs and implicates interaction between the receptor and DNA. Binding to TREs can occur in an apo- and holo-state of the receptor, thus presence of TH is not necessary for DNA binding. The conformation of the receptor in an apo-state, with a displaced helix 12, enables binding of corepressor complexes to the receptor. Two known corepressors which interact with TRs are NCoR (nuclear receptor corepressor) and SMRT (silencing mediator for retinoid and thyroid hormone receptors) (Astapova *et al.*, 2008; Makowski, Brzostek, Cohen, & Hollenberg, 2003; Nagy *et al.*, 1999). Bound corepressors build a scaffold for histone deacetylases (HDACs). Recruitment of HDACs leads to deacetylation of lysine residues of histones in close proximity where the unliganded TR has bound (Figure 7). This results in an inactivated chromatin structure and ends up in a decreased expression of the target gene (Yen, 2015). T3 binding to TRs causes the transition from an apo- into a holo-state. The conformational change moves helix 12 closer to the LBD and traps T3 in its binding pocket (Nagy & Schwabe, 2004). Additionally, it induces the release of corepressors and allows the binding of coactivators, such as the steroid receptor coactivator family (SRC-1, -2, -3) and p300 (McKenna & O'Malley, 2002; Vella *et al.*, 2014). The coactivators bind to the AF2 domain in the LBD via their LXXLL motif in a helix-12-dependent manner (Nagy *et al.*, 1999; Nolte *et al.*, 1998; Rastinejad, Huang, Chandra, & Khorasanizadeh, 2013). The coactivator complex engages histone

acetylases (HATs) and mediators like TRAPs (TR associated proteins) and DRIPs (vitamin D receptor interacting proteins) which form a multi-subunit complex. HATs transform the chromatin structure into an activated condition by increasing histone acetylation. Additionally, the multi-subunit mediator complex initiates recruitment of several transcription factors and RNA polymerase II to induce gene transcription (Bassett, Harvey, & Williams, 2003; Yen, 2001).

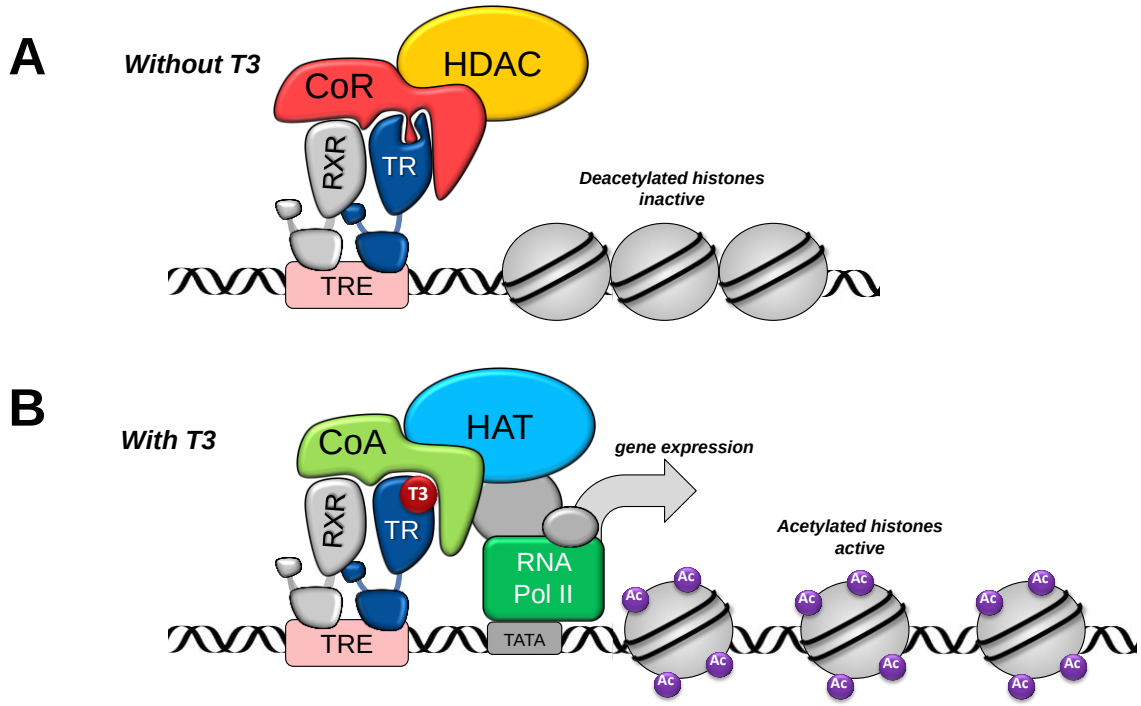

Figure 7: Schematic view of canonical action of thyroid hormone receptors. *(**A**) In absence of T3 (apo-state) TR/RXR heterodimer are bound to thyroid hormone response elements (TREs) and recruit corepressors (CoR). CoR build a scaffold for histone deacetylases (HADC). HDACs inactivate chromatin structure by deacetylating histones. (**B**) Binding of T3 (holo-state) leads to conformational changes which enables the exchange of CoR by coactivators (CoA). CoA recruitment engages histone acetylases (HAT) which activate chromatin structure by histone acetylation. Further recruitment of RNA polymerase II (RNA Pol II) complex results in gene expression. (Ac = acetylated lysine residue)*

It is worth mentioning, that many of the studies were restricted to one TR isoform, mainly TRβ. Thus, it remains unclear whether the coactivator and corepressor recruitment is mechanistically the same between the different TR isoforms. This issue is currently under investigation. However, the induction of gene expression by TRs acting as hormone-dependent transcription factors is considered as the current paradigm of TH/TR action.

Non-canonical TR action –Rapid activation of second-messenger signaling pathways

Canonical action of TR consists of gene induction and protein synthesis, as described above. However, in the early 80`s Segal and Ingbar showed that T3 can stimulate sugar up-take in rat thymocytes within a few minutes. Moreover, they used cycloheximide, an inhibitor of mRNA translation, to prove that these rapid TH effects are independent from protein synthesis (Segal, Buckley, & Ingbar, 1985; Segal & Ingbar, 1981, 1985). Thus, such an effect cannot be mediated by canonical TR action.

In 2000 Simoncini *et al.* reported that ERα could increase intracellular PIP_3 (phosphatidylinositol-3,4,5-phosphate) after stimulation with 17β-estradiol (E_2). Formation of PIP_3 is mediated by PI3K (phosphatidylinositol-4,5-phosphate-3 kinase). PIP_3 functions as a lipid mediator to recruit proteins with PIP_3-binding or pleckstrin homology domains such as the PIP_3-dependent kinase B (PKB, also known as AKT). Moreover, Simoncini *et al.* demonstrated that this mechanism is transferable to some other nuclear receptors including TRs (Simoncini *et al.*, 2000). The downstream signaling mainly depends on phosphorylation cascades. Hence, this signaling is rapid and only takes a couple of minutes. On top of that, the formation of PIP_3 in a hormone-dependent manner is fully preserved in a cell free system after immunoprecipitation of ERα or TR. Hence, it implies that this mode of action is independent from DNA binding and protein synthesis. Therefore, it is considered as non-canonical action of nuclear receptors.

During the following years of TR research many other different TR effects that are mediated in a DNA-binding independent manner have been reported in *in vitro* experiments. For instance, it was shown that TRβ can rapidly activate the ether-a-go-go related potassium channel (Kcnh2) in a rat pituitary cell line after T3 stimulation. This non-canonical TH/TR effect was abrogated by wortmannin, a PI3K inhibitor, implying that this effect is mediated by the same or at least a similar mechanism which was previously described by Simoncini *et al.* (Storey *et al.*, 2006; Storey, O'Bryan, & Armstrong, 2002). Even though TRα failed to induce Kcnh2 activity, Cao *et al.* proved interaction of TRα with PI3K and downstream phosphorylation of AKT after T3 stimulation (Cao, Kambe, Yamauchi, & Seo, 2009). Hiroi *et al.* reported a rapid activation of eNOS (endothelial nitric oxide synthase) by T3 through TRα in an Akt dependent manner in mouse embryotic fibroblasts (Hiroi *et al.*, 2006). The

interaction between PI3K and TRα or TRβ was further confirmed by the group of Sheue-yann Cheng. They showed that TRs with a C-terminal frameshift mutation were unable to bind T3 but binding to PI3K was enhanced (Furuya, Lu, Willingham, & Cheng, 2007). In 2014, the group of David Armstrong described a mechanism by which TRβ activates PI3K. Briefly, they found that phosphorylation of tyrosine at position 147 in the second zinc-finger of TRβ is necessary for binding Lyn-kinase. Lyn is a non-receptor tyrosine kinase, belonging to the Src family kinases. Thus, Lyn is able to phosphorylate and activate PI3K. Substitution of tyrosine by phenylalanine (Y147F) abrogated Lyn binding to TRβ and prevented T3 mediated activation of PI3K (Martin *et al.*, 2014) (Figure 8).

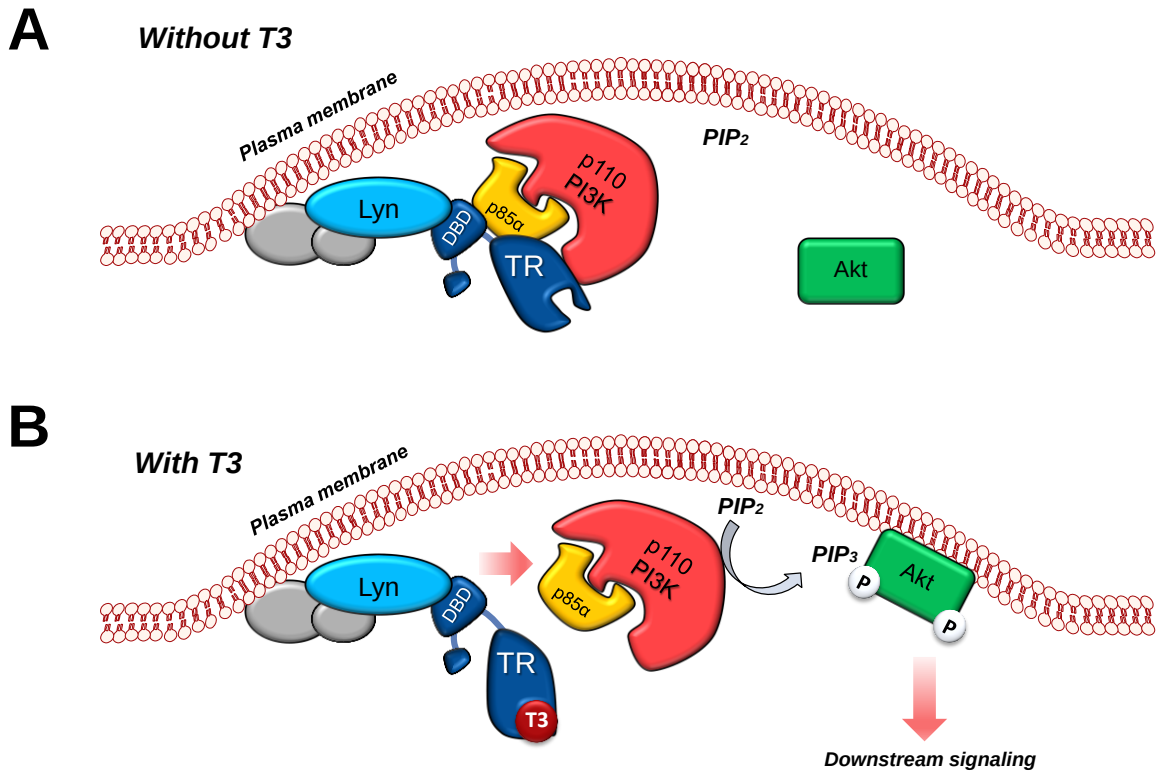

Figure 8: Proposed mechanism for non-canonical action of TRβ. *Lyn kinase (Lyn) sequesters TRβ at the plasma membrane by binding to a motif in the DBD of TRβ. (**A**) In absence of T3, p85α subunit of PI3K is bound to TR. (**B**) Conformational changes of TR after T3 binding releases PI3K which is now able to convert PIP_2 to PIP_3. This enables membrane translocation and phosphorylation of Akt with activation of downstream signaling cascades. (DBD = DNA-binding domain; PI3K = phosphatidylinositol 3-kinase; PIP_2 = phosphatidylinositol-2-phosphate; PIP_3 = phosphatidylinositol-3-phosphate; P = phosphorylates amino acid residue; Akt = serine/threonine specific protein kinase B)*

These authors also state, that non-canonical TR signaling via TR and PI3K is solely mediated by TRβ, as the SRC homology 2 binding motif (IYVGM) for PI3K binding

only exists in TRβ and not in TRα. Even though, other groups demonstrated that there is a direct protein-protein interaction between PI3K and TRα (Cao *et al.*, 2009). Taken together, the mechanisms by which TRs mediate non-canonical action are still incompletely understood. Noteworthy, it is known that among anti-apoptotic effects, activation of PI3K/Akt signaling pathway can result in transcription of PI3K dependent genes. Moeller *et al.* showed that T3 could induce the expression of hypoxia inducible factor-1α in primary cultures of human fibroblasts. Furthermore, this induction was TRβ dependent and sensitive to the PI3K inhibitor LY294002 (Moeller, Dumitrescu, & Refetoff, 2005; Moeller, Dumitrescu, Walker, Meltzer, & Refetoff, 2005). Thus, non-canonical action of TRs might not solely be restricted to activation of second messenger signaling, but might also result in induction of non-canonically regulated TH target genes.

Recapitulating, non-canonical action of TRs seems to be closely related to PI3K activation. Thus, non-canonical TH/TR mediated effects are rapid and might have anti-apoptotic effects on target tissues. However, hitherto studies on non-canonical TR action were performed *in vitro,* often using artificial conditions like experiments based on TR overexpression in immortalized cell lines. Even though these studies convincingly prove the existence of a DNA-binding independent TR action, they fail to confirm the physiological relevance of this non-canonical TR signaling pathway.

Hypothesis and Aims of the Study

State of the art at a glance

More than 20 years of TR research have resulted in discovering many physiological TH/TR effects. Contribution of TR signaling to maintain several physiological effects like organ development, growth, regulation of body temperature and heart rate is a well-accepted fact. The regulation of these physiological TH/TR effects are based on the current paradigm that TRs are canonical ligand dependent transcription factors, thus DNA binding and protein synthesis is fundamentally required. This paradigm is still valid, even though it was shown more than 30 years ago, that TH can mediate rapid functions independent of protein synthesis (Segal *et al.*, 1985; Segal & Ingbar, 1985).

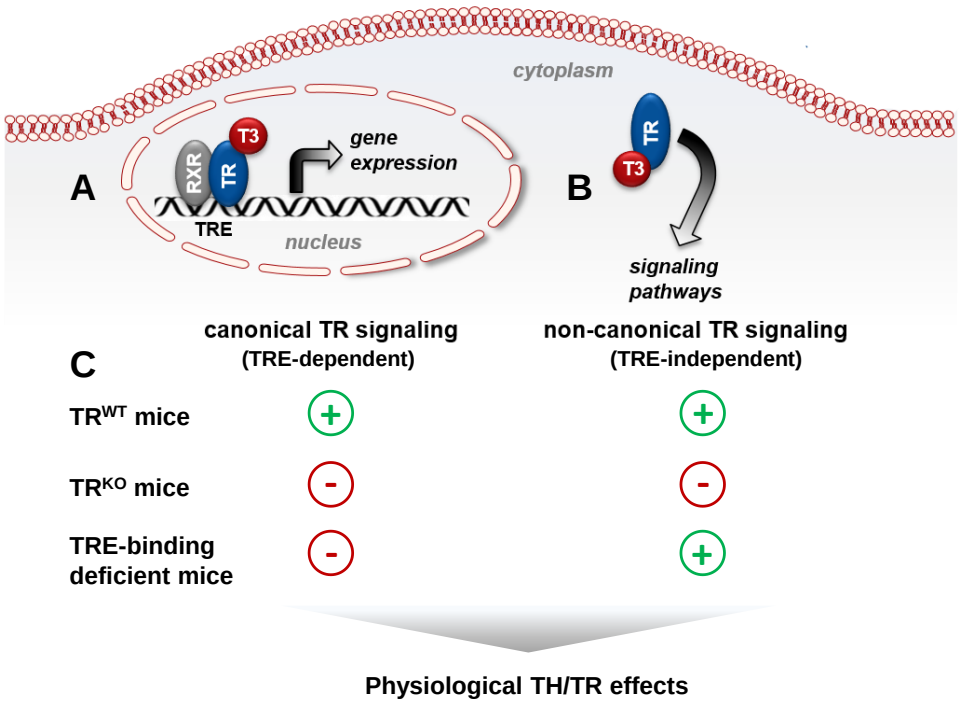

Figure 9: Phenotypical comparison of different mouse models for distinguishing between canonical and non-canonical TR action. *(**A**) Canonical TR signaling requires binding of TR to regulatory DNA sequences, the thyroid hormone response elements (TREs), primary as a heterodimer with retinoic X receptor (RXR). Binding of T3 leads to an exchange of cofactors which initiates or represses transcription of the target gene. (**B**) Non-canonical action of TRs involves rapid activation of signaling pathways without DNA-binding. (**C**) Present (+) and absent (-) TR signaling in mouse models. In wild-type mice (TR^{WT}), the TR can mediate both canonical and non-canonical signaling. In TR-knockout mice (TR^{KO}), both effects are absent. In mice with TRE-binding deficient TRs, canonical signaling is abolished and only non-canonical signaling is preserved. Thus, a comparison of these mice allows determining whether the signaling mechanism responsible for TH effects is canonical or non-canonical.*

This non-canonical TR action has been widely overlooked throughout the last decades, mainly, because adequate models for distinguishing between canonical and non-canonical TR signaling *in vivo* are missing. With the currently available mouse models (TR wild-type (WT) mice and TR^{KO} mice) it is impossible to distinguish between canonical and non-canonical TR signaling, because TRs can mediate canonical and non-canonical actions of TH in WT mice, whereas both actions are absent in TR^{KO} mice (Figure 9).

Major hypothesis of this study

1) *Non-canonical signaling contributes to the overall effect of TH and is physiological relevant.*
2) *TRα and TRβ may act non-canonically in an organ- or tissue-specific manner.*
3) *Comparison of WT, TR^{KO} and TR-mutant mice with abrogated canonical action, will determine the underlying TR signaling pathways that result in a range of physiological TH responses (Figure 9).*

Aims of this study

To address this question, this study aims to:

1) *Develop a mouse model with abrogated canonical TRE-dependent TR signaling for investigating non-canonical TR action separately.*
2) *Determine which physiological TH effect is mediated by which mechanism, canonical or non-canonical.*
3) *Reveal the contribution of non-canonical TR signaling in an isoform-specific manner.*

THs are crucial for physiology and homeostasis, as well as maintaining energy metabolic processes. Even after more than 30 years of TR research the mechanisms behind TH signaling are not fully understood. Thus, the purpose of this project is to elucidate the physiological role of non-canonical TR signaling and extend the understanding of TR action.

Materials and Methods

Materials

Chemicals

Table 1: Register of chemicals and reagents

Chemicals and Reagents	Manufacturer/Supplier
3,5,3'-Triiodothyronine	Sigma-Aldrich, St. Louis, USA
Acetic acid 99.7%	Sigma-Aldrich, St. Louis, USA
Agarose	Sigma-Aldrich, St. Louis, USA
Amberlite Resine IRA-400 chloride form	Sigma-Aldrich, St. Louis, USA
Ammonium per sulfate	Bio-Rad, Munich, Germany
Beta-mercaptoethanol	Sigma-Aldrich, St. Louis, USA
BlueJuice Loading Buffer (10x)	Invitrogen/Life Technologies, Carlsbad, California, USA
Bovine serum albumin (BSA)	Sigma-Aldrich, St. Louis, USA
Charcoal, Dextran Coated	Sigma-Aldrich, St. Louis, USA
Clarity Western ECL substrat	Bio-Rad, Munich, Germany
cOmplete protease inhibitor cocktail	Roche, Berlin, Germany
cOmplete Ultra, EDTA-free protease inhibitor	Roche, Berlin, Germany
Dimethyl sulfoxide (DMSO)	Sigma-Aldrich, St. Louis, USA
Dithiothreitol (DTT)	Thermo Fischer Scientific Inc. Waltham, USA
Dulbecco´s modified Eagle´s Medium	Thermo Fischer Scientific Inc. Waltham, USA
Ethanol (technical grade)	Pharmacy, UK Essen, Essen Germany
Ethylenediaminetetraacetic acid disodium salt	Sigma-Aldrich, St. Louis, Missouri, USA
Fetal calf serum	Thermo Fischer Scientific Inc. Waltham, USA
Formafix, buffered formalin	Formafix Global Technologies Ltd., Düsseldorf, Germany
FuGene6	Promega GmbH, Mannheim, Germany

Gel Pilot 1kb Ladder	Qiagen, Hilden, Germany
GelPilot 100bp Plus Ladder	Qiagen, Hilden, Germany
Heparin-Natrium-5000	Ratiopharm, Ulm, Germany
Hydrochloride acid (36.5-38.0%)	Sigma-Aldrich, St. Louis, USA
Isoflurane	Baxter, Oslo, Norway
Isopropanol (2-propanol)	Sigma-Aldrich, St. Louis, USA
LightCycler® 480 SYBR Green I Master Mix	Roche, Berlin, Germany
Methimazole (MMI)	Sigma-Aldrich, St. Louis, USA
N,N,N′,N′-Tetramethylethylenediamine	Sigma-Aldrich, St. Louis, USA
Nonident P-40 Substitude	Sigma-Aldrich, St. Louis, USA
Nuclease free water	Promega GmbH, Mannheim, Germany
Oil-Red O	Sigma-Aldrich, St. Louis, USA
Panthenol	Ratiopharm, Ulm, Germany
Peptone	Carl Roth GmbH & Co. KG, Karlsruhe, Germany
PhosSTOP	Roche, Berlin, Germany
PhosStop Phosphatase Inhibitor	Roche, Berlin, Germany
Protein-Marker IX	VWR Interntional GmbH, Langenfeld, Germany
Rotiphorese A	Carl Roth GmbH & Co. KG, Karlsruhe, Germany
Rotiphorese B	Carl Roth GmbH & Co. KG, Karlsruhe, Germany
Roti-GelStain	Carl Roth GmbH & Co. KG, Karlsruhe, Germany
Sodium dodecyl sulfate (SDS)	Sigma-Aldrich, St. Louis, USA
Sodium hydroxide (NaOH)	Sigma-Aldrich, St. Louis, USA
Sodium orthovanadate ($NaVO_4$)	Sigma-Aldrich, St. Louis, USA
Sodium perchlorate	Sigma-Aldrich, St. Louis, USA
Sodiumdeoxycholate	Sigma-Aldrich, St. Louis, USA
Sodiumfluoride (NaF)	Sigma-Aldrich, St. Louis, USA

Triiodothyronine (T3)	Sigma-Aldrich, St. Louis, USA
Tris-Base	Sigma-Aldrich, St. Louis, USA
Tris-HCl	Sigma-Aldrich, St. Louis, USA
Triton X-100	Sigma-Aldrich, St. Louis, USA
Tween 20	Sigma-Aldrich, St. Louis, USA
Yeast extract	Carl Roth GmbH & Co. KG, Karlsruhe, Germany
ZellShield	Minerva Biolabs, Berlin, Germany

Technical devices

Table 2: Register of technical devices

Device	**Manufacturer/Supplier**
ADVIA2400	Siemens, Munich, Germeny
Autoclave VX-150	Systec, Linden, Germany
Bendelin Sonoplus HD 2070	Bandelin, Berlin, Germany
Biometra electrophorese chamber	Biometra, Jena, Germany
Bio-Rad SDS-PAGE chamber	Bio-Rad, Munich, Germany
Faxitron MX20	Qados, sandhurst, Great Britain
Heracell 150i, Incubator	Thermo Fischer Scientific Inc. Waltham, USA
Heraeus Fresco17	Thermo Fischer Scientific Inc. Waltham, USA
Heraeus Megafuge 16R	Thermo Fischer Scientific Inc. Waltham, USA
Heraeus Megafuge 40R	Thermo Fischer Scientific Inc. Waltham, USA
Herasafe 2020, Safty Cabinet	Thermo Fischer Scientific Inc. Waltham, USA
Incubator shaker innova42	New Brunswick Scientific, Edison, USA
Kern EMB 100-3	Kern & Sohn, Balingen, Germany
LeicaDMLB2 microscope	Leica, Wetzlar, Germany
LightCycler® 480 II	Roche, Berlin, Germany
Magnet stirrer IKA RH digital	IKA, Staufen, Germany

NanoDrop 2000	Thermo Fischer Scientific Inc. Waltham, USA
Olympus BX51 microscope	Olympus, Waltham, USA
Olympus CK40	Olympus, Waltham, USA
ProfessionalTrio Thermocycler	Biometra, Jena, Germany
Rectal temperature probe	TempJKT, Eutech Instruments Europe, Netherlands
SevenCompact pH meter	Mettler Toledo, Columbus, USA
Shaker WT12	Biometra, Jena, Germany
SI-114A scale	Denver Instruments, Bohemia, USA
Sirius Luminometer	Berthold detection systems, Pforzheim, Germany
Skyscan 1172a	Bruker micro CT, Kontich, Belgium
Standard Power Pack P 25T	Biometra, Jena, Germany
Ultrasonic bath Sonorex	Bandelin, Berlin, Germany
Ultra-Turrax T25	Janke & Kunke IKA,
Versadoc 4000MP	Bio-Rad, Munich, Germany
Versamax	Molecular Devices, Biberach an der Riß, Germany
Vortex 4 Basic	IKA, Staufen, Germany
Water bath 1008	GFL Gesellschaft für Labortechnik, Bergwedel, Germany
Zeiss, Primo Vert	Zeiss, Oberkochen, Germany

Antibodies

Table 3: Register of primary and secondary antibodies

Antibody	**Concentration**	**Catalog#**	**Supplier**
Anti-mouse IgG HRP linked	1:2000	7076S	Cell Signaling
FASN mAb	1:1000	MA5-14887	Pierce Antibodies
H-300 anti-SCD1	1:1000	Sc-30081	Santa Cruz, USA
ME1 antibody	1:1000	PA5-21550	Pierce Antibodies
Mouse anti-Gapdh	1:6000	ACR001P	Acris Antibodies

Plasmids

Table 4: Register of plasmids

Plasmid	Description	Antibiotic resistance
TRβ1-pcDNA3	expression vector for human TRβ1	AmpR
TRα1-pcDNA3	expression vector for human TRα1	AmpR
DR+4-*Firefly* Luciferase Reporter	DR+4 regulated luciferase reporter vector	AmpR
RL-TK Renilla-Luciferase expression vector	Vector for expression of *Renilla* firefly	AmpR

All plasmids listed above were a kind gift of Prof. Dr. Refetoff.

Kits

Table 5: Register of kits

Kit	Catalog#	Manufacturer/Supplier
CompoZr® Targeted Integration Kits	CSTZFN	Sigma-Aldrich, St. Louis, USA
Dual-Glo® Luciferase Assay System	E2920	Promega GmbH, Mannheim, Germany
EndoFree Plasmid maxi Kit	12362	Qiagen, Hilden, Germany
Free T3 ELISA	EIA-2385	DRG Diagnostics GmbH, Marburg, Germany
Free T4 ELISA	EIA-2386	DRG Diagnostics GmbH, Marburg, Germany
PCR Mycoplasma Test Kit	A3744	AppliChem, Darmstadt, Germany
Pierce™ BCA Protein Assay Kit	23225	Thermo Fischer Scientific Inc. Waltham, USA
Q5® Site-Directed Mutagenesis Kit	E0554S	New England Biolabs GmbH, Frankfurt am Main, Germany
QIAGEN Plasmid Maxi Kit	12162	Qiagen, Hilden, Germany
QIAprep Spin Miniprep Kit	27104	Qiagen, Hilden, Germany
QiaPrep Spin Miniprep Kit (50 applications)	27104	Qiagen, Hilden, Germany

QIAshredder	79654	Qiagen, Hilden, Germany
RNeasy Mini Kit	74106	Qiagen, Hilden, Germany
SuperScript™ III Reverse Transcriptase	18080-051	Thermo Fischer Scientific Inc. Waltham, USA
Total T3 RIA	RIA-4534	DRG Diagnostics GmbH, Marburg, Germany
Total T4 ELISA	EIA-1781	DRG Diagnostics GmbH, Marburg, Germany

Consumables

Table 6: Register of consumables

Consumables	**Manufacturer/Supplier**
10 ml syringe BD Discard II	Becton Dickinson, Franklin Lakes, USA
2 ml reaction tubes	Eppendorf, Hamburg, Germany
2 ml syringe BD Discard II	Becton Dickinson, Franklin Lakes, USA
8 ml tubes	Sarstedt, Nümbrecht, Germany
BD Microfine Insulin U-100	Becton Dickinson, Franklin Lakes, USA
Blue crew cap tube, 15 ml, steril	Greiner bio-one, Essen, Germany
Blue crew cap tube, 50 ml, steril	Greiner bio-one, Essen, Germany
Cellstar 24 well, Tissue culture treated	Greiner bio-one, Essen, Germany
Cellstar 6 well, Tissue culture treated	Greiner bio-one, Essen, Germany
Cellstar dish 150 x 15mm, non TC Petri	Greiner bio-one, Essen, Germany
DB Eclipse Needle 20G	Becton Dickinson, Franklin Lakes, USA
DB Eclipse Needle 23G	Becton Dickinson, Franklin Lakes, USA
DB Eclipse Needle 25G	Becton Dickinson, Franklin Lakes, USA
DB Eclipse Needle 25G	Becton Dickinson, Franklin Lakes, USA
Filter paper	Machery-Nagel, Düren, Germany
Microvette	Sarstedt, Nümbrecht, Germany
Pasteur pipettes	Brand, Wertheim, Germany
Pipette tips 100-1000 µl	Eppendorf, Hamburg, Germany

Pipette tips 2-200 µl	Sarstedt, Nümbrecht, Germany
96-well white bottom plates	4titude, Berlin, Germany
96-well clear bottom plates	Greiner bio-one, Essen, Germany
2-50 ml pipettes (Cellstar)	Greiner bio-one, Essen, Germany
0.2 ml PCR soft tubes	Biozym Biotech Trading, Wien, Austria
0.5 ml reaction tubes	Biozym Biotech Trading, Wien, Austria
Rotilabo Syringe-filter 0.22 µm and 0.45 µm	Biozym Biotech Trading, Wien, Austria
1.5 ml reaction tubes	Eppendorf, Hamburg, Germany
Pipette tips 0.1-10 µl	Sarstedt, Nümbrecht, Germany

Molecular biological methods

Cloning of TR expression vectors and luciferase-reporter vectors

Point mutations for TRα71GS, TRαG291R, TRβ125GS and TRβG345R were introduced into pcDNA3 vectors expressing TRα1 and TRβ1 by site-directed mutagenesis (Quickchange Site Directed Mutagenesis Kit, Agilent Technologies, USA). For generation of TRE/GRE1 and TRE/GRE2 luciferase reporter constructs, the DR+4-*Firefly*-Luciferase reporter vector served as a template. Primers were designed back-to-back, while one primer carried the desired point mutations (Table 7). 12.5 µl of Q5 Hot Start High-Fidelity 2x Master Mix was mixes with 1.25 µl of each mutagenesis primer (final concentration of 0.5 µM), 1 µl template plasmid (20 ng) and filled up to 25 µl with nuclease-free water. Cyclin conditions were chosen as follows: Initial denaturation at 98 °C for 30 sec, followed by 25 cycles of 98 °C for 10 sec, for 20 sec at an appropriate annealing temperature (annealing temperature was calculated with the average T_m + 3 °C) and extension at 72 °C for 30 sec. Mutagenesis PCR was terminated after a final extension at 72 °C for 2 min. Linear PCR-product was ligated and the template was digested by incubating a mixture of 1 µl of PCR-product, 5 µl of 2x KLD Reaction Buffer, 1 µl of 10x KLD Enzyme Mix and 3 µl of nuclease-free water, for 15 min at RT.

Table 7: List of mutagenesis primers

Primer	Sequence (5'→3')
TRb125GS-mut-F	GAA GCT GCA AGG GTT TCT TTA G
TRb125GS-mut-R	ACA ACG TGA TAC AGC GGT AG
TRa71GS-mut-F	GTA TCA CTT GTG GGA GCT GCA AGG G
TRa71GS-mut-R	AGC GGT AGT GAT AAC CAG
TRbG345R-mut-F	GGC CAG CTG AAA AAT GGG CGT CTT GGG GTG
TRbG345R-mut-R	AAA CTT TTT CAG CTG GCC CCG TGT CAC TGC
TRaG291R-mut-F	CAG CCA TTG GAA ACA GAG GCA GAA ATT CCT GC
TRaG291R-mut-R	GCC TCT GTT TCC AAT GGC TGC CCT GGG CAT
TRE/GRE1-mut-F	TAC CTC AGG TCA CAG GAG ATC AGA C
TRE/GRE1-mut-R	CAA GGT CAC AGG AGA TCA TGT ACC C
TRE/GRE2-mut-F	TAC CTC AGG TCA CAG GAG GAC AGA C
TRE/GRE2-mut-R	CAA GGT CAC AGG AGG ACA TGT ACC C

Transformation

For amplification of plasmids, 50 µl chemically competent NEB 5-α *E. coli* (supplied with *Q5 mutagenesis Kit*) were thawed on ice. 10 ng of plasmid was given to the tube of thawed cells and mixed carefully by flicking the tube. After 30 min incubation on ice, heat shock was performed at 42 °C for 30 sec before the tube was put back on ice for additional 5 min. 950 µl of room temperature SOC medium was added and the mix was incubated at 37 °C for 60 min with shaking at 225 rpm. An appropriate amount of cells was plated on lysogeny broth-agar (10 g peptone, 5 g yeast extract, 10 g NaCl, 15 g agarose, solved in 1 L $H_2O_{dest.,}$ pH 7.0) with 70 µg/ml ampicillin overnight at 37 °C. Only clearly separated single colonies were picked for further plasmid preparation.

Mini- and maxi-plasmid preparation

For mini- and maxi-plasmid-preparation volumes of 5 ml or 250 ml inoculated LB-culture (10 g peptone, 5 g yeast extract, 10 g NaCl, solved in 1 L $H_2O_{dest.,}$ pH 7.0)

were used, respectively. Briefly, 5 ml cultures were inoculated by picking a single colony from the agar plate with a pipette tip. 250 ml cultures were inoculated with a 50 µl of the 5 ml culture. Liquid cultures were incubated at 37 °C for 16-18 hours, shaking at 225 rpm.

For mini-preparation the *Qiaprep® Miniprep kit* was used. Bacteria were pellet by centrifugation at 4600xg for 5 min. After discarding the supernatant, bacteria pellet was resuspended in 250 µl of *buffer P1* and transferred to a 1.5 ml reaction tube. For induction of cell lysis, 250 µl of *buffer P2* was added and thoroughly mixed by inverting the tube 6 times. Lysates were neutralized by adding 350 µl of *buffer N3* and mixing thoroughly (tubes were inverted up to 10 times). Cell debris was removed via centrifugation at 17000xg for 10 min. The supernatant (~800 µl) was transferred to *QIAprep 2.0 spin columns* and the columns were centrifuged for 1 min at full speed. After discarding the flow-through, columns were washed with 750 µl of *PE buffer* and centrifuged again for 1 min at full speed. Another centrifugation step was done to remove residual wash buffer. 30-50 µl of *EB buffer* (10 mM Tris-HCl, pH 8.5) to the center of the column and incubated for 1 min at RT. Plasmids were eluted by centrifugation at full speed for 1 min.

For maxi-preparation the *EndoFree® Plasmid Maxi Kit* (Qiagen) was used. The 250 ml of liquid culture were separated into five 50 ml tubes. Bacteria were pelleted by centrifugation at 4600xg for 20 min. Supernatant was discarded and the five pellets were resuspended and combined in 10 ml of buffer P1. Lysis was induced by adding 10 ml of *buffer P2* and suspension was incubated at RT for 5 min. After adding 10 ml of cold *buffer P3* and gently mixing, the lysate was poured into the barrel of the *QIAfilter Cartridge* and incubated for 10 min at RT before being filtered into a new 50 ml tube. 2.5 ml *ER buffer* was added to the filtered lysate and incubated on ice for 30 min. After incubation, the lysate was transferred to an equilibrated *QIAGEN-tip 500 column* (equilibrated with 10 ml *QBT buffer*) and allowed to enter the resin by gravity flow. The column was washed two times with 30 ml of QC buffer (also via gravity flow). DNA was eluted by adding 15 ml of *QN buffer* following DNA precipitation by adding 10.5 ml of isopropanol. DNA was pelleted by centrifugation for 1 h at 4600xg. The supernatant was discarded and the pellet was washed with 5 ml of endotoxin-free 70% EtOH. After another centrifugation at 4600xg for 60 min, again the supernatant was carefully discarded and the pellet was air-dried. The dried pellet was redissolved in an appropriate volume of endotoxin-free *TE buffer*.

Concentration and purity of isolated plasmids was determined by NanoDrop (*NanoDrop2000*, ThermoFisher).

Cell culture based assays

Cell lines and culturing

HEK293 cells (human embryonic kidney cells) were obtained from ATCC and used for *in vitro* experiments. Cells were maintained in DMEM (Dulbecco´s modified Eagle´s Medium) containing 4.5 g/L glucose (DMEM+GlutaMAX, Gibco, USA), 1% ZellShield (Minerva Biolabs GmbH, Germany) and 10% FCS (Gibco, USA). Prior to experiments, cells were tests for mycoplasma contamination using the *PCR Mycoplasma Test Kit* (AppliChem), according to manufacturer´s instructions.

Generation of TH-depleted FCS

For depletion of FCS from TH a method described by Samuels *et al.* was used (Samuels, Stanley, & Casanova, 1979). Briefly, 500 g of resin (Amberlite® IRA-400 chloride form, Sigma-Aldrich) was washed 6 times with 2 L $H_2O_{dest.}$ and 250 ml of the washed resin was autoclaved after drying. 500 ml of FCS was added to the resin and stirred for 24 h at 37 °C. Aliquots of 50 ml were stored at -20 °C after sterile filtration of TH-depleted FCS.

Luciferase assay

For transient transfection, $4x10^4$ HEK293 cells were grown to 80% confluence in 24-well plates. FuGENE6 (Promega, USA) transfection reagent was used in a 1:3 DNA:FuGENE ratio. After 24 h cells were transfected using 280 ng/well of pDR+4-reporter, 33 ng/well RL-TK-control and 17 ng/well of plasmid encoding for TRα1 or TRβ1 variants (TRαWT, TRα71GS, TRαG291R, TRβWT, TRβ125GS, TRβG345R or empty vector pcDNA3) in the absence of FCS. After 24 h, transfection medium was replaced by fresh medium containing 5% TH-depleted FCS, which was generated by treatment with anion exchange resin as described above (Samuels *et al.*, 1979). Cells were stimulated with 10 nM T3 (dissolved in 40 mM NaOH, 0.02% BSA) or treated with vehicle for another 48 h. Cells were harvested and the activities of firefly

and renilla luciferases were determined (Dual-Glo Luciferase Assay System, Promega, USA) with a Sirius luminometer (Berthold Detection Systems GmbH, Germany). *Firefly* luciferase luminescence was normalized on *Renilla* luciferase luminescence from the same transfection sample to correct for differences in transfection efficiency.

Animal generation and genotyping

Study approval

All animal experiments were approved by the local authorities (Landesamt für Natur, Umwelt und Verbraucherschutz Nordrhein-Westfalen).

Generation of TRα^{GS} and TRβ^{GS} knock-in mouse strains

The GS point mutations were introduced into the *Thra* (NM_178060.3) and *Thrb* (NM_001113417.1) gene loci of C57BL/6J mice using custom made zinc finger nucleases (ZFNs) (CompoZr™ Targeted Integration-Kit-AAVS, Sigma-Aldrich, USA) and a donor plasmid containing the desired sequence (Carbery *et al.*, 2010; Cui *et al.*, 2011) (Suppl. Figure 1). For *Thra*, a ZFN cutting site within exon 3, 42 bp upstream from the target codons and for *Thrb*, the ZFN cutting site downstream of exon 3 was chosen (ZNF recognition sequence for *Thra*, 5´-TCC CTA GTT ACC TGGA *CAAAGAC* ACG AGC AGT GTG TCG TGT GTG-3´; for *Thrb*, 5´-CCA GAC AAC CAC *TGGACAT* CAGG CTT ACA GAA AGA GAT-3´; underlined = ZFN binding sites; italic = *FokI* cutting site). The donor vectors pTRα^{GS}-donor and pTRβ^{GS}-donor (both in pUC57-Kan, GENEWIZ, UK) contained the mutations changing the amino acid sequence in the P-box from glutamic acid and glycine (EG) to glycine and serine (GS). The codons 71, GAG, and 72, GGC, of exon 3 of *Thra* were mutated to GGG and AGC, respectively. Corresponding codons in *Thrb* (125, GAA and 126, GGC) were changed to GGA and AGC, respectively. Additionally, silent mutations created artificial restriction sites for *Eco32I* (TRα^{GS}) and *Mph1103I* (TRβ^{GS}) to facilitate genotyping by restriction fragment length polymorphism PCR (RFLP-PCR). C57BL/6JCrl oocytes were injected with microinjection solution (MIS) containing 20 ng/µl of ZFN mRNA and 1.3 ng/µl of donor vector. Injection of 1 pl MIS per pronucleus was performed with Leica micromanipulators. Manipulated oocytes were transplanted into oviducts of 0.5 days p.c. pseudopregnant mice. Offspring were

screened by PCR and sequencing. Generation of TR^{GS} mouse strains was done in cooperation with the Transgene Unit of the animal facility of the University Hospital Essen.

TR-knockout mouse strains

TR^{KO} ($TR\alpha^{0/0}$ and $TR\beta^{-/-}$) mice were obtained from the European Mouse Mutant Archive (https://www.infrafrontier.eu). All mouse strains were kept on a C57BL/6JCrl backcross for at least five generations and experiments were performed with homozygous mice and WT littermates.

General animal housing

All mice were housed in individually ventilated cages (IVC) at an ambient temperature of 21 ±1 °C and an alternating 12-hour light and 12-hour dark cycle. Standard chow (Sniff, Soest, Germany) and tap water were provided *ad libitum*, unless indicated otherwise.

Genotyping of the different mouse strains

DNA was extracted from ear punches which were used to identify animals. Therefore, ear punches were boiled for 45 min at 95 °C in 75 µl of lysis-buffer (25 mM NaOH, 0.2 mM EDTA, pH 12) and neutralized with an equal amount of neutralization-buffer (40 mM Tris-HCl, pH 5) afterwards. After vortexing thoroughly, all samples were directly used for PCR. PCR-reaction buffer consisted of 1x PCR buffer, 3.5 mM $MgCl_2$, 20 mM dNTPs and 2,5 U recombinant *Taq* DNA polymerase and 0.5 µl of specific forward and reverse primer (5 pM each) for the different mouse strains (Table 8).

Nuclease free water was added to fill up the volume to 18 µl. After adding 2 µl of DNA sample, everything was mixed carefully by flipping the reaction tube and spun down afterwards. The PCR-program was started with an initial denaturation at 95 °C for 3 min followed by 40 cycles consisting of 30 sec at 95 °C, 20 sec at 60 °C and 30 sec at 72 °C. A final step at 72 °C for 3 min was used to ensure complete PCR product synthesis. Samples of TR^{KO} mouse strains ($TR\alpha^{0/0}$ and $TR\beta^{-/-}$) were mixed

with 2 µl of loading buffer (*BlueJuice*) and proceeded directly to gel electrophoresis. Therefore, a 2% agarose gel (w/v in TAE buffer, 40 mM Tris-acetate, 1 mM EDTA, pH 8) was run at 100 V for 40 min. For determining the band size 3 µl of 100 bp ladder was used.

For TR^{GS} mouse strains RFLP-PCR was used. 10 µl of PCR product was digested with 0.5 µl of *Eco32I* or *Mph1103I* at 37 °C for 1 h for TRαGS or TRβGS, respectively.

Table 8: List of primers used for genotyping PCRs

Strain	Primer	Sequence (5'→3')	Amplicon size [bp]
$TR\beta^{-/-}$	*ThrbKO-fwd*	TGA ACC TAT TAT CTC GGG TCT TTC TC	150
	ThrbKO-rev	GCC TCT TCG CTA TTA CGC CA	
$TR\beta^{+/+}$	*ThrbWT-fwd*	CCT CTC ACC TTT CTA CTT TGC	250
	ThrbWT-rev	CAG GAA TTT CCG CTT CTG CTT	
$TR\alpha^{0/0}$	*ThraKO-fwd*	GCA TCG CCT TCT ATC GCC TT	660
	ThraKO-rev	GAG GAT GAT CTG GTC TTC GCA A	
$TR\alpha^{+/+}$	*ThraWT-fwd*	TCC TGA AGA GTG GGA CCT GAT	110
	ThraWT-rev	GCC TTC TTA CCA GGA ATT TTC GC	
$TR\beta^{GS/GS}$	*ThrbGS-fwd*	TCT GAA GCA CCA ACA CTT TCC T	1299
	ThrbGS-rev	AGA AAG GCT GTG GAG CAA AC	
$TR\alpha^{GS/GS}$	*ThraGS-fwd*	GTT TTG GCC CCA TCT AAG CC	1421
	ThraGS-rev	AGC CGT GCC AGG TGA ATT AG	

Animal phenotyping and *in vivo experiments*

Monitoring of linear growth and gain of body weight

Linear growth was determined through measuring the length from anus to the tail tip with a ruler (tail length). Gain of body weight was measured by weighting the mice. Tail length and body weight were weekly recorded from *postnatal* day P21 to P70.

Measurement of body temperature

Body temperature of 12 to 13-week-old male mice was measured every other day between 9 and 10 a.m. with a rectal probe (TempJKT, Eutech Instruments Europe, Netherlands). Briefly, the rectal probe was covered with Panthenol and carefully inserted into the anus of the mice. Temperature was stable 3 sec after inserting the probe.

Non-invasive ECG measurements

Heart rate was determined with non-invasive electrocardiography (ECG) in at least three recordings per mouse. 13-week-old conscious mice were restrained in a tunnel with their paws on electrodes covered with a small amount of electrode gel. One week prior to measurements mice were trained to get used to handling and restraining to minimize stress-induced effects. ECG data were recorded and analyzed with *PicoScope6* (Pico Technology, UK).

Blood glucose measurements

To measure the blood glucose response to T3, euthyroid mice were injected i.p. with T3 (7 ng/g BW) or vehicle. Before injection and 60, 120, 180 and 240 minutes after T3 injection, blood was drawn by tail vein puncture and blood glucose concentration was determined using Contour® XT (Bayer, Leverkusen, Germany).

Induction of hypothyroidism

For *in vivo* studies of T3 effects it is recommended to render mice hypothyroid before T3 treatment to ensure low and comparable TH concentrations within the different genotypes (Bianco *et al.*, 2013). Therefore, mice at the age of 10 to 11 weeks were treated with an iodine-deficient diet (LID) (TD.95007, Harlan-Teklad, USA), 0.05% 2-mercapto-1-methylimidazole (MMI) and 1% sodium perchlorate (Sigma-Aldrich) administered via the drinking water for at least three weeks.

Long-term and acute thyroid hormone treatment for gene expression analysis

After induction of hypothyroidism, as described above, mice were separated into T3 treatment and control groups for each genotype. Long-term T3-treated animals (5 days) received daily i.p. injections of 5 µg/100 g BW T3 (T3 stock solution was prepared as 1 mM in 40 mM NaOH containing 0.02% BSA; for injections T3 stock solution was diluted in sterile PBS) for 5 consecutive days. Animals of the control group were i.p. injected with equally diluted vehicle (40 mM NaOH with 0.02% BSA). For acute T3-treatment mice were given 20 µg/100 g BW by a single i.p. injection. The mice were euthanized with CO_2, 6 hours after the single dose of acute T3-treatment or 2 hours after the last injection on day 5 for the long-term treated groups. Blood was collected via heart puncture from the right ventricle. After that, mice were perfused via the left ventricle with 10 ml PBS/heparin (5 U/ml heparin) first, followed by a second perfusion with 10 ml of pure PBS.

Tissue sampling for histological or biochemical analysis

After sacrifying mice with CO_2 and perfusion as described above liver tissue was shock frozen in liquid nitrogen or embedded in *TissueTek® O.C.T™* (Sakura Finetek, Germany). Liver tissue, as well as thyroids were embedded in *TissueTek®* and quickly frozen in the gas phase of liquid nitrogen. Samples were stored -80 °C until used morphological analysis or Oil-Red-O staining. Shock frozen tissue (liver and heart) was also stored at -80 °C until used biochemical analysis e.g. protein or mRNA isolation. For analysis of bone histology, right limps, as well as distal tail were placed in buffered formalin (10%) over night at 4 °C. Left limbs and proximal tail parts were directly stored in 70% EtOH. The next day, formalin was exchanged by 70% EtOH.

Preparation of serum

Blood was collected by heart puncture in *Microvette®* tubes for capillary blood collection (Sarstaed, Germany) and stored on ice for at least 30 min to enable coagulation. After centrifugation at 4 °C with 17.000xg for 20 min, 50 µl of serum were aliquoted in 500 µl reaction tubes and stored at -80°C.

Methods for histological *ex vivo* analysis

Histological analysis and microscopy

Thyroids, embedded in *TissueTek*®, were cut in 5 µm thick sections and transferred to *SuperFrost*® microscopy slides (VWR). Sections were rinsed with $H_2O_{dest.}$ and incubated for 5 min in hematoxylin (1:5 dilution in $H_2O_{dest.}$). Samples were rinsed with tap water for 10 min and after that with $H_2O_{dest.}$. Eosin staining was done by incubating the slides in a 0.3% eosin solution (1 drop of glacial acetic acid was added per 100 ml) for 45 sec. Slides were rinsed again with $H_2O_{dest.}$. Stained sections were covered with mounting medium (Immu-Mount, ThermoScientific) and coverslips and dried over night at RT.

Brightfield microscopy images were taken with an *Olympus BX51 upright* microscope using the *Cell sense Dimension* software.

Bone histology

Analysis of bone samples was done in cooperation with the group of Prof. Graham Williams and Prof. Duncan Bassett at the Imperial College in London.

Tibias were decalcified in 10% EDTA and embedded in paraffin wax. Sections (5 µm) were stained with alcian blue and van Gieson (Bassett *et al.*, 2010). Measurements from at least 4 separate positions across the growth plate were obtained to calculate the mean height using *a LeicaDMLB2 microscope* and *DFC320 digital camera* (Leica Microsystems). Results from 2 levels of sectioning were compared.

Faxitron digital x-ray microradiography

Femurs were imaged at 10 µm resolution using a *Faxitron MX20*. Bone mineral content was determined relative to steel, aluminum and polyester standards. Images were calibrated with a digital micrometer and bone length, cortical bone diameter, and thickness were determined (Bassett *et al.*, 2010; Bassett *et al.*, 2014).

Micro-computed tomography (CT)

Femurs were analyzed by micro-CT (*Skyscan 1172a*) at 50 kV and 200 µA with a detection pixel size of 4.3 μm^2 and images were reconstructed using *Skyscan NRecon* software. A 1 mm^3 region of interest was selected 0.2 mm from the growth plate and trabecular bone volume as proportion of tissue volume (BV/TV), trabecular number and trabecular thickness were determined (Bassett *et al.*, 2010). Representative femurs from each treatment group were rescanned using a *SCANCO µCT 40* (SCANCO Medical AG) operating at 55 kVp peak energy detection, 6 µm resolution to obtain approximately 2500 cross-sections per specimen in 766 X 763 pixel 16 bit DICOM files. Raw data were imported using 32-bit Drishti v2.0.221 (Australian National University Supercomputer Facility, http://anusf.anu.edu.au/Vizlab/drishti/) and rendered using 64-bit Drishti v2.0.000 to generate high-resolution images.

Methods for biochemical analysis

Gene expression analysis via qRT-PCR

Total RNA was isolated from liver and heart with the *RNeasy™ Kit* with minimal modifications (QIAGEN, Hilden, Germany). 30 mg of heart and liver tissue were homogenized in 300 µl or 600 µl of *RLT-buffer* (containing 10 µl of β-mercaptoethanol per 1 ml *RLT-buffer*), respectively, using round bottom tubes and a rotor-stator homogenizer (*Ultra-Turrax*). Homogenates were loaded on *QIAshredder™* columns for further cell disruption (2 min centrifugation at full speed). Lysates from heart tissue were additionally digested with *proteinase K* (for 10 min at 55 °C). One Volume of 70% ethanol (technical grade) was added to the lysates and RNA was bound to matrix of *RNeasy columns* by centrifugation (15 sec at full speed). Columns were washed with 350 µl of *RW1-buffer* (15 sec at full speed). 10 µl DNaseI in 70 µl *RDD-buffer* was added to the columns and incubated for 15 min at RT. After an additional washing step with 350 µl *RW1-buffer*, the column was washed two times with 500 µl of *RPE-buffer* (15 sec at full speed). The columns were dried by centrifugation (1 min at full speed) and 30 µl of RNase-free water was pipetted directly onto the column matrix. After 2 min of incubation at RT, RNA was eluted by centrifugation (1 min at full speed). The flow-through containing the eluted RNA was again pipetted onto the column matrix and incubated for another 2 min at RT and

centrifuged as described above (this increased the RNA yield). RNA concentration and purity was determined via *NanoDrop* measurements (*NanoDrop2000*, ThermoScientific, USA).

2 µg of total RNA were reverse transcribed into cDNA with *SuperScript® III* (Invitrogen, USA) and random hexamer primers. Briefly, 2 µl random hexamer primer and 1 µl dNTP mix was added to 2 µg RNA and the volume was brought up to 10 µl by adding nuclease-free water. The mix was incubated at 65 °C for 5 min and chilled at 4 °C for at least 1 min. 10 µl of a cDNA-synthesis Master Mix, containing 2 µl of 10x *RT Buffer*, 4 µl of 25 mM $MgCl_2$, 0.1 M DTT, 1 µl of each *RNaseOUT™* and *SuperScript® III* were added and incubated at 25 °C for 10 min followed by 50 min at 50 °C. Reaction was terminated by incubation at 85 °C for 5 min. 1 µl of RNase H was added to the 20 µl reaction volume and RNA digestion was induced by incubation at 37 °C for 20 min.

qRT-PCR was performed using *Roche SYBR Green I Master Mix* on a light cycler LC480® (Roche, Switzerland). 2.5 µl of cDNA were mixed with 5 µl of *SYBR Green I Master Mix*, 2.4 µl PCR-grade water (Roche) and 0.05 µl of forward and reverse primer (100 pM) in white bottom 96-well plate. The PCR program was run with an initial melting at 95 °C for 5 min (ramp rate, 4.4 °C/s), followed by 40 cycles of 95 °C for 15 sec, 60 °C for 10 sec and 72 °C for 20 sec (ramp rate for every step was set at 2 °C/s). A melting curve analysis was performed to identify and exclude unspecific PCR products and formation of primer dimers. For primer sequences see table 9.

Table 9: List of qRT-PCR primers for gene expression analysis

Gene	Forward	Reverse	Accession No.
18s	CGG CTA CCA CAT CCA AGG AA	GCT GGA ATT ACC GCG GCT	NR_003278.3
Acc1	TGG CCT TTC ACA TGA GAT CC	TGC AAT ACC ATT GTT GGC GA	NM_133360.2
Acly	ATG CCC CAA GGA AAG AGT GC	CGT CTC GGG AAC ACA CGT AG	NM_001199296.1
Bcl3	CTG AAC CTG CCT ACT CAC CC	AGT ATT CGG TAG ACA GCG GC	NM_033601.3
Dio1	GGG CAG GAT CTG CTA CAA GG	CGT GTC TAG GTG GAG TGC AA	NM_007860.3
Fasn	TGC CCGAGT CAG AGA ACC TA	TAG AGC CCA GCC TTC CAT CT	NM_007988.3
Gapdh	CCT CGT CCC GTA GAC AAA ATG	TGA AGG GGT CGT TGA TGG C	NM_001289726.1
Gpam	TCG CCT CGG GCA ATA ATC TC	ATC TGG GGT TTC ATC GAG CC	NM_008149.3
Gpd2	CGA CTC CTA GAC GCC TTT CT	TGA GCA AAC GGA GAG AGT CC	NM_001145820.1
Hcn2	CCA GTC CCT GGA TTC GTC AC	TCA CAA TCT CCT CAC GCA GT	NM_008226.2

Hcn4	CAG CGT CAG AGC GGA TAC TT	CTT CTT GCC TAT GCG GTC CA	NM_001081192.1
Hprt	TGG GCT TAC CTC ACT GCT TT	TCA TCG CTA ATC ACG ACG CT	NM_013556.2
Kcnb1	TAC GGC GAT GTT GTT GGT CA	ATG CCC GTC ACT GTT CTG AG	NM_008420.4
Kcnd2	CTC CAC TAT CCA ACA GCC GA	TGC TGT GGT CAC GTA AGG TT	NM_019697.3
Kcne1	GCA GAG CCT CGA CCA TTT AGC	GCA GAA CAG TCG TGG AAT TGG	NM_008424.3
Kcnq1	ACT TCA CCG TCT TCC TCA TTG T	ACC AGA GGC GGA CCA CAT A	NM_008434.2
Me1	TAA GGG TCG TGC ATC TCT CAC	TGC AGC AAC TCC TAT GAG GG	NM_001198933.1
Myh6	CAG ACA GAG ATT TCT CCA ACC CA	GCC TCT AGG CGT TCC TTC TC	NM_010856.4
Myh7	CAC GTT TGA GAA TCC AAG GCT C	CTC CTT CTC AGA CTT CCG CA	NM_080728.2
Pdk4	TCT GAG GAT TAC TGA CCG CC	CAA AAC CAG CCA AAG GGG CA	NM_013743.2
Ppia	CTT GGG CCG CGT CTC CTT CG	GCG TGT AAA GTC ACC ACC CTG GC	NM_008907.7
Rpl13a	GGG CAG GTT CTG GTA TTG GA	GGG GTT GGT ATT CAAT CCG CT	NM_009438.5
Scd1	AAT ATC CTG GTT TCC CTG GGT G	GAA CTC AGA AGC CCA AAG CTC	NM_009127.4
Tbg	TGG GCA TGT GCT ATC ATC TTC A	GAG TGG CAT TTT GTT GGG GC	NM_177920.5
Thra	GAA AAG CAG CAT GTC AGG GTA	GGA TTG TGC GGC GAA AGA AG	NM_001313983.1
Thrb	GGA CAA GCA CCC ATC GTG AA	ACA TGG CAG CTC ACA AAA CAT	NM_001113417.1
Thrsp	GAG GTG ACG CGG AAA TAC CA	TGT CCA GGT CTC GGG TTG AT	NM_009381.2

In compliance with the MIQE guidelines for qRT-PCR (Bustin *et al.*, 2009), a set of three reference genes per tissue was used for accurate normalization and calculation (liver: *18S*, *Ppia*, *Rpl13a*; heart: *18S*, *Gapdh*, *Hprt1*). Ct values <35 were used for analysis and calculation of the fold change in gene expression by the efficiency corrected method (Pfaffl, 2001).

Microarray analyses

For microarray analyses, the *Affymetrix GeneChip* platform employing the *Express Kit* protocol for sample preparation and microarray hybridization was used. First, integrity of isolated mRNA (expressed as RNA integrity number, RIN) was determined with an *Agilent 2100 Bioanalyzer* (Agilent Technologies, Santa Clara, CA, USA). Only samples with a RIN ≥ 8 were used. Total RNA (200 ng) was converted into biotinylated cRNA, purified, fragmented and hybridized to *MG-430_2.0 microarrays* (Affymetrix, Santa Clara, CA, USA). The arrays were washed and stained according to the manufacturer's recommendation and finally scanned in *a GeneChip scanner 3000* (Affymetrix, Santa Clara, CA, USA).

Array images were processed using the *PartekGS* software (Robust Multi-Array algorithm, RMA algorithm). Differentially expressed probe sets were identified using the implemented ANOVA method and the step-up procedure to correct for multiple testing.

Immunoblot analysis

Whole protein lysates were generated from shock frozen liver tissue homogenized in RIPA buffer (150 mM NaCl, 50 mM Tris-HCl, 1% NP-40, 0.5% sodiumdesoxycholate, 0.1% sodiumdodecylsulfate, 2 mM EDTA, 50 mM NaF and *cOmplete-protease inhibitor cocktail*). Lysates were treated with an ultrasonic probe and afterwards incubated on ice with gentle agitation for 30 min. After 10 min of centrifugation at 17.000xg at 4 °C, supernatant was collected and the cell debris was discarded. Samples 20 µg/lane were separated by SDS-PAGE and transferred to a polyvinyl difluoride membrane (*Roti-Fluoro® PVDF*, Roth). After blocking with 5% milk in TBS-T (Tris-buffered saline with 150 mM NaCl, 0.5% Tween20 and pH 7.4), membranes were incubated for 16 h at 4 °C under gentle agitation with desired primary antibodies (table 3). Horseradish peroxidase-labeled secondary antibodies were used in an appropriate dilution for detection with *VersaDocMP4000* (BioRad). Band densities of desired proteins were determined with *Image Lab* software (BioRad) and normalized to intensity of Gapdh. For Scd1 the specific band at 37 kDa was used for quantification (Hashimoto *et al.*, 2013).

Thyroid function tests and analysis of serum parameters

Serum thyroid-stimulating hormone (TSH) concentration was measured with a sensitive, heterologous disequilibrium double-antibody precipitation RIA (Pohlenz *et al.*, 1999) (in cooperation with the Refetoff Lab at the University of Chicago). Results are expressed in mU/L. Serum concentrations of TT4, FT4 an FT3 were determined with ELISAs from DRG Instruments. Measurements were done according to the manufacturer´s instructions except that only the half of the recommended serum volume was used for analysis. TT3 were measured by RIA (DRG Instruments, Germany) (TT3 measurements were done in cooperation with the Köhrle group at the Charité Universitätsmedizin Berlin, within the SPP1629 consortium).

Triglyceride measurements in serum and liver tissue homogenates

30 µl of serum were used to measure TG on an *ADVIA2400 Chemistry System* (Siemens Healthcare, Germany). Therefore, serum samples were diluted with diluent up to 300 µl which were needed for a single measurement. 50 mg of shock frozen liver tissue was homogenized in 300 µl PBS with 1% Triton-X100. Lysates were boiled for 10 min at 95 °C and the supernatant was collected after 10 min of centrifugation at 17.000xg. Whole lysates were used for analysis of TG with *ADVIA2400*.

Oil-Red O staining of liver section

0.3 g of Oil-Red was dissolved in 100 ml isopropanol. 48 ml of that stock solution was filtered and diluted with 32 ml of H_2O_{milli}. Microscope slides with frozen sections of liver tissue were first washed with H_2O_{milli} and 50% EtOH before incubated in Oil-Red for 10 min at RT. After washing two times with H_2O_{milli} and 50% EtOH sections were counterstained with hematoxylin for 30 sec at RT. Slides were washed thoroughly with tap water and two times with H_2O_{milli} before covering with mounting medium (Immu-Mount, ThermoScientific) and coverslips.

Statistics and software

Statistics

One-way ANOVA with Tukey's *post hoc* test for statistical analysis for normally distributed data sets was used unless otherwise noted. Differences were considered significant when $P<0.05$. For gene expression data, statistical significance was calculated on log-transformed data (to obtain normal distribution) as recommended by the MIQE guidelines (Bustin *et al.*, 2009). Analysis and plotting were done with *GraphPad Prism6* (GraphPad Software, USA).

Primer design -software and conditions

Primers for mutagenesis PCR were designed with *SnapGene® Viewer 1.4* (GSL Biotech, USA). Mutagenesis primers were designed back-to-back with one primer carrying the desired point mutation which should be integrated. Primers used for

genotyping and qRT-PCR were designed via *Primer-BLAST* (NCBI, Bethesda, USA). If possible, primers should span exon-exon junctions, or at least being separated by an intron ≥1500 bp. The desired amplicon size was restricted to a range of 70-200 bp and the average melting temperature was set to 60 ±3 °C. Primers were designed to detect all physiological transcript variants.

Software used for graphical design

For graphical design and imaging *Microsoft PowerPoint*, *Adobe Photoshop* and *Mind-The-Graph* was used.

Results

The GS mutation abrogates canonical TR signaling *in vitro*

Canonical TR signaling consists of TR binding to TREs in regulatory regions of target genes and subsequent activation of gene expression. ChIP-seq (chromatin immunoprecipitation sequencing) analyses of mouse liver samples revealed a DR4 motif, a repeat of two 5'-AGGTCA-3' half-sites in the same orientation separated by 4 nucleotides, as the most prevalent TRE in T3 induced genes (Ayers *et al.*, 2014; Grontved *et al.*, 2015; Ramadoss *et al.*, 2014). Thus, this consensus DR4 TRE was used in a thyroid hormone-responsive luciferase reporter plasmid (DR4-TKLuc) to test the transcriptional activity of TRα71GS and TRβ125GS mutants *in vitro* in comparison to WT TRs (TRαWT and TRβWT). Empty vector (EV) and TR mutants TRβG354R and TRαG291R served as controls. These mutant TRs cannot bind T3 and cannot activate gene transcription after T3 treatment.

10 nM T3 increased luciferase activity more than 15-fold with WT TRα and TRβ, but not with empty vector or TRβG354R and TRαG291R (Figure 10 A and B). Luciferase activity was not increased by T3 through the TRα71GS and TRβ125GS mutants. Moreover, WT TRs without T3, as well as mutant TRs incapable of T3 binding, showed a reduction in basal luciferase activity. This dominant negative effect by apo-TR and mutant TR, was not present in $TR\alpha^{GS}$ and $TR\beta^{GS}$ transfected HEK293 cells. These data were confirmed by repeating the experiment using a common DR4-variant with an alternative 3'-half-site (AGGACA) (Figure 10 C and D).

Referring to Shibusawa *et al.,* this experiment was extended to two artificial TRE/GRE variants (AGGTAcaggAGATCA and AGGTCAcaggAGAACA, also referred to as TRE/GRE1 and TRE/GRE2, respectively). Again, transactivation by WT TRs and the complementary TR^{GS}-variants was tested with and without T3. Neither WT TRs nor the GS-variants could increase luciferase expression on a TRE/GRE1. Only WT TRs showed residual, but negligible transactivation on artificial TRE/GRE2 (Figure 10 C and D). In conclusion, these data demonstrate *in vitro* that the GS mutation in the DNA-binding domain abolishes the canonical TRE-mediated transcriptional activity of TRα and TRβ.

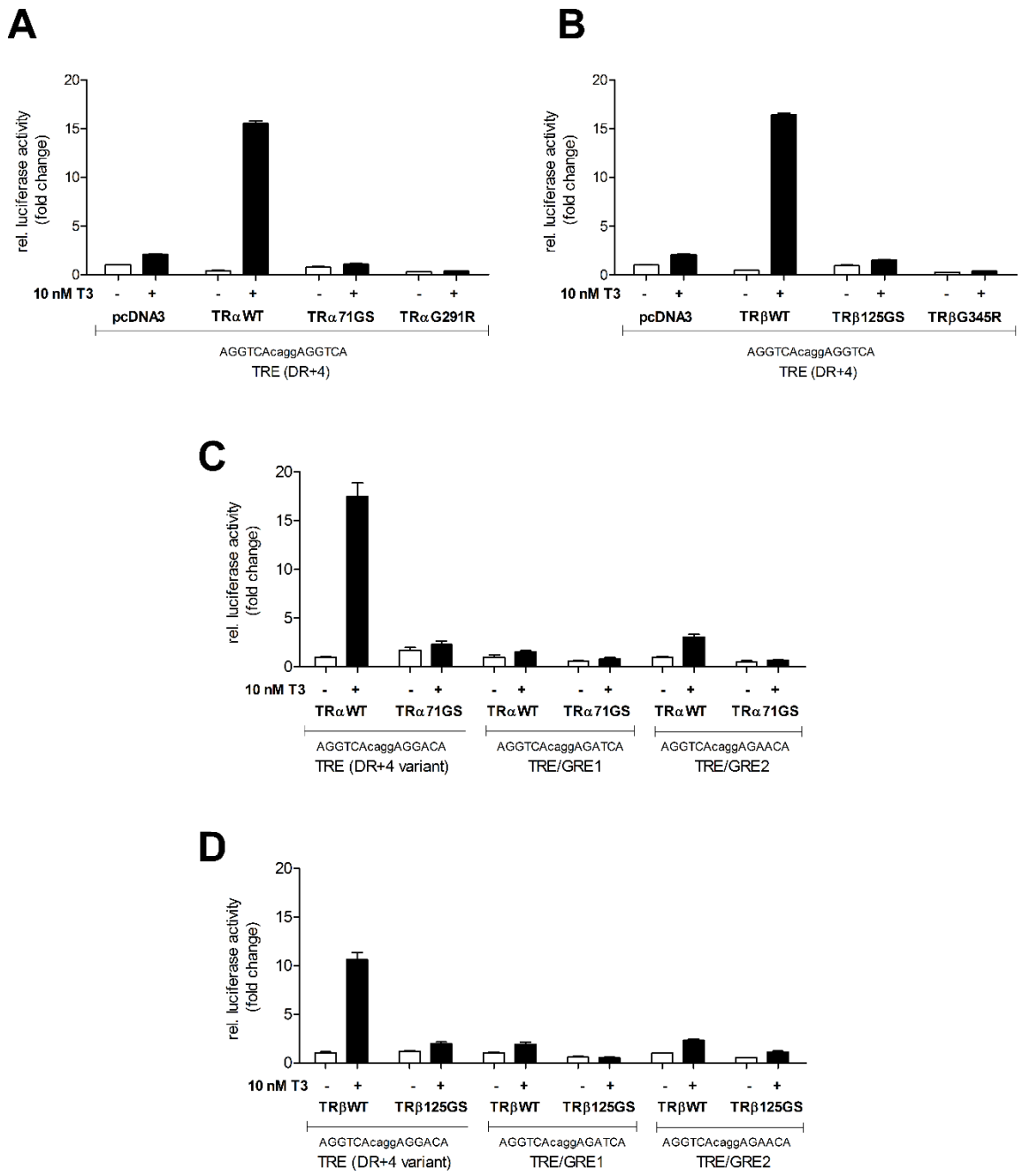

Figure 10: Luciferase reporter assay for detection of canonical TR action. *HEK293 cells were cultured in TH-depleted medium and transfected with plasmids encoding for WT TRα and TRβ and the corresponding GS-variants and the indicated DR4-luciferase reporter plasmids. TR mutants without T3 binding served as negative controls (TRαG291R and TRβG345R). Cells were treated with 10 nM T3 for 24 h (black bars) to induce luciferase expression via canonical TR/TRE-mediated action for TRα (**A** and **C**) and (**B** and **D**) TRβ-variants. Besides the most established DR4 half-site (AGGTCA; **A** and **B**) two artificial TRE/GRE hybrid sequences and a DR4-variant were tested for transactivation by WT TRs and the complementary GS-variants (**C** and **D**).*

TRα$^{GS/GS}$ and TRβ$^{GS/GS}$ mice are viable

For generation of the TRα^{GS} and TRβ^{GS} mouse models to study non-canonical TR action *in vivo*, ZFN technology was used to introduce the desired mutations into the murine WT *Thra* and *Thrb* gene loci, respectively. Offspring were screened by RFLP-PCR and sequencing, which confirmed the successful knock-in of the GS mutation in TRα$^{GS/+}$ and TRβ$^{GS/+}$ mice. One pup out of 29 for TRα$^{GS/+}$ and one out of 39 for TRβ$^{GS/+}$ was positive for the targeted integration, which equals a mutation rate of 3.5% and 2.6%, respectively (Figure 11; similar data for *Thra* are not shown).

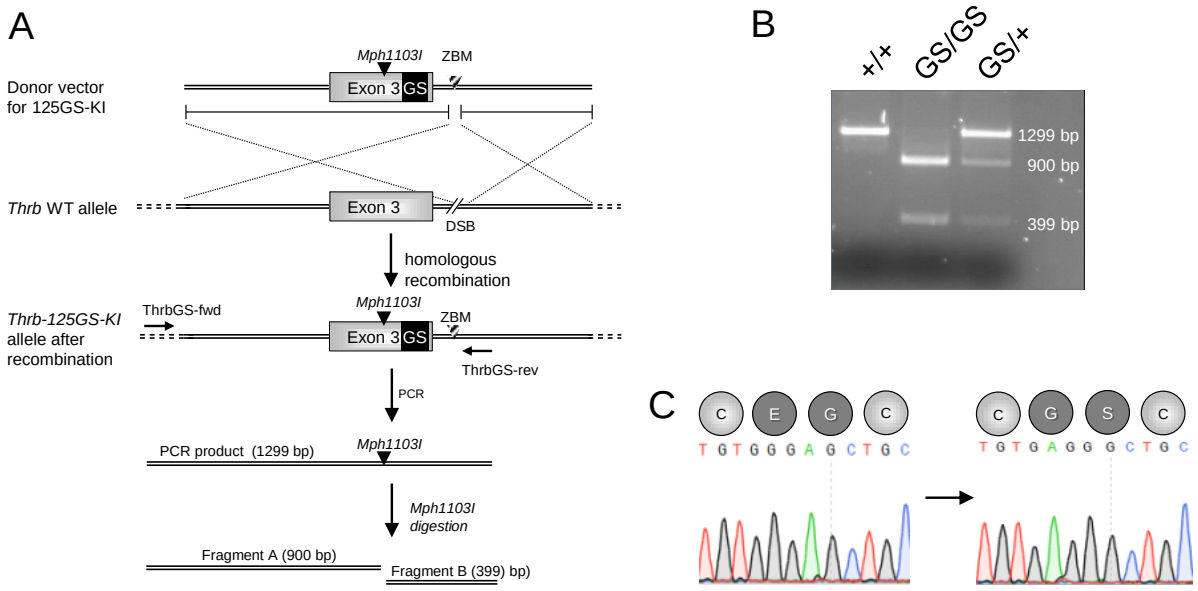

Figure 11: Generation of TRβ^{GS} knock-in mice by zinc finger nuclease technology. *(**A**) A donor vector (DV) bearing the desired point mutations and zinc finger nuclease (ZFN) mRNA were microinjected into the pronucleus of an oocyte. A zinc finger binding mutation (ZMB) was introduced into the DV sequence to protect it from ZFN. The genomic WT allele was cut by ZFN and the double strand break (DSB) was repaired via homologous recombination using the DV sequence as a template. In addition to the point mutations generating the amino acid exchange from EG to GS, a silent mutation was introduced to generate an Mph1103I restriction site for genotyping by restriction fragment length polymorphism PCR (RFLP-PCR). For identification of positive founder animals, RFLP-PCR using a forward primer (ThrbGS-fwd), which binds to a sequence of the Thrb gene outside the left homologous sequence of the DV, and a reverse primer (ThrbGS-rev) located downstream of exon 3 was performed. (**B**) Restriction digestion of the PCR product determined homo- and heterozygosity for the mutated allele. (**C**) Integration of GS mutation was confirmed by sequencing. TRα^{GS} mice were generated in parallel using the same techniques.*

Litter size and genotype distribution were monitored to exclude embryonic lethality of GS-mutation. For the TRα^{GS} mouse strain the mean litter size of heterozygous breeding pairs was 5-6, whereas the mean litter size for the TRβ^{GS} mouse strain was

7-8. Recording of genotype distribution revealed that mutant mice are born in Mendelian proportions and are viable (Table 10 and 11). No negative effect on fertility was observed among breeding animals up to the age of eight months.

Table 10: List of genotype distribution for TRα^{GS} strain

		Genotype		
	total	*TRα$^{+/+}$*	*TRα$^{+/GS}$*	*TRα$^{GS/GS}$*
Male:	73	17	40	16
	(50.0%)	*(23.3%)*	*(54.8%)*	*(21.9%)*
Female:	73	19	37	17
	(50.0%)	*(26.0%)*	*(50.7%)*	*(23.3%)*
Σ:	146	36	77	33
	100%	*24.7%*	*52.7%*	*22.6%*

Table 11: List of genotype distribution for TRβ^{GS} strain

		Genotype		
	total	*TRβ$^{+/+}$*	*TRβ$^{+/GS}$*	*TRβ$^{GS/GS}$*
Male:	86	23	40	23
	(51.2%)	*(26.7%)*	*(46.5%)*	*(26.7%)*
Female:	82	20	45	17
	(48.8%)	*(24.4%)*	*(54.9%)*	*(20.7%)*
Σ:	168	43	85	40
	(100%)	*(25.6%)*	*(50.6%)*	*(23.8%)*

Introduction of GS-mutations does not alter TRα and TRβ expression

For determining the expression of known TH responsive genes in TRα$^{GS/GS}$ and TRβ$^{GS/GS}$ mice in comparison to WT and the respective TR^{KO} mice (TRα$^{0/0}$ and TRβ$^{-/-}$ mice) qRT-PCR was performed. TRα is predominantly expressed in heart and TRβ in liver, thus these two tissues were studied. First, expression of TRα and TRβ was determined to ensure that the introduced GS-mutation does not alter systemic expression of the receptors. qRT-PCR analysis revealed equal expression of WT and mutated receptors for TRα, as well as for TRβ (Figure 12, A and B). Additionally, KO of the receptors in TRα$^{0/0}$ and TRβ$^{-/-}$ mice was confirmed. In hearts of TRα$^{GS/GS}$ mice, expression of the two TH target genes *Myh6* and *Myh7* was comparable to that in

TRα$^{0/0}$ mice and both differed significantly from expression in WT mice (Figure 11, middle and right panel). Of note, there was also a significant difference in expression of *Myh7* between TRα$^{0/0}$ and TRα$^{GS/GS}$ mice.

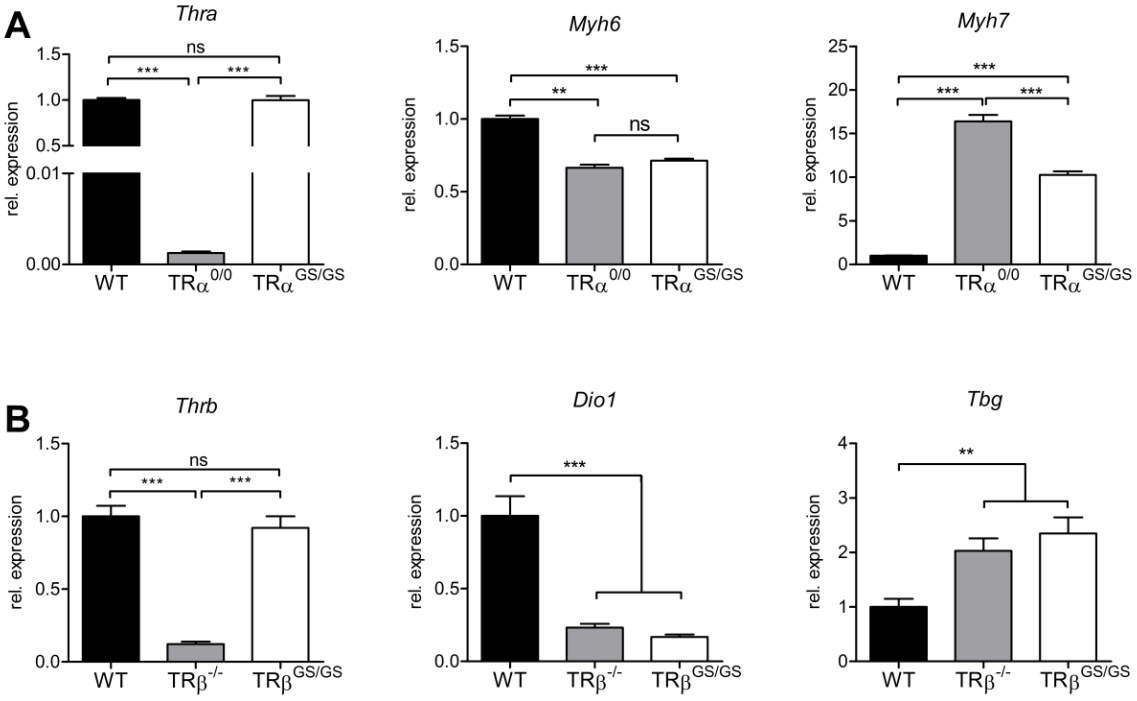

Figure 12: Gene expression analysis revealed loss of canonical action for GS-mutants. *qRT-PCR analysis of heart (**A**) and liver (**B**) tissue of untreated mice confirmed equal expression of TRs bearing the GS-mutation and WT TRs (**A** and **B**; left panel). Expression of Myh6 and Myh7, two known TH target genes in heart, was altered in TRα$^{0/0}$ (grey bar) and TRα$^{GS/GS}$ (open bar) mice in comparison to WT (black bar) hearts (**A**; middle and right panel). (**B**) Similar results were obtained for expression of Dio1 and Tbg in livers of TRβ$^{-/-}$ (grey bar) and TRβ$^{GS/GS}$ (open bar). (n=6; mean ± SEM; ANOVA and Tukey's post hoc test; ns=not significant, **P<0.01, ***P<0.01)*

For TRβ, similar results were obtained for TH target genes *Dio1* and *Tbg* in liver (Figure 12, B middle and right panel). Expression of both genes were significantly altered in TRβ$^{-/-}$ and TRβ$^{GS/GS}$ mice in comparison to WT. These data suggest that the GS-mutation in the DBD of TRα, as well as in TRβ abrogates canonical TH/TR action *in vivo.*

T3 response of known TH target genes is abolished by GS-mutation

It is well known that TRβ$^{-/-}$ and TRβ$^{GS/GS}$ mice have elevated TH serum concentration due to disrupted negative feedback regulation of the HPT axis. Hence, serum TH concentrations are expected to differ significantly from their WT littermates. For generating a suitable initial basis for comparison of the genotypes, different basal TH concentrations in WT, TRβ$^{GS/GS}$ and TRβ$^{-/-}$ mice had to be mitigated. Therefore, TH-induced gene expression was determined in hypothyroid animals without and with T3 treatment for five consecutive days. ELISA measurements confirmed successful induction of hypothyroidism with dramatically reduced TT4 concentration in all genotypes, while FT3 concentrations were only slightly decreased (Figure13).

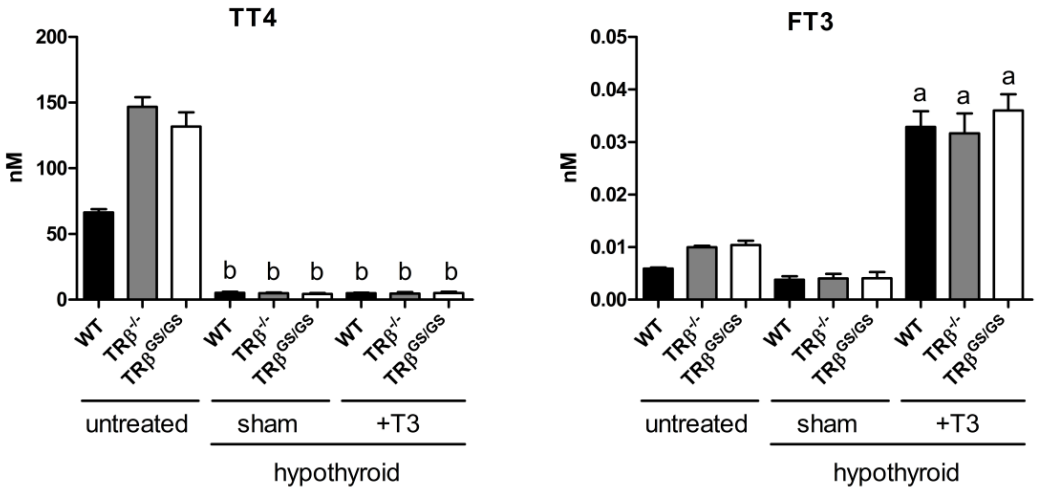

Figure 13: TH serum concentrations after induction of hypothyroidism and T3 treatment. *Systemic differences in TH concentration found in WT, TRβ$^{-/-}$ and TRβ$^{GS/GS}$ mice (untreated) was mitigated by induction of hypothyroidism. Hypothyroidism was induced through administration of methimazole and perchlorate via the drinking water and feeding a low-iodine-diet for 3 weeks. After 3 weeks of treatment, mice received daily i.p. injection of 5 µg/100 g BW T3 for 5 consecutive days (+T3) or were sham treated by i.p. injection of solvent (sham). (b=below detection limit of assay; a=above upper detection limit of assay, extrapolated values)*

Injection of 5 µg/100 g BW T3 resulted in a strong increase in FT3 serum concentration, whereas TT4 concentrations were unaffected. These data successfully confirmed pharmacological induction of hypothyroidism and T3 treatment.

In livers of hypothyroid WT mice, T3 induced expression of the TH target genes *Dio1*, *Thrsp*, *Me1* and *Bcl3* mRNAs. This induction was absent to the same extent in TRβ$^{-/-}$ mice as wells as in TRβ$^{GS/GS}$ mice (Figure 14). These results indicate that the GS-

mutation eliminates canonical TH/TR mediated gene expression in the same manner like a global TR^{KO}.

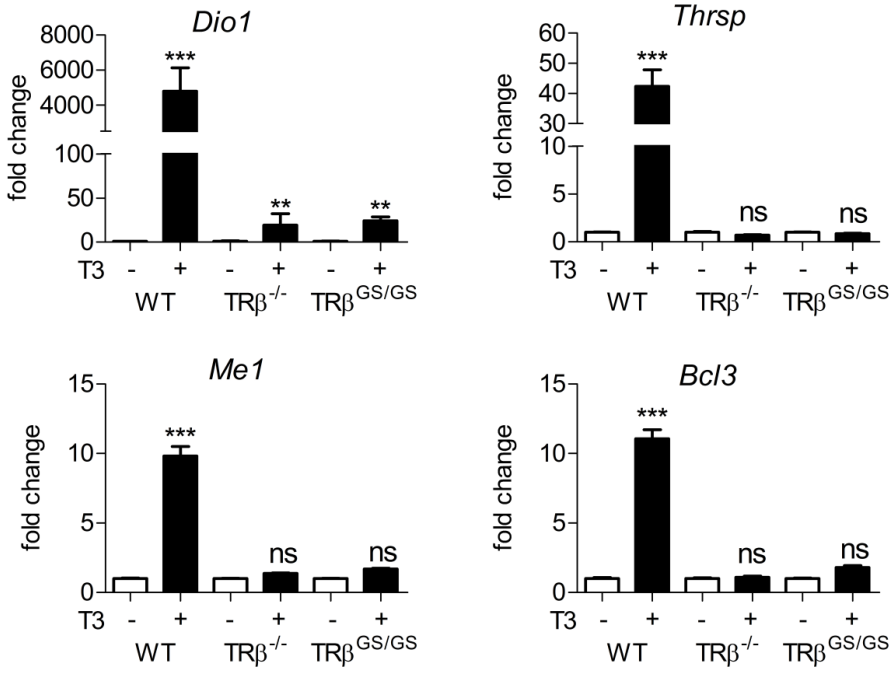

Figure 14: Response of TH target genes to T3 in livers of hypothyroid WT, TRβ$^{-/-}$ and TRβ$^{GS/GS}$ mice. *Mice were rendered hypothyroid and either injected with vehicle (open bars) or with 5 µg/100 g BW T3 (black bars) for 4 consecutive days. qRT-PCR analysis revealed loss of TH/TRβ-mediated gene expression of Dio1, Thrsp, Me1 and Bcl3 in TRβ$^{-/-}$ and TRβ$^{GS/GS}$ mice (n=6; mean ± SEM; ANOVA and Tukey's post hoc test; **P<0.01, ***P<0.001, ns=not significant).*

Microarray analysis revealed loss of canonical action on a genome-wide scale

The broad set of TH target genes also includes genes which encode for other transcription factors and cofactors (Dugas, Ibrahim, & Barres, 2012). These transcription factors and cofactors can also regulate expression of certain genes. In relation to a T3 stimulus these indirectly regulated genes are called secondary target genes. Secondary effects might mask primary TH/TR induced gene expression, which in turn makes it impossible to distinguish whether the affected gene was directly or indirectly induced by TR. Besides pharmacological inhibition of secondary effects (via cycloheximide, which has high toxic adverse effects and therefore only accounts for cell culture experiments), a reduction in time after T3 stimulation can be a compromise (Picou, Fauquier, Chatonnet, Richard, & Flamant, 2014). Studying TH/TR gene expression kinetics over a period of 16 h should reveal an optimal time

point for measuring principal primary TH/TR regulated gene expression. Hypothyroid WT mice received a single injection of T3 and were sacrificed after 2, 4, 8 and 16 hour of injection. For known TH target genes like *Dio1*, *Thrsp* and *Bcl3* induction of gene expression was significantly increased within the first two hours, reaching a maximal expression between 4 and 8 hours (Figure 15, A).

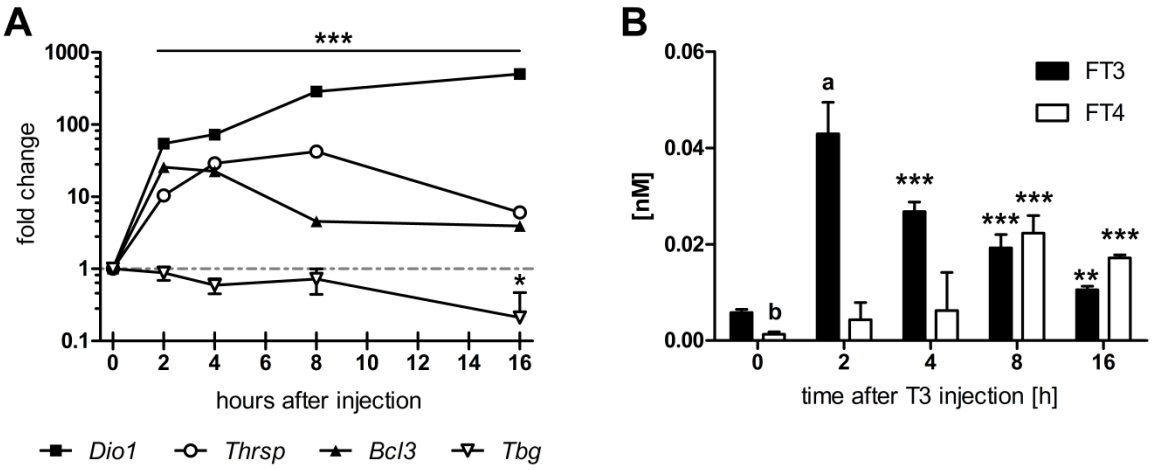

Figure 15: Kinetic of TH-induced hepatic gene expression and free TH concentration. *Hypothyroid WT mice were i.p. injected with 5 µg /100 g BW T3. (**A**) TH target gene expression was measured via qRT-PCR at 2, 4, 8 and 16 h after injection. An increased expression of Dio1, Thrsp and Bcl3 was detected 2 h after injection. Decreased expression of Tbg was observed 16 h after T3 administration. (**B**) Determination of free T3 (FT3; black bar) and free T4 (FT4; open bar) concentration in sera of mice revealed a 7-fold increase of FT3 2 h after injection. A delayed but severe increase in FT4 concentration was detected 8 h after injection. (n=3; mean ± SEM; t-test test; *P<0.05, **P<0.01, ***P<0.001; a=above upper detection limit, b=below lower detection limit)*

Hence, for further experiments 6 hours were chosen to study directly TH/TR induced gene expression. Due to the fact that a significant repression of thyroxin binding globulin (*Tbg*) was only observed after 16 hours, a time point of 6 hours would not allow detection of negatively regulated genes that are directly affected by TRs but the risk to detect secondarily induced genes will be diminished. Interestingly, FT3 and FT4 measurements revealed and 17-fold increase in FT4 serum concentration 8 hours after i.p. injection of T3 (Figure 15, B).

Investigating the expression of a small set of known TH target genes, as described above, is not sufficient to show that canonical TR action on TRE-mediated gene expression is abrogated globally, as it is likely that that not all TRE-variants are covered by this study. In other words, this study lacks proving, whether the TR^{GS} mutants possess residual transcriptional activity on other known TH target genes. Moreover, off-target effects caused by the DBD mutation can only be excluded by

studying gene expression on a genome-wide scale. Therefore, gene expression was studied using microarray analysis of mRNA from liver tissue. Hypothyroid WT, TRβ$^{-/-}$ and TRβ$^{GS/GS}$ mice were treated with an acute single dose of T3 (20 µg/100 g BW) and gene expression was measured after 6 hours by microarray analysis (in cooperation with the BioChip Lab of the University Hospital Essen). Figure 16A shows the results in a dendrogram and a heat map with mice grouped not by genotype, but clustered by similarity of their gene expression patterns. WT mice were clearly different from TRβ$^{-/-}$ and TRβ$^{GS/GS}$ mice and form their own branch in the hypothyroid and T3-treatment groups. Importantly, TRβ$^{-/-}$ and TRβ$^{GS/GS}$ mice were grouped together, indicating the similarity of their gene expression patterns.

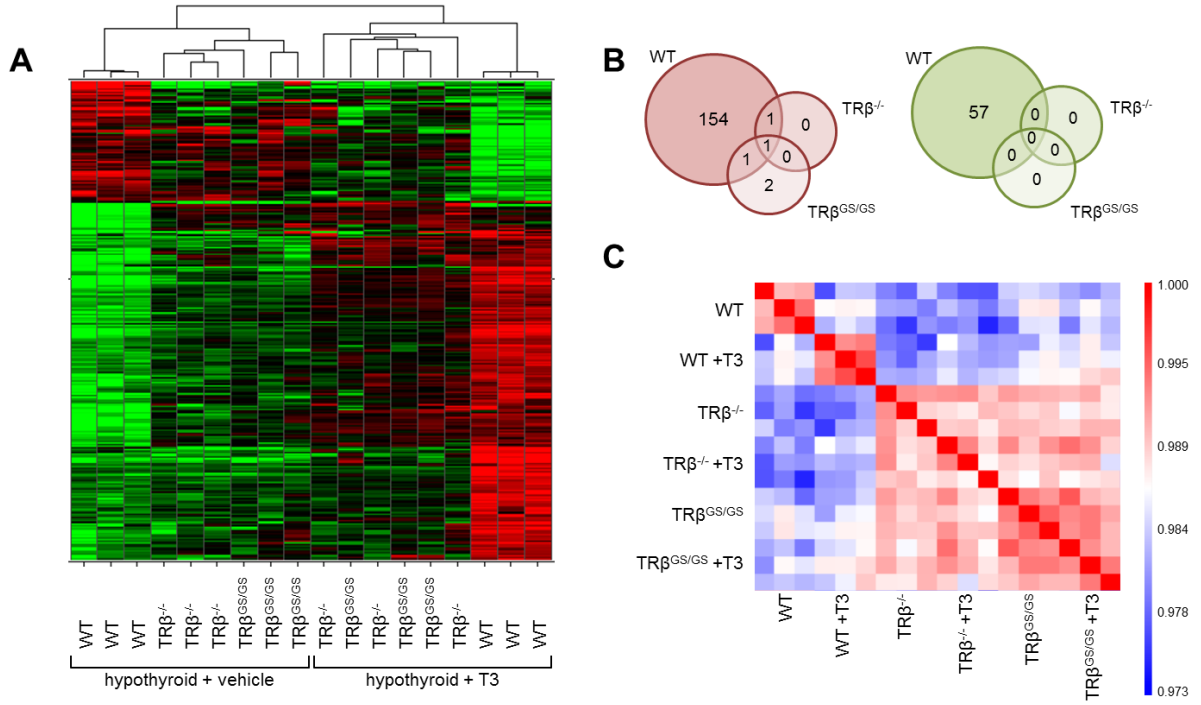

Figure 16: Microarray analysis confirmed genome-wide loss of TRE-mediated transcriptional activity via integrated GS-mutation. *(**A**) Hierarchical clustering of gene expression data (including 302 probe sets; ANOVA, FDR<0.01) from livers of hypothyroid WT, TRβ$^{-/-}$ and TRβ$^{GS/GS}$ mice were treated either with 20 µg/100 g BW T3 or with vehicle (PBS) for 6 h. The signal was log$_{10}$-transformed and a color gradient from green (0.5-fold of mean signal) to red (2-fold of mean signal) was used to visualize changes in expression in a heat map (n=3). (**B**) Venn diagrams for overlap analysis of differentially expressed probe sets (upregulated probe sets, red; fold change > 2 and down regulated probe sets, green; fold change < 0.5; ANOVA, FDR<0.05). (**C**) Pearson´s correlation of the signal between the different groups (high correlation, red = 1.000, low correlation, blue = 0.973). (In cooperation with the BioChip Lab of the University Hospital Essen)*

In fact, the gene expression pattern of T3-treated TRβ$^{-/-}$ and TRβ$^{GS/GS}$ mice was not distinguished by genotype. This is also demonstrated by a comparison of differentially regulated gene expression in the three genotypes, showing that the

TRβ^{GS}-variant possesses no significant residual transcriptional activity and also does not acquire a new set of target genes (Figure 16, B). The GS-mutation abolishes TRE-mediated transcriptional function of TR *in vivo*.

Loss of DNA-binding ability of TRβ disrupts hypothalamic-pituitary-thyroid axis

Thyroid hormone production and secretion is regulated by the negative feedback loop of the HPT axis. Inhibition of TSH is mediated by TRβ (Abel, Ahima, Boers, Elmquist, & Wondisford, 2001; Forrest, Erway, *et al.*, 1996; Weiss *et al.*, 1997) and had been shown to depend on DNA binding of TRβ (Shibusawa, Hashimoto, *et al.*, 2003). In accordance with these reports, basal serum TSH was significantly higher in TRβ$^{-/-}$ and in TRβ$^{GS/GS}$ mice compared to WT mice (Figure 17, A). As a consequence of elevated TSH, T3 and T4 concentrations were also significantly higher in TRβ$^{-/-}$ and TRβ$^{GS/GS}$ mice compared to WT mice (Figure 17, B and C). The combination of elevated circulating TH concentrations and elevated TSH demonstrates central resistance to thyroid hormone due to the lack of the receptor in TRβ$^{-/-}$ mice and, more importantly, also lack of canonical TRβ action in the HPT axis of TRβ$^{GS/GS}$ mice. TSH, TT4 and TT3 concentrations in TRα$^{0/0}$ mice and TRα$^{GS/GS}$ mice were not different from those in WT mice.

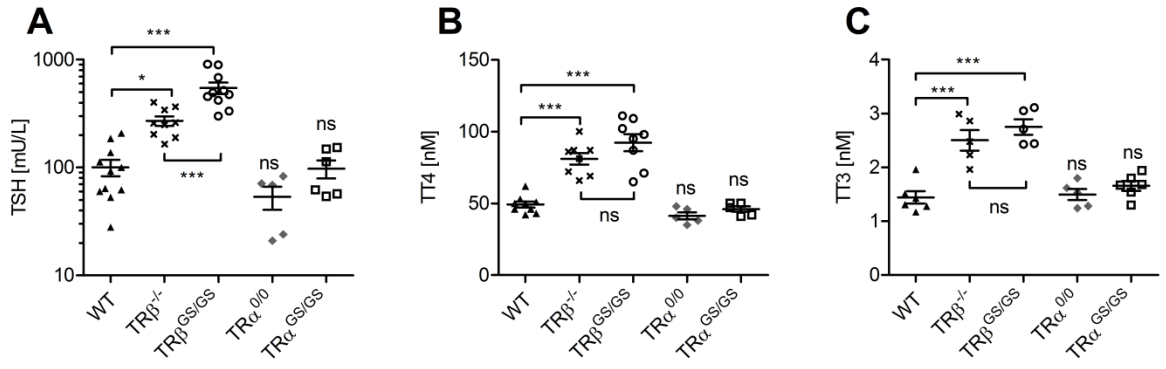

Figure 17: Loss of DNA-binding ability of TRβ disrupts negative feedback loop of HPT axis. *(**A**-**C**) TSH, TT4 and TT3 in serum of 15-week old WT (▲; n=11) TRβ$^{-/-}$ (**x**; n=9), TRβ$^{GS/GS}$ (○; n=10), TRα$^{0/0}$(◆; n=5) and TRα$^{GS/GS}$ (□; n=6) male mice (mean ± SEM; ANOVA and Tukey's post hoc test; *P<0.05, ***P<0.001, ns = not significant) (TSH was measured in cooperation with the Refetoff´s Lab in Chicago and TT3 was determined in cooperation with the Köhrle group in Berlin)*

Because of the increased TSH serum concentration it is quite likely that thyroid morphology is affected. Thus, cross sections of thyroids from 15-week-old male WT,

TRβ$^{-/-}$ and TRβ$^{GS/GS}$ mice were stained with hematoxylin and eosin and analyzes microscopically (Figure 18, A). Thyroids of TRβ$^{-/-}$ and TRβ$^{GS/GS}$ mice were significantly enlarged in comparison to WT thyroids. This enlargement was statistically confirmed by measuring the mean lobe area of serial transverse sections (Figure 18, B).

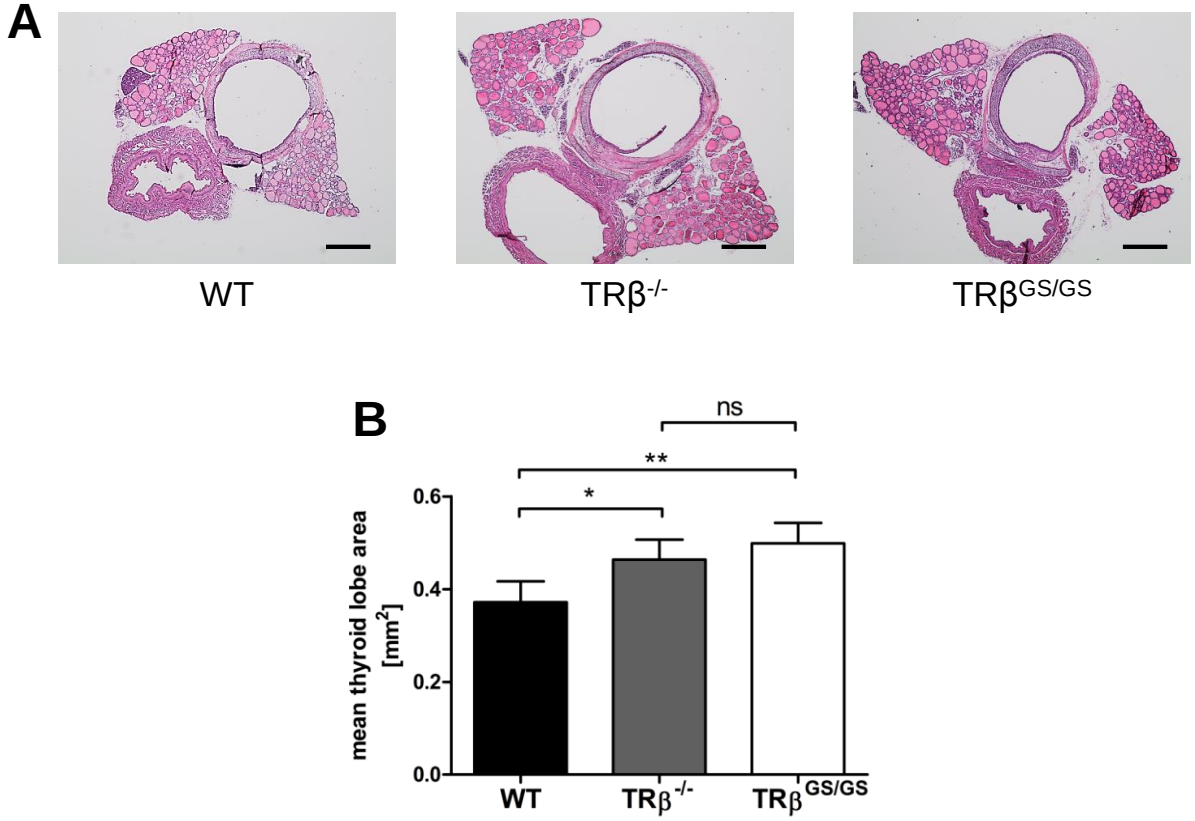

Figure 18: Microscopic thyroid morphology and lobe size. *(**A**) Transverse sections of thyroids from WT, TRβ$^{-/-}$ and TRβ$^{GS/GS}$ mice stained with hematoxylin and eosin (black bar=200 µm). (**B**) Mean thyroid lobe size was determined by measuring the lobe area of a series of transverse sections. (n=5; mean ± SD; ANOVA and Tukey's post hoc test; *P<0.05, **P<0.01, ns=not significant)*

Linear growth and gain of body weight is canonically mediated via TRα

Growth is one of the most prominent physiological effects regulated by TH. Thyroid dysfunction, as well as loss-of-function mutations in TRα can lead to a severe growth phenotype (Bochukova *et al.*, 2012; Moran & Chatterjee, 2015; van Mullem *et al.*, 2013). Therefore, linear growth of mice from all genotypes WT, TRα$^{0/0}$, TRα$^{GS/GS}$, as well as the complementary TRβ genotypes, TRβ$^{-/-}$ and TRβ$^{GS/GS}$, was monitored from *postnatal* day 21 to 70 by measuring tail length. Additionally, gain of body weight was studied by weighting mice once a week. There were no differences in linear growth

and gain of body weight detectable between WT and the TRβ mutants (Figure 19, A). However, TRα$^{0/0}$ and TRα$^{GS/GS}$ mice had a delayed linear growth with significant differences regarding tail length from day 21 to 56 (Figure 19, B and C). Gain of body weight was also affected in TRα$^{0/0}$ and TRα$^{GS/GS}$ mice. Consequently, linear growth and gain of body weight during early *postnatal* stages seem to be mediated by canonical action of TRα.

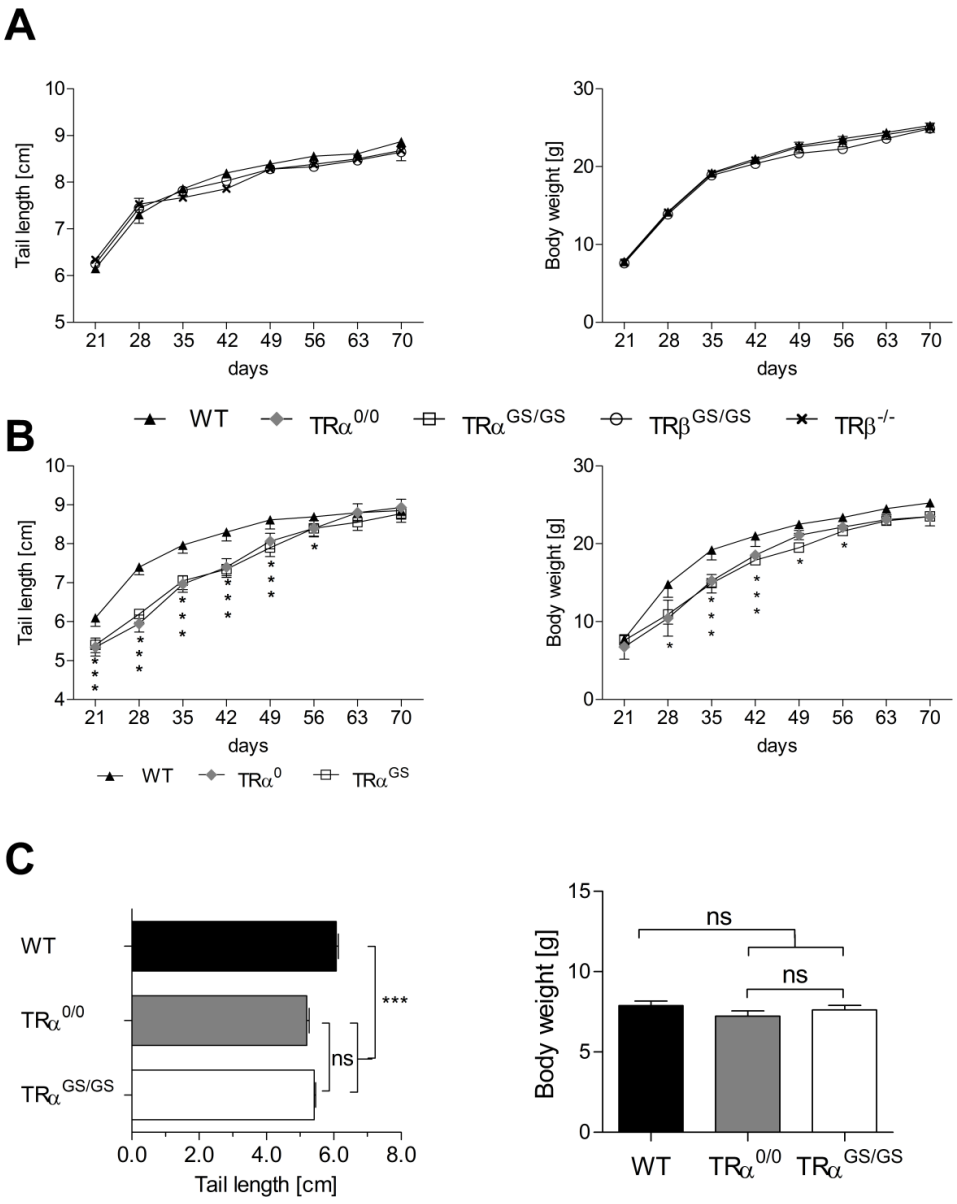

Figure 19: Monitoring of linear growth and gain of body weight. *(**A**) Tail length and body weight of WT, TRβ$^{-/-}$ and TRβ$^{GS/GS}$ mice between postnatal day 21 and 70. (**B**) Progression of linear growth and gain of body weight of WT, TRα$^{0/0}$ and TRα$^{GS/GS}$ mice from day 21 to 70. (**C**) Tail length measurements revealed an early delay in linear growth of TRα$^{0/0}$ and TRα$^{GS/GS}$ mice, while body weight was unaffected. (n=5-7; mean ± SEM; ANOVA and Tukey's post hoc test; *P<0.05, ***P<0.001, ns=not significant)*

Skeletal development requires canonical TH/TRα signaling

The difference in linear growth of TRα$^{0/0}$ and TRα$^{GS/GS}$ mice, detected between P21 and P56, might be a result of bone dysgenesis caused by a loss of canonical TRα action (Bassett *et al.*, 2010; Bassett *et al.*, 2014). To investigate the underlying cause, skeletal analysis of juvenile WT, TRα$^{0/0}$ and TRα$^{GS/GS}$ mice was performed after weaning at *postnatal* day 21 (in cooperation with the group of Williams and Bassett in London).

X-ray microradiography of femurs and caudal vertebrae (Figure 20) revealed a similar decrease in bone length and vertebral height in both TRα$^{GS/GS}$ and TRα$^{0/0}$ mice in comparison to WT littermates. These significant differences correlate with genotype-specific differences in tail length, previously described (Figure 19, B and C).

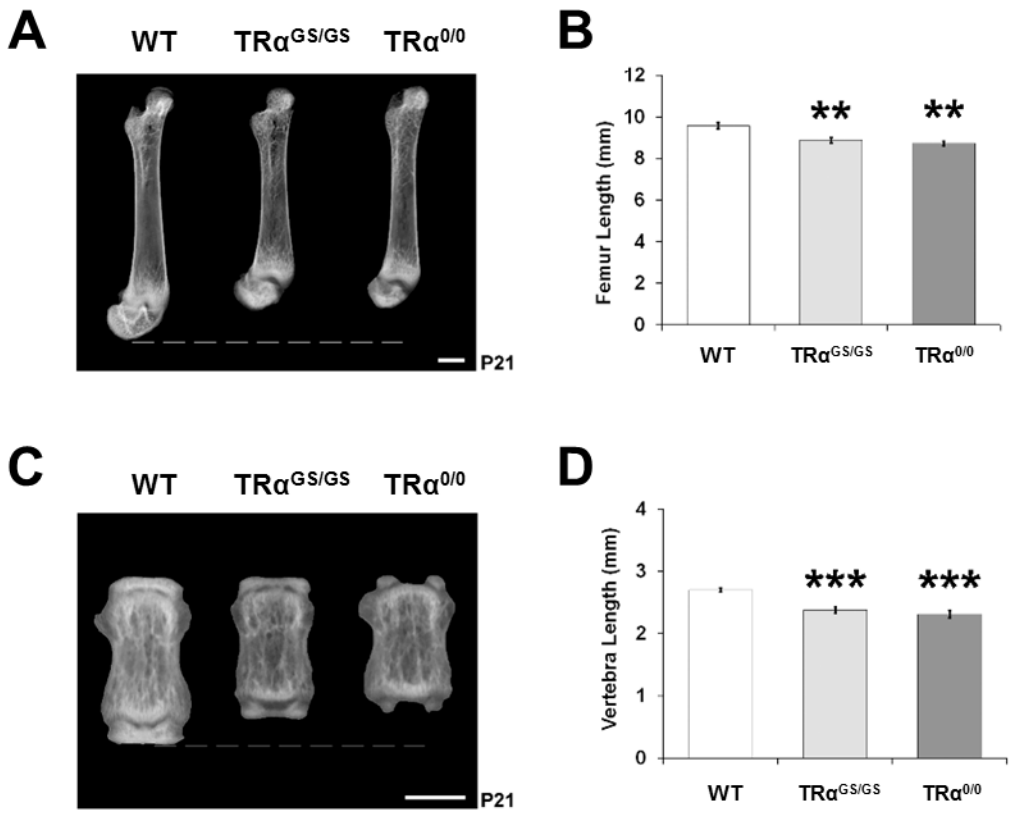

Figure 20: X-ray microradiography of femurs and caudal vertebrae from P21 TRα mutant mice. *Representative grey scale images of femurs from P21 WT (n=5), TRα$^{GS/GS}$ (n=5) and TRα$^{0/0}$ (n=3) mice (Bar=1000 µm) reveal differences in longitudinal growth for femurs (**A**), as well as caudal vertebrae (**C**) of TRα$^{GS/GS}$ and TRα$^{0/0}$ mice. Graph (**B**) displays femur length of WT (open column) TRα$^{GS/GS}$ (light gray) and TRα$^{0/0}$ (dark gray) mice. (**D**) Plot of caudal vertebra length in WT, TRα$^{GS/GS}$ and TRα$^{0/0}$ mice. (mean ± SEM; ANOVA and Tukey's post hoc test; **P<0.01, ***P<0.001). (In cooperation with the group of Williams and Bassett in London)*

Pseudocolored X-ray images of femurs and vertebrae allow investigation of bone mineral content (Figure 21). Femurs of juvenile P21 old WT, TRα$^{GS/GS}$ and TRα$^{0/0}$ mice showed no alterations in mineral content. However, analysis of vertebrae demonstrated a significantly reduced mineral content for TRα$^{0/0}$ and TRα$^{GS/GS}$ mice.

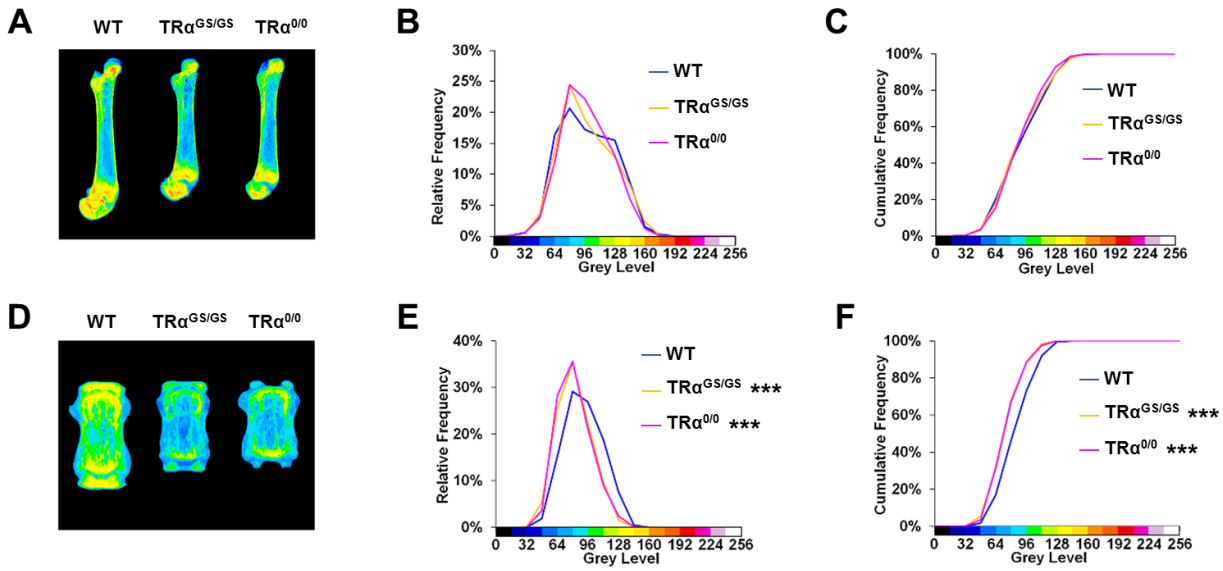

Figure 21: Pseudocolored X-ray microradiography of femurs and vertebrae from P21 TRα mutant mice. *Representative X-ray images of femurs (**A**) and caudal vertebrae (**D**) were pseudocolored according to a 16-colour palette in which low mineral content is blue and high mineral content is red. Relative (**B** and **E**) and cumulative frequency (**C** and **F**) histograms display bone mineral content of femurs and vertebrae from TRα$^{GS/GS}$ (yellow curve; n=5) and TRα$^{0/0}$ mice (pink curve; n=3) vs WT mice (blue curve; n=5). Significant differences in bone mineral content was only found for vertebrae of TRα$^{GS/GS}$ and TRα$^{0/0}$ mice in comparison to WT mice (Kolmogorov-Smirnov test, ***P<0.001). (In cooperation with the group of Williams and Bassett in London)*

Long bones like femur and tibia are formed by endochondral ossification. Longitudinal bone growth takes place in the epiphyseal growth plate. The highly complex process of endochondral bone formation requires chondrocyte maturation, proliferation and apoptosis to form a cartilage scaffold, which is used by osteoblast to form new bone (Hunziker, 1994; Robson, Siebler, Stevens, Shalet, & Williams, 2000). Determining, whether the underlying TH-dependent mechanism in endochondral ossification are related to canonical TRα signaling, the proximal tibia growth plates of WT and TRα-mutant mice were histologically analyzed. Analysis of the growth plates revealed a delay in endochondral ossification similarly affecting both TRα$^{GS/GS}$ and TRα$^{0/0}$ mice (Figure 22). This delay comprised a decrease in the size of the secondary ossification center (Figure 22, A). While the proliferation zone width (PZ) remained constant within the three genotypes, an increase in the reserve zone (RZ) width and a decrease in the hypertrophic zone (HZ) width were

determined (Figure 22, B, C and D). These findings display a phenotypic accordance between TRα$^{GS/GS}$ and TRα$^{0/0}$ mice related to epiphyseal dysgenesis with alterations in endochondral ossification processes at the growth plate. Thus, it suggests that canonical action of TRα is essential for these processes.

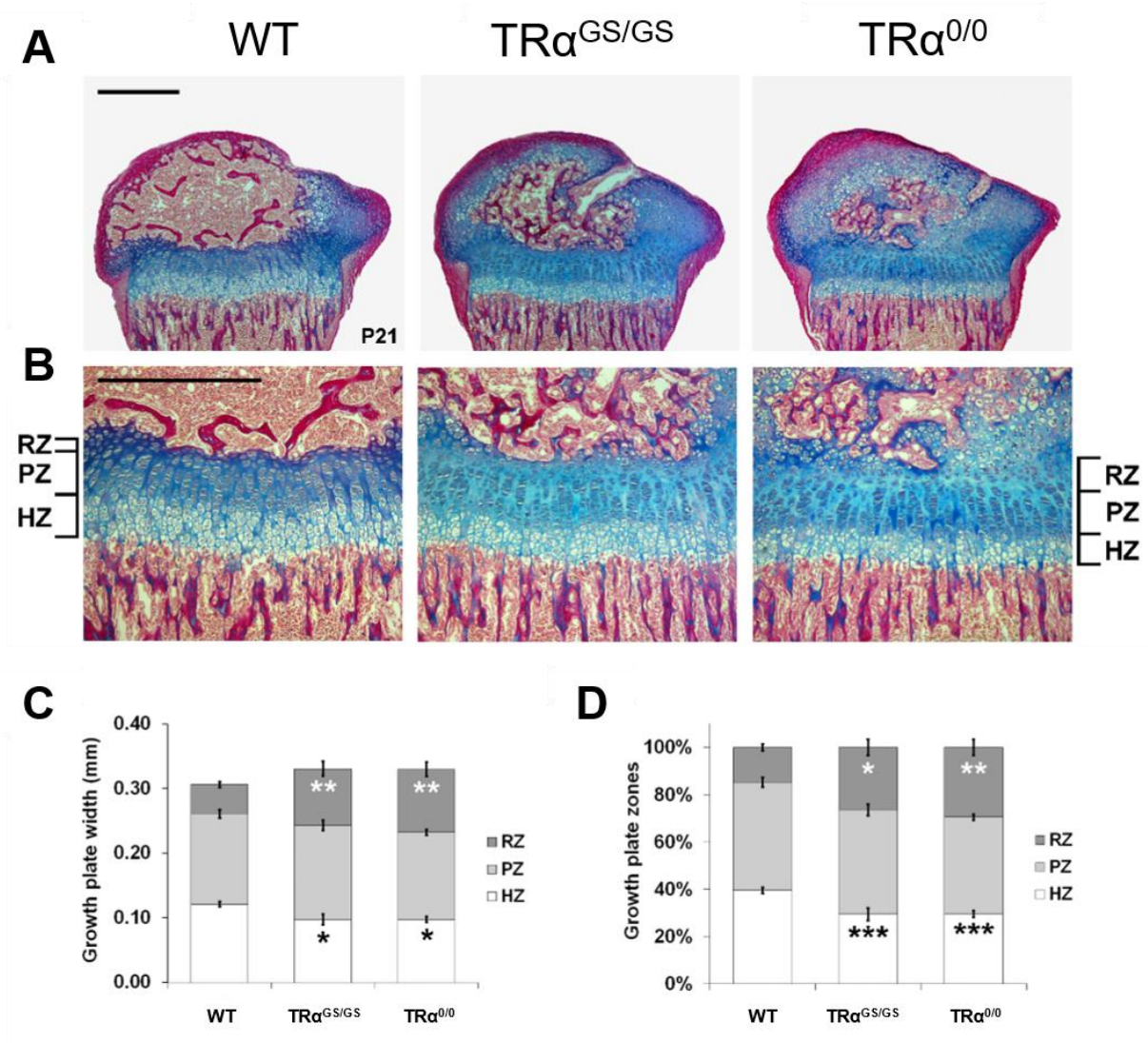

Figure 22: Histological analysis of proximal tibia growth plates. *Proximal tibia growth plate sections stained with alcian blue (cartilage) and van Gieson (bone) (magnification ×50 (**A**) and ×100 (**B**); Bars=500 µm; RZ, reserve zone; PZ, proliferative zone; HZ, hypertrophic zone). Growth plate chondrocyte zone measurements (**C**) and relative proportions corrected for total growth plate height (**D**) are shown for WT (n=5), TRα$^{GS/GS}$ (n=5) and TRα$^{0/0}$ (n=3) (mean ± SEM; ANOVA and Tukey's post hoc test; *P<0.05; **P<0.01; ***P<0.001). (In cooperation with the group of Williams and Bassett in London)*

Long bone architecture was studied via high resolution micro-CT. Images of femur midline sections demonstrated epiphyseal dysgenesis, increased trabecular bone mass and reduced metaphyseal inwaisting consistent with a bone modelling defect and delayed endochondral ossification (Figure 23).

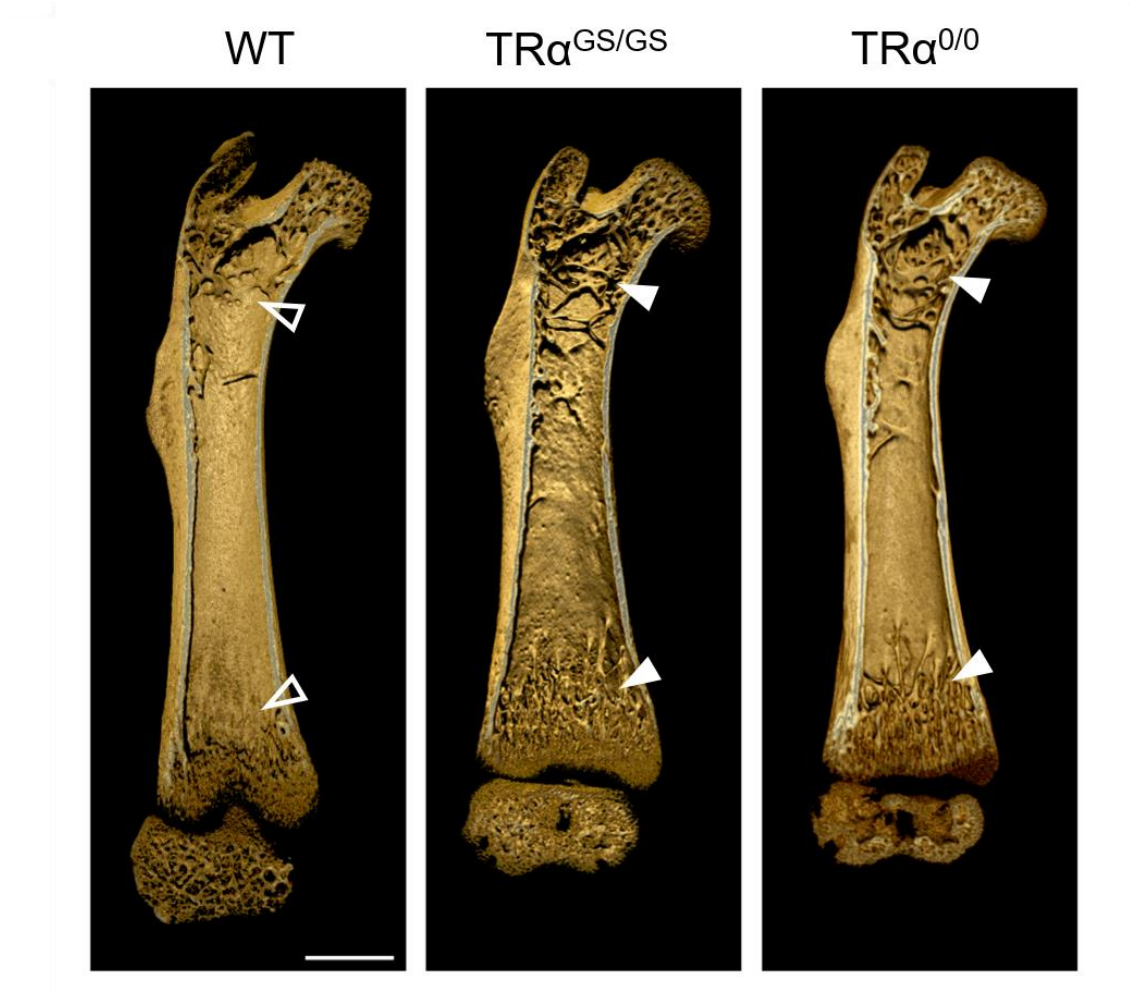

Figure 23: Micro-CT images of longitudinal femur midline sections demonstrate bone morphology. *Micro-CT images (3 µm voxel resolution) of midline sections revealed differences in bone morphology with areas of low trabecular number (open triangle) in femurs of WT mice and areas with increased trabecular number (solid triangle) in femurs of TRα$^{GS/GS}$ and TRα$^{0/0}$ mice. (Bar=1000 µm). (In cooperation with the group of Williams and Bassett in London)*

Micro-CT images of transverse section of the distal metaphysis and the bone shaft confirmed previous findings and enabled statistical analysis for trabecular number (Tb.N), trabecular thickness (Tb.Th), trabecular spacing (Tb.Sp), cortical bone area (Ct. Ar), cortical thickness (Ct.Th) and bone mineral density (Figure 24). Significant differences between the TRα mutants and WT mice were observed for Tb.N and Tb.Sp.

In summary, these data demonstrate an equivalent delay in skeletal development due to similar loss of TRE-mediated canonical TRα signaling in both TRα$^{0/0}$ and TRα$^{GS/GS}$ mice. These phenotypical concordances between TRα$^{0/0}$ and TRα$^{GS/GS}$ mice establish that T3 actions in the juvenile skeleton are mediated by canonical actions of TRα on TREs.

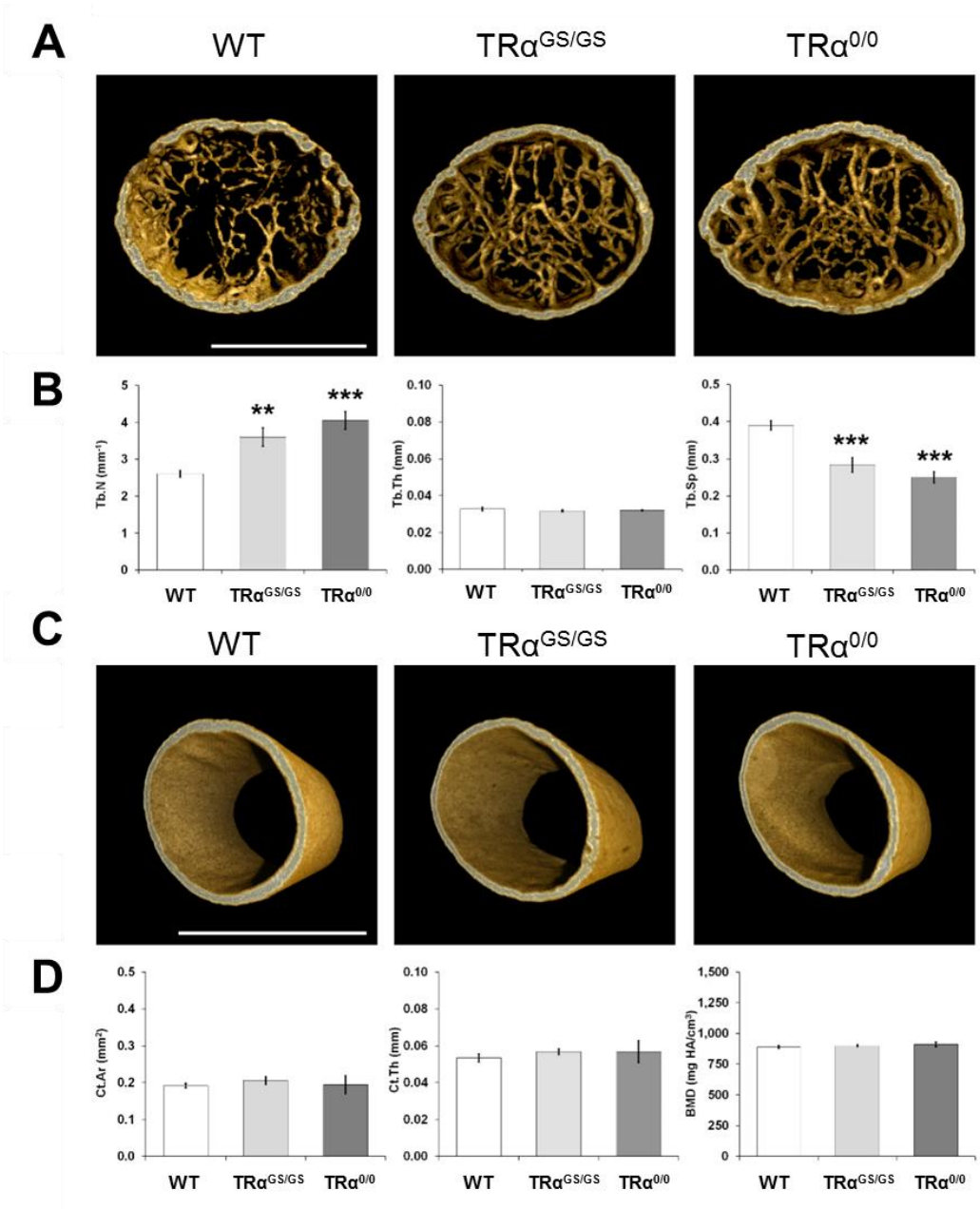

Figure 24: Micro-CT images showing transverse sections of the distal metaphysis and mid-diaphyseal cortical bone. *(**A**) Micro-CT images (3 µm voxel resolution) of transverse sections display increased trabecular structure in femurs of TRα$^{GS/GS}$ and TRα$^{0/0}$ mice (Bar=1000 µm). Graphs (**B**) demonstrate trabecular number (Tb.N; left), trabecular thickness (Tb.Th; middle) and trabecular spacing (Tb.Sp; right) (mean ± SEM; ANOVA and Tukey's post hoc test; **P<0.01; ***P<0.001). (**C**) Micro-CT images showing transverse sections of mid-diaphyseal cortical bone (Bar=1000 µm). Graphs (**D**) display cortical bone area (Ct.Ar; left), cortical thickness (Ct.Th; middle) and bone mineral density (BMD; right). (mean ± SEM; ANOVA and Tukey's post hoc test, not significant) (In cooperation with the group of Williams and Bassett in London)*

Non-canonical action of TRβ mediates TH-dependent decrease in blood glucose

In 2011, Lin *et al.* showed that a single i.p. injection of T3 reduced serum glucose concentration in lean and adipose mice within one hour after injection (Y. Lin & Sun, 2011a). This led to the hypothesis that such a rapid TH effect could be non-canonically mediated by TRs, as involvement of transcriptional and translational events would not allow such fast changes. Thus, these effects should be present in WT and either $TR\alpha^{GS/GS}$ or $TR\beta^{GS/GS}$ mice, but absent in the corresponding KO strain. To determine which receptor isoform mediates this TH effect, this hypothesis was first tested in WT and $TR\beta^{-/-}$ mice. Under fasting conditions, a single injection of T3 (7 ng/g BW) reduced serum glucose about 20% within 60 min in WT. This effect was absent in $TR\beta^{-/-}$ mice (Figure 25). Consequently, the TH-dependent reduction of blood glucose is mediated by TRβ and not by TRα. Strikingly, $TR\beta^{GS/GS}$ mice showed the same phenotype like WT mice after T3 injection.

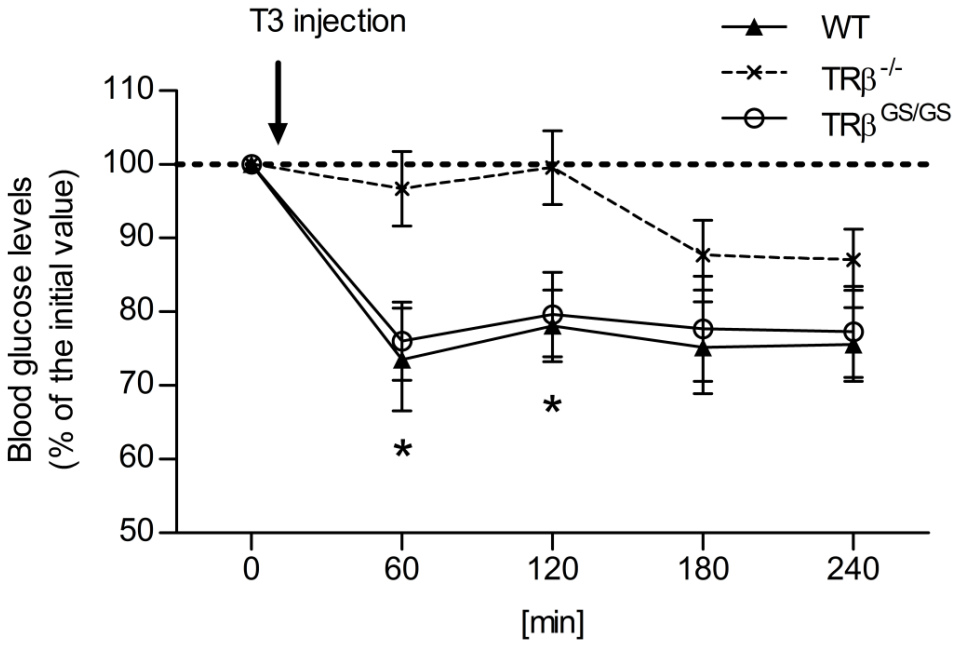

Figure 25: Rapid effect of T3 on blood glucose. *Under fasting conditions, WT (▲), $TR\beta^{GS/GS}$ (○) and $TR\beta^{-/-}$ (x) mice received a single injection of T3 (7 ng/g BW) and blood glucose concentration was measured by tail vein puncture with a glucometer at indicated time points (n=4; mean ± SEM; student's t test; *P<0.05).*

Measurements of systemic serum glucose revealed no significant differences between the TRβ genotypes (WT 374±11 mg/dl, TRβ$^{-/-}$ 350±31 mg/dl, TRβ$^{GS/GS}$ 342±18 mg/dl; n.s.).

These data suggest that the decrease in blood glucose after T3 treatment is TRβ-mediated, because it is absent in TRβ$^{-/-}$ mice. Consequently, TRα apparently plays no role in glucose decrease as it cannot compensate lack of TRβ in TRβ$^{-/-}$ mice. Strikingly, the similarity of the phenotype with an identical decrease in blood glucose in WT and TRβ$^{GS/GS}$ mice clearly demonstrates that non-canonical TRβ signaling mediates this effect. Furthermore, this effect occurs within 60 minutes, which is likely too rapid to depend on RNA transcription and translation into new proteins.

Non-canonical action of TRβ is required to maintain normal serum and hepatic triglycerides

Triglyceride (TG) concentration is another metabolic parameter under TH control. Serum TG concentration was elevated in TRβ knock-in mice with RTHβ (TRβPV), indicating that TRβ might mediate TH-dependent regulation of TG (Araki, Ying, Zhu, Willingham, & Cheng, 2009). Therefore, serum TG concentration in untreated WT, TRβ$^{-/-}$ and TRβ$^{GS/GS}$ mice was determined. TG concentration was significantly higher in TRβ$^{-/-}$ mice compared to WT mice (300±61 mg/dl vs. 152±23 mg/dl; *P<0.05*), but not in TRβ$^{GS/GS}$ mice (123±34 mg/dl; n.s.) (Figure 26, A). Additionally, TG content in liver homogenates was also significantly elevated only in TRβ$^{-/-}$ mice (Figure 26, B). As mentioned above, there was no significant difference in serum glucose of WT, TRβ$^{-/-}$ and TRβ$^{GS/GS}$ mice. The total cholesterol concentration in sera of TRβ$^{-/-}$ was slightly increased compared to WT and TRβ$^{GS/GS}$ mice (WT, 134±4 mg/dl; TRβ$^{-/-}$, 163±17 mg/dl; TRβ$^{GS/GS}$ 146±11 mg/dl). The genotype specific incidence of high TG concentration was confirmed by Oil-Red-O staining resulting in an increased staining of liver sections from TRβ$^{-/-}$ mice (Figure 26, C). The phenotype similarity between WT and TRβ$^{GS/GS}$ mice suggests that non-canonical TRβ signaling, preserved in TRβ$^{GS/GS}$ but absent in TRβ$^{-/-}$, maintains TG metabolism. Moreover, these regulatory effects seem to take place in liver, as the high TG serum concentration are confirmed by Oil-Red-O staining of liver section and liver is known to be the major organ for TG synthesis.

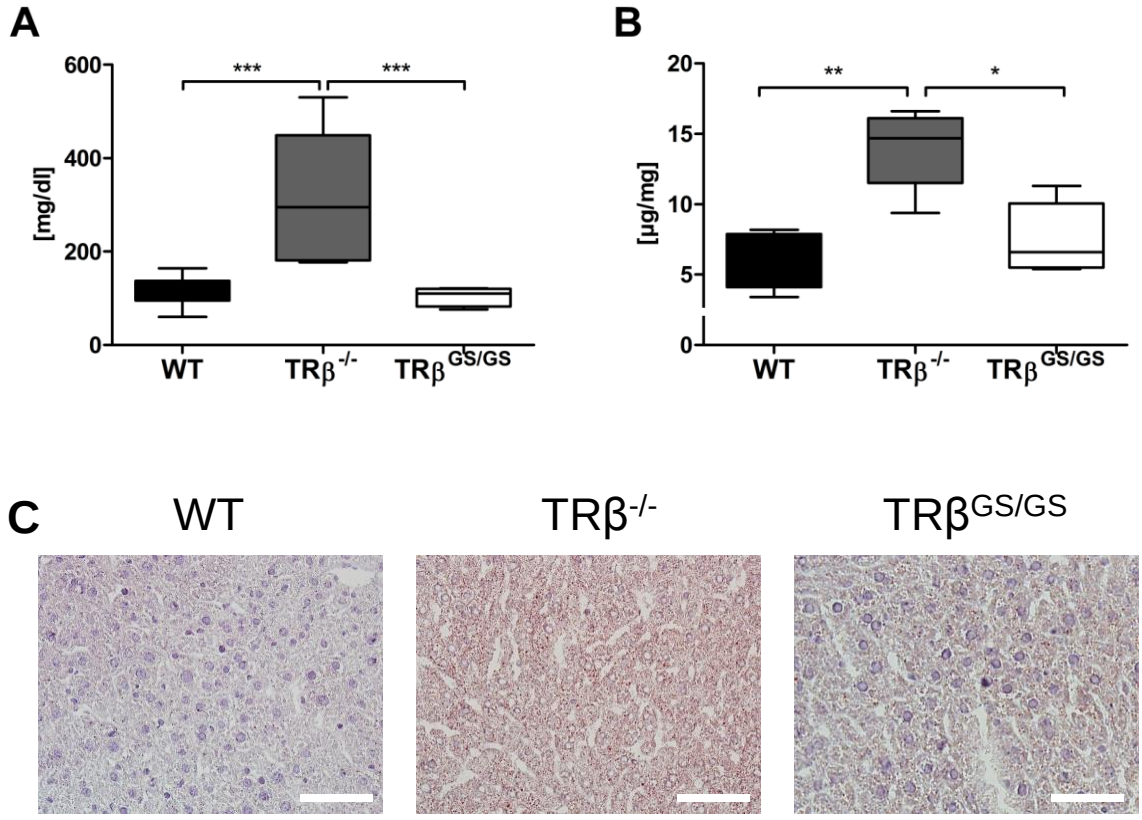

Figure 26: Measurement of triglyceride concentration in serum and liver tissue*. (**A**) Determination of TG concentration in sera from WT, TRβ$^{-/-}$ and TRβ$^{GS/GS}$ mice revealed increased TG concentration in sera of TRβ$^{-/-}$ mice only. No significant difference was detected between WT and TRβ$^{GS/GS}$ mice. (**B**) Liver TG content reflects the results obtained from serum measurements with an increased TG content in livers of TRβ$^{-/-}$ mice. (**C**) Hepatic lipid accumulation in livers of TRβ$^{-/-}$ mice was confirmed via Oil-Red-O staining (n=4-6; box plot [whiskers min to max] and mean; ANOVA with Tukey´s post hoc test; significant differences are indicated as follows: *P<0.05, **P<0.01***P<0.001; white bar = 50 µm)*

Expression of key enzymes of TG synthesis correlates with elevated TG concentration

As TG synthesis takes place in liver expression of key enzymes of the TG synthesis pathway were next investigated by qRT-PCR. Therefore, expression of acetyl-CoA carboxylase (*Acc1*), fatty acid synthase (*Fasn*), ∆9-steaoryl-CoA desaturase (*Scd1*), ATP-citrate lyase (*Acly*), malic enzyme (*Me1*), glycerol-3-phosphate dehydrogenase (*Gpd2*), mitochondrial glycerol 3-phosphate acyltransferase (*Gpam*), all genes encoding for key enzymes involved in TG synthesis, was analyzed in livers from WT, TRβ$^{-/-}$ and TRβ$^{GS/GS}$ mice (Figure 27, A-G). Additionally, expression of metabolic regulator proteins like pyruvate dehydrogenase kinase 4 (*Pdk4*) and thyroid hormone responsive (*Thrsp*) was determined, too (Figure 27, H and I). The most obvious differences in gene expression between the three genotypes were found for *Fasn,*

Scd1, *Acly*, *Me1*, *Thrsp* and *Gpam*. These genes showed a significantly increased expression in TRβ$^{-/-}$ mice compared to WT and TRβ$^{GS/GS}$ mice. Noteworthy, for all genes analyzed, there was a trend towards an increased expression in TRβ$^{-/-}$ mice. These expression patterns resemble the elevated TG concentration found in serum and liver homogenates of TRβ$^{-/-}$ mice compared to WT and TRβ$^{GS/GS}$ mice (Figure 26).

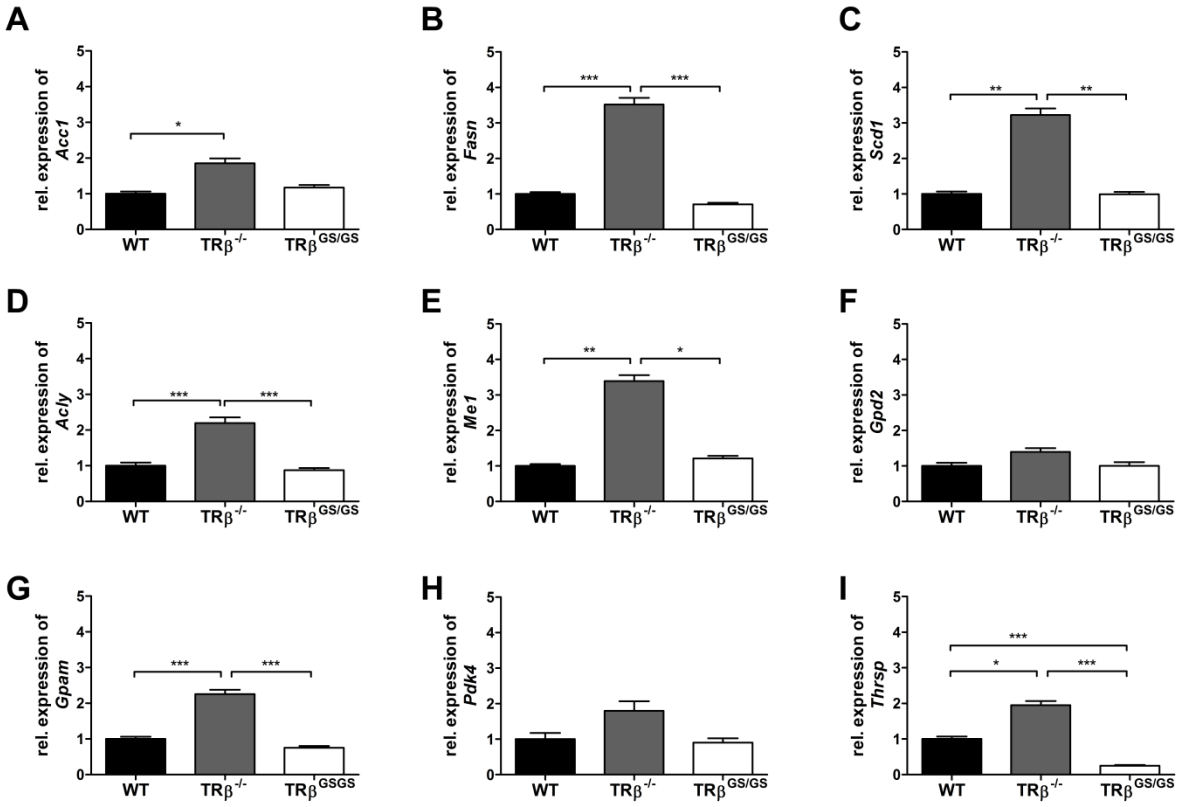

Figure 27: Hepatic mRNA expression profile of key enzymes and regulatory proteins involved in triglyceride synthesis*. (**A-G**) mRNA expression of enzymes (acetyl-CoA carboxylase (Acc1), fatty acid synthase (Fasn), ∆9-steaoryl-CoA desaturase (Scd1), ATP-citrate lyase (Acly), malic enzyme (Me1), glycerol-3-phosphate dehydrogenase (Gpd2), mitochondrial glycerol 3-phosphate acyltransferase (Gpam) involved in TG synthesis in livers of WT, TRβ$^{-/-}$ and TRβ$^{GS/GS}$ mice. (**H-I**) mRNA expression of proteins regulating fuel demand (pyruvate dehydrogenase kinase 4; Pdk4) and lipogenesis (thyroid hormone responsive; Thrsp). (n=4-6; ANOVA with Tukey´s post hoc test on log-transformed qRT-PCR data; significant results are indicated as follows: *P<0.05, **P<0.01, ***P<0.001)*

Next qRT-PCR data was validated for the three key enzymes of TG synthesis, Fasn, Scd1 and Me1 by immunoblot of whole liver protein lysates. Immunoblot analysis revealed higher hepatic protein content of Fasn, Scd1 and Me1 in livers of TRβ$^{-/-}$ mice and moreover, confirmed phenotypical similarity between WT and TRβ$^{GS/GS}$

mice (Figure 28, A). Significant differences in expression determined by immunoblot were semi-quantitatively analyzed by densitometry (Figure 28, B).

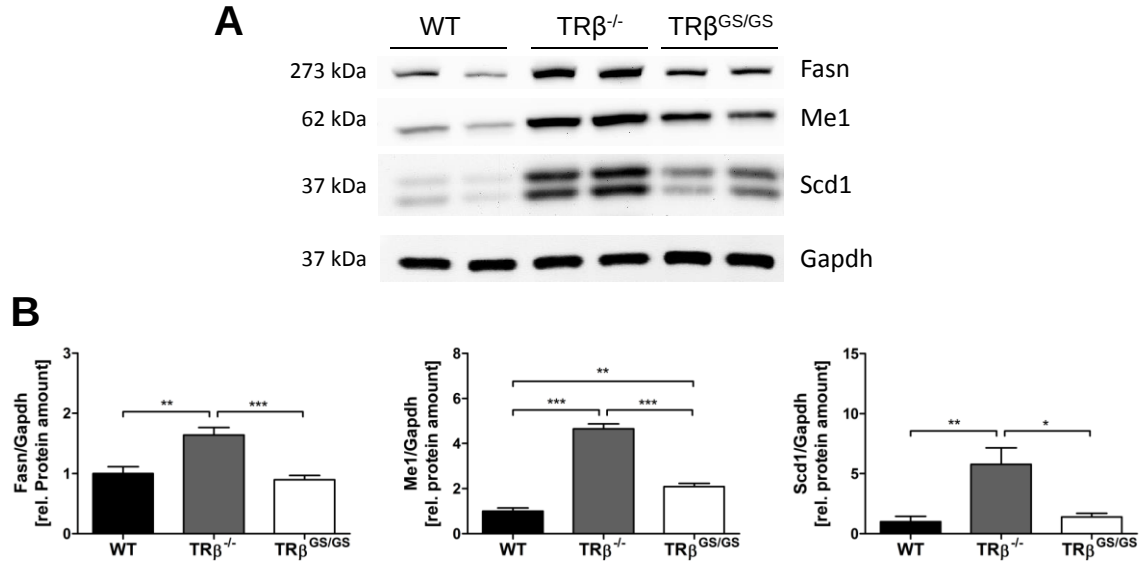

Figure 28: Protein content of Fasn, Me1 and Scd1 in liver tissue. *(**A**) Immunoblot (n=2) of Fasn, Me1 and Scd1 revealed increased lipogenic enzyme expression in livers of TRβ$^{-/-}$ mice. (**B**) Band densities (n=4) were calculated to determine the expression semi-quantitatively and perform statistical analysis (n=4; ANOVA with Tukey´s post hoc test; *P<0.05, **P<0.01, ***P<0.001)*

Non-canonical action of TRβ contributes to body temperature homeostasis

Body temperature homeostasis is an important physiological function of TH. Thus, core body temperature (BT_c) was assessed for WT, TRβ$^{-/-}$ and TRβ$^{GS/GS}$ mice by rectal measurements with a temperature probe. Deletion of TRβ did not significantly alter BT_c. Interestingly, mean BT_c of TRβ$^{GS/GS}$ mice was 0.9 °C higher than that of TRβ$^{-/-}$ mice (Figure 29, left panel). To exclude any interference by TRα, BT_c measurements were repeated in mice with a TRα$^{0/0}$ genetic background. In TRα$^{0/0}$;TRβ$^{-/-}$ double KO mice, temperature was markedly reduced from 37.0 °C in WT mice to 34.9 °C (Figure 29, right panel), which has been described before (Gauthier *et al.*, 2001; Macchia *et al.*, 2001; Wikstrom *et al.*, 1998). However, in the TRα$^{0/0}$ genetic background body temperature of TRβ$^{GS/GS}$ mice was also approximately 1°C higher than that of TRβ$^{-/-}$ mice (Figure 29 right panel). These results suggest that TRβ exerts specific effects on thermogenesis, that are independent from TRα and that these effects are non-canonically mediated.

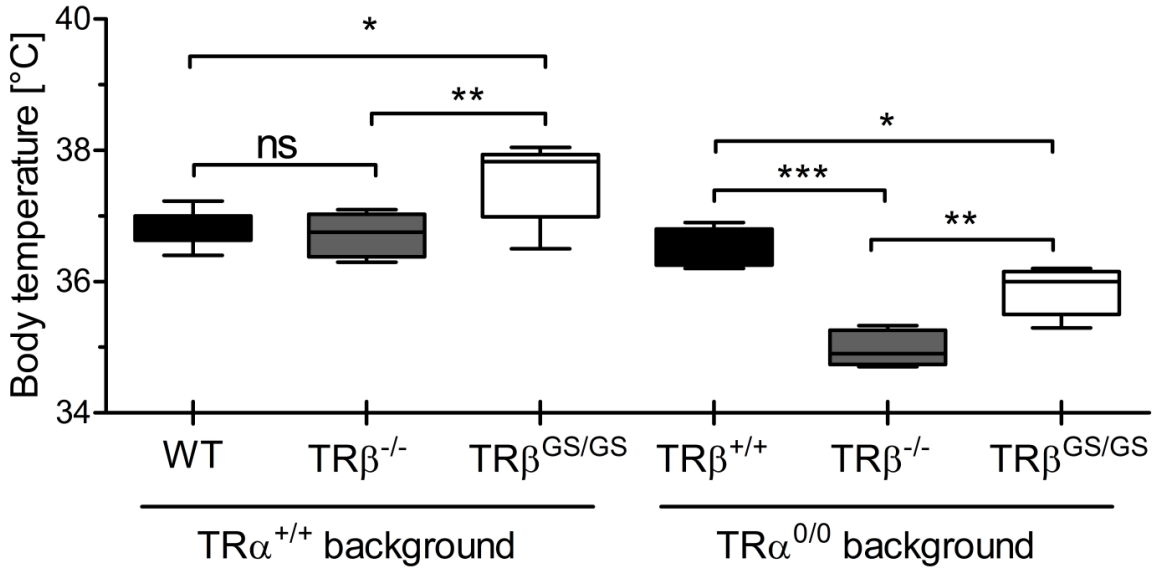

Figure 29: Body temperature of male mice in a TRα$^{+/+}$ and TRα$^{0/0}$ genetic background. *BT_c was measured rectally in TRβ$^{+/+}$ (WT, black box), TRβ$^{-/-}$(grey box) and TRβ$^{GS/GS}$ mice (open box). (n=6; box plot [whiskers min to max] and mean; ANOVA and Bonferroni's post hoc test for multiple comparison; ns = not significant; *P<0.05; **P<0.01; ***P<0.001; BT_c, body core temperature).*

Regulation of heart rate requires non-canonical action of TRα

TRα is the predominant TR isoform in the heart and regulation of heart rate (HR) is a well-known physiological effect of TH and TRα (Macchia *et al.*, 2001). Basal HR of untreated WT, TRα$^{0/0}$ and TRα$^{GS/GS}$, TRβ$^{GS/GS}$ and TRβ$^{-/-}$ mice was determined with a non-invasive ECG. Depletion of TRβ, as well as loss of canonical TRβ action resulted in an increased HR (Figure 30, A), due to elevated TH serum concentration (compare to Figure 17), as expected. Loss of TRα in TRα$^{0/0}$ mice was associated with significantly reduced HR compared to WT mice (Figure 30, A). Strikingly, HR was not reduced in TRα^{GSGS} mice. Remarkably, expression of TH responsive genes, which are thought to be involved in regulation of HR, were similarly altered in hearts of TRα$^{GS/GS}$ and TRα$^{0/0}$ mice (e.g. *Hcn2*, *Hcn4* and *Kcne1*; Figure 30, B). These data suggest that TH-dependent expression of several ion channels is not solely responsible for TH-dependent regulation of HR. Moreover, the phenotype concordance between WT and TRα$^{GS/GS}$ mice demonstrates that non-canonical TRα signaling significantly contributes to normal HR in TRα$^{GS/GS}$ mice.

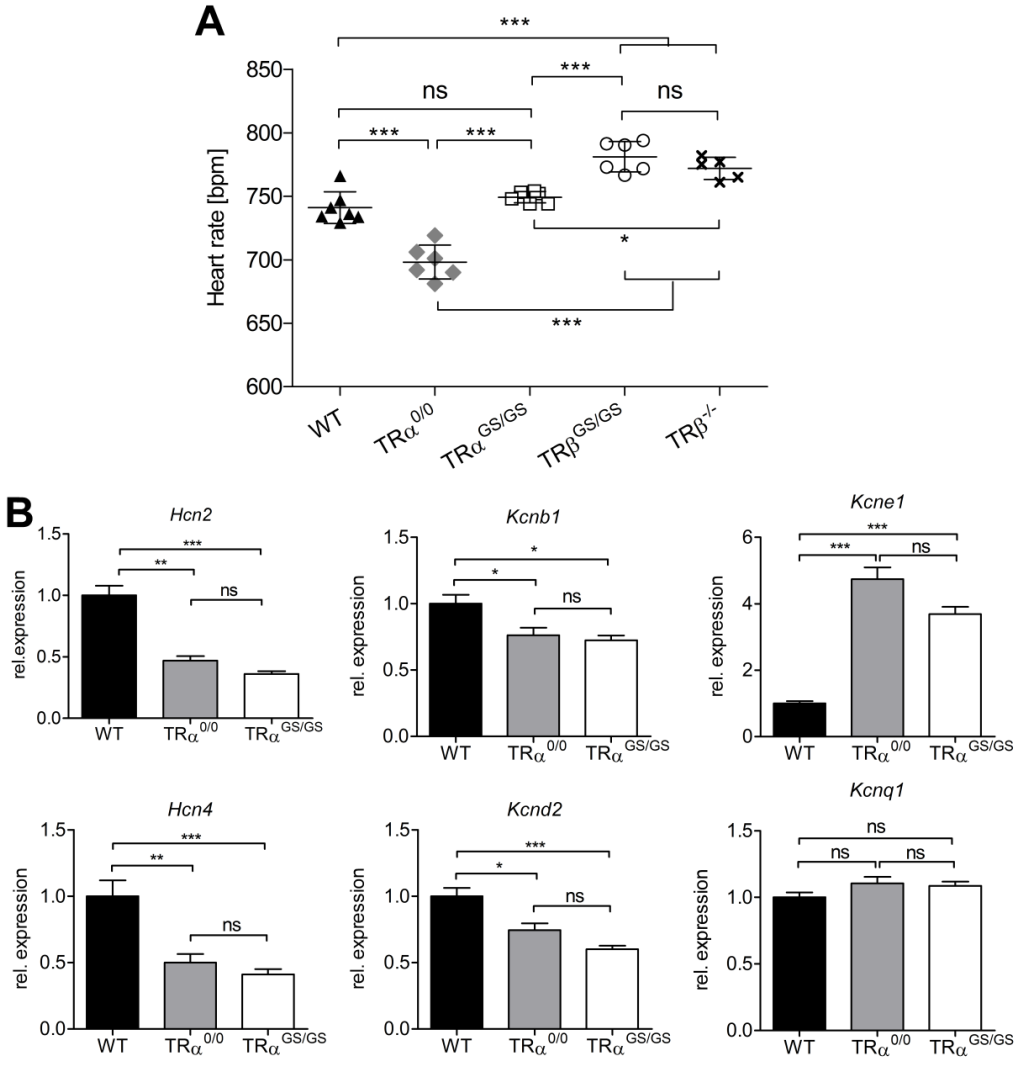

Figure 30: Non-canonical TRα signaling maintains normal systemic heart rate independent of cardiac pacemaker channel gene expression *(**A**) HR of non-sedated male WT (▲; n=7), TRα$^{0/0}$ (◆; n=6), TRα$^{GS/GS}$ (□; n=6), TRβ$^{GS/GS}$ (○; n=6) and TRβ$^{-/-}$ (x; n=5) mice were measured via ECG (mean ± SD; ANOVA followed by Bonferroni's post hoc test for multiple comparisons; *P<0.05, ***P<0.0001, ns=not significant). (**B**) Relative expression of pacemaker channels Hcn2 and Hcn4 and of potassium channel subunits with importance for repolarization, Kcnb1, Kcnd2, Kcne1 and Kcnq1, in hearts of TRα$^{0/0}$ (grey bars), TRα$^{GS/GS}$ (open bars) mice and WT mice (black bars) were determined via qRT-PCR (n=6; mean ± SEM; ANOVA and Tukey's post hoc test; *P<0.05, **P<0.01, ***P<0.001, ns=not significant).*

Discussion

TH controls development, growth, regulation of HR and body temperature and maintains several metabolic functions via the TH receptors TRα and TRβ. The current paradigm of TH/TR signaling is that TRs are ligand-dependent transcription factors, thus the main TH effects are determined by the genes that are induced via canonical TR action. The paradigm in its current form cannot explain TH-mediated effects which were reported to be independent of protein synthesis (Segal & Ingbar, 1985). Moreover, the existence of a non-canonical TR signaling pathway has been suggested more than a decade ago, when signaling pathway activation by TRs and TH was reported *in vitro* (Cao, Kambe, Moeller, Refetoff, & Seo, 2005; Hiroi *et al.*, 2006; Simoncini *et al.*, 2000; Storey *et al.*, 2006). However, its relevance *in vivo* remained unresolved. This may be explained by the fact that both canonical and non-canonical TR signaling are present in WT mice and absent in TR^{KO} mice so that these mouse models cannot distinguish between the two mechanisms. Thus, non-canonical TR signaling was not recognized and physiological effects of TH were attributed to the established canonical TR signaling pathway.

This issue was addressed in this study by generating mouse models with abolished canonical TR signaling ($TR\alpha^{GS}$ and $TR\beta^{GS}$ mouse models). Therefore, canonical TRE/TR dependent action should be abrogated and in turn, that allows studying the effects of non-canonical TR signaling alone. Further, this study aimed to investigate the contribution of non-canonical TR action to the overall physiological effects of TH by comparing WT mice with TR^{KO} and TR^{GS} mice.

In vitro validation of the GS-mutation model for abrogating canonical TR action

Prior to generating the TR^{GS} *in vivo* models the general principle of terminating canonical TR action by mutating the DBD was tested *in vitro*. Shibusawa *et al.* demonstrated that an amino acid substitution of EG to GS in the P-box of the first zinc-finger of the TRβ DNA-binding domain severely impaired TRE recognition and DNA binding (Shibusawa *et al.*, 2002). Those *in vitro* results were confirmed in this study and successfully extended to TRα by testing canonical action of TRα71GS on DR4-TREs with the two most prevalent canonical half sites (AGGTCA and AGGACA) (Ayers *et al.*, 2014; Katz & Koenig, 1994; Ramadoss *et al.*, 2014). A limitation of this experiment might be that only two DR4-variants were used in this study. But for the

TRβ125GS mutant other TREs like PAL and IP have been tested previously (Shibusawa *et al.*, 2002). On top of that, a genome-wide analysis of TRα and TRβ mediated gene expression and chromatin occupancy (by ChIP-seq analysis) revealed the DR4 consensus sequence 5'-AGGTCAnnnnAGGNCA-3' as the most prevalent TRβ binding sites, in which the TR binds to the 3'-half site (Chatonnet, Guyot, Benoit, & Flamant, 2013). Additionally, TRα and TRβ are highly homologous regarding their DBD and especially their amino acid sequence of the first zinc finger including the recognition helix with the P-box (Figure 5). Thus, it is reasonable to assume that the results for TRβ are well transferable to TRα.

However, the principle of abolishing canonical action of nuclear receptors by integrating the GS-mutating into the P-box was also successfully shown for ER by Jakacka *et al.* (Jakacka, 2002; Jakacka *et al.*, 2001). It is worth mentioning that the choice of glycine and serine as substitutional amino acids was not arbitrary. Glycine and serine and valine (GSV) is the P-box amino acid motif of the glucocorticoid receptor (GR) (Hard *et al.*, 1990). Thus, the substitution is based on similar molecular characteristics like size and charge. This has the advantage that the general tertiary structure of the zinc finger and hence the DBD is left intact and therefore other functions e.g. dimerization and cofactor binding are not affected (Shibusawa *et al.*, 2002). Additionally, Baumann *et al.* proved that a mutation in the DBD of TR does neither alter TR shuttling between the nucleus and the cytoplasm nor affect the steady-state of TR distribution among cellular compartments (Baumann *et al.*, 2001).

But of note, by substitution of the TR´s P-box amino acids EG by GS (obtained from the GR´s P-box motif: GSV) might not fully abrogate the TR´s DNA-binding ability but rather enable the mutated TR adopting an affinity for GRE-like regulatory DNA sequenced. Thus, besides the established DR4 sequences, transcriptional activation by TR was tested on artificial TRE/GRE hybrid sequences (hybrid of a 5'-TRE and a 3'-GRE spaced by 4 nucleotides) 5'-AGGTCAcaggAGATCA-3' and 5'-AGGTCAcaggAGAACA-3') (Shibusawa, Hollenberg, & Wondisford, 2003). While no significant increase in transcriptional activity by neither TRα71GS nor TRβ125GS was detectable in this study, previous work by Shibusawa *et al.,* came to the result that TRβ125GS has transcriptional activity on an artificial TRE/GRE sequence (AGGTCAcaggAGAACA). Additionally, this activation is increased in cells, cotransfected with RXRα (Shibusawa *et al.*, 2002). In the present study, all *in vitro* experiments were carried out without cotransfection of RXRα. Noteworthy, no

residual transcriptional activation of TRβ125GS was detectable on this sequence. Of course, it might be possible that RXRα can bind TRβ125GS and direct it to the TRE/GRE sequence. Another considerable fact is that, Shibusawa *et al.* used a TRβ2 mutant, while in this study all *in vitro* experiments were done with TRβ1 mutants. TRβ2 differs only at the N-terminus and therefore has a different AF1 domain than TRβ1. But, heterodimerization of TR with RXRα was shown to depend on motifs in the DBD and the AF2 sequence (Y. Wu, Yang, & Koenig, 1998). However, one should keep in mind, that the reported activation by the TRE-binding deficient TRβ125GS was related to an artificial TRE/GRE sequence. Thus, this activation might be of no physiological relevance. Additionally, cell culture experiments based on overexpression of proteins can result in promiscuous protein interactions and pathway activation (Moriya, 2015).

Generation of the TR^{GS} mouse models

The targeted integration of the mutation into the murine *Thra* and *Thrb* gene loci was done by zinc-finger nuclease (ZFN) technology (Carbery *et al.*, 2010). The mutation rate for the successful targeted integration of the $TR\alpha^{GS}$ and $TR\beta^{GS}$ mutation was 3.5% and 2.6%, respectively. These values are within the range of mutation frequency for ZFN-induced targeted integration for mice described in literature (Carbery *et al.*, 2010; Cui *et al.*, 2011).

Viability of $TR\beta^{GS/GS}$ mice has been proven previously by others (Shibusawa, Hashimoto, *et al.*, 2003) and remarkably viability of $TR\alpha^{GS/GS}$ was also not affected by the mutation. This is in a way surprising, because other groups showed that a $TR\alpha^{KO}$ mouse model ($TR\alpha^{-/-}$, a specific KO of the TRα1 and TRα2 isoforms) had a severe phenotype during early *postnatal* development resulting in growth retardation, weight loss and death after only 3-4 weeks (Fraichard *et al.*, 1997). Almost at the same time, Wikström *et al.* published data from a different $TR\alpha^{KO}$ mouse model and by contrast, these mice were viable and survived. The difference between these two $TR\alpha^{KO}$ mouse models is that Fraichard *et al.* targeted exon 2, which leads to a KO of the TRα1 and TRα2 isoforms but does not affect the internal promoter located in intron 7, which regulates the expression of the truncated TRαΔ1 and TRαΔ2 variants. In contrast to this, Wikström *et al.* targeted the region around exon 9, which mediates the alternative splicing to form TRα1 and TRα2, as well as the two corresponding Δ-

isoforms. Hence, the expression of TRα1 and TRαΔ1 was abrogated in this model. Further an inhibitory effect of TRαΔ1 on TRα mediated gene expression was demonstrated *in vitro* (Chassande *et al.*, 1997), concluding that expression of TRαΔ1 in absence of TRα1 has a dominant negative effect on TRα1 mediated physiological functions which results in early lethality. This hypothesis was supported by the generation of the $TR\alpha^{0/0}$ mouse, devoid of all known TRα isoforms including the Δ-isoforms (the $TR\alpha^{KO}$ model which was also used in this study). These mice also survived and had a milder phenotype than the $TR\alpha^{-/-}$ mice which still express the TRαΔ1 isoform (Gauthier *et al.*, 2001).

Considering these results, it is surprising that the $TR\alpha^{GS/GS}$ mice are viable, because these mice express a canonically non-functional TRα1 isoform, as well as the TRαΔ1 and TRαΔ2 isoforms. Strictly speaking, the $TR\alpha^{GS/GS}$ mice rather resemble the TRα-related isoform expression of $TR\alpha^{-/-}$ mice than that of $TR\alpha^{0/0}$ mice. Hence, one could expect that these mice would have a severe phenotype such as the $TR\alpha^{-/-}$ mouse model. But strikingly, this was not the case. For some physiological effects the $TR\alpha^{GS/GS}$ mice closely resembled the milder $TR\alpha^{0/0}$ phenotype and moreover TRα-mediated regulation of HR was like in WT mice.

On the one hand, these findings cast doubt on the *in vitro* results demonstrating the dominant negative inhibitory effect of TRαΔ1 on TRα gene expression. But on the other hand the data, presented in this study, might support the hypothesis made by Gauthier *et al.* in 2001. They proposed that presence of TRα1 is sufficient to interfere with TRαΔ1 function and induce degradation of TRαΔ1 in a T3-independent manner (Gauthier *et al.*, 2001). Due to the fact, that the GS-mutation does not affect systemic TRα expression, as demonstrated, the mutated receptor could interfere with TRαΔ1 and induce its degradation, thus preventing the severe and lethal phenotype described for $TR\alpha^{-/-}$ mice.

In vivo validation of the TR^{GS} mouse models

The loss of canonical TR action proven in a cell culture experiment might be essential but not sufficient, as experiments based on overexpression of certain proteins can lead to artificial outcomes. Thus, for validation of the TR^{GS} mouse models it is necessary to confirm loss of DNA-binding ability *in vivo*. For this, gene expression of known TH target genes in heart and liver were analyzed.

Systemic expression of Thra, Thrb and TH target genes in heart and liver

As expected, introduction of the GS-mutation did not alter systemic expression of TRα and TRβ in heart and liver, respectively. In contrast, expression of TH target genes *Myh7, Myh6* in $TR\alpha^{GS/GS}$ and additionally *Dio1* and *Tbg* in $TR\beta^{GS/GS}$ mice, resembled the expression detected in the corresponding TR^{KO} strains. For *Myh6* the presence of a regulatory positive TRE has been described about 30 years ago (Izumo & Mahdavi, 1988). Thus, a lack of TRα in $TR\alpha^{0/0}$, as well as a loss of canonical TR action would result in a decreased expression of *Myh6,* as observed. TH/TR dependent downregulation of *Myh7* has been shown by independent studies and thus was suggested to depend on a negative TRE, although evidence for the existence of such a negative TRE is still missing (Edwards, Bahl, Flink, Cheng, & Morkin, 1994; Iwaki *et al.*, 2014; Morkin, 1993). However, increased expression of *Myh7* further confirmed loss of canonical action of TRE binding deficient $TR\alpha^{GS}$ mutant.

Similar results were obtained for *Dio1* and *Tbg* expression in livers of WT, $TR\beta^{-/-}$ and $TR\beta^{GS/GS}$ mice. Here again, expression of *Dio1* and *Tbg* in livers from $TR\beta^{GS/GS}$ mice were different to WT mice but resembled the expression pattern of $TR\beta^{-/-}$ mice. Regarding *Dio1,* DR4-like TREs close to the transcriptional start site have been described (Toyoda, Zavacki, Maia, Harney, & Larsen, 1995). Additionally, it was shown that Klf-9 (Krüppel-like-factor 9) can also induce *Dio1* expression (Ohguchi *et al.*, 2008). Klf-9 is also a TH target gene (Denver *et al.*, 1999; Dugas *et al.*, 2012; Moeller, Wardrip, Niekrasz, Refetoff, & Weiss, 2009), thus Klf-9 acts synergistically on *Dio1* expression. This explains the rapid and strong response of *Dio1* on T3 treatment also shown in this study. In turn, absence of *Dio1* expression in $TR\beta^{GS/GS}$ mice indicated loss of canonical action. The reverse regulation of *Tbg* in relation to TH concentration was described earlier, as treatment with propylthiouracil increased *Tbg* expression, while acute T4 treatment decreased its expression (Engels *et al.*, 2016; Vranckx *et al.*, 1990). As it turned out, a lack of TRβ or DNA-binding ability of the receptor resulted in an increased expression of *Tbg* (Figure 12), resembling a hypothyroid state due to RTHβ.

Confirming loss of TH/TRβ target gene expression under T3 stimulation

As expression of *TSH* is also under control of canonical TRβ2 action, in $TR\beta^{-/-}$ and $TR\beta^{GS/GS}$ mice, TSH and subsequently T3 and T4 were elevated due to lack of TRβ mediated negative feedback in the pituitary, constituting resistance to thyroid hormone, congruent with earlier reports (Shibusawa, Hashimoto, *et al.*, 2003). Even though this confirms loss of canonical action of TRβ2 isoform by the GS-mutation, it also results in an uneven TH steady-state between WT, $TR\beta^{-/-}$ and $TR\beta^{GS/GS}$ mice. To overcome this issue all mice were rendered hypothyroid before T3 treatment for 5 consecutive days. Determining gene expression of hepatic TH target genes in hypothyroid and T3-treated mice revealed a residual increase of *Dio1* expression in $TR\beta^{-/-}$ and $TR\beta^{GS/GS}$ mice. As the small but significant increased expression of *Dio1* is present in both genotypes it is doubtful that this is due to residual DNA binding by the GS-mutant receptor. More likely, residual TRα expression in $TR\beta^{GS/GS}$ and $TR\beta^{-/-}$ hepatocytes explains the residual transcriptional action. Of note, TRβ is the predominant but not the solely expressed TR isoform in liver.

Diverse kinetics of positive and negative TR target gene expression

To determine the optimal time point for measuring direct TH-induced gene expression, a kinetic study was performed. It was obvious that the negative regulated TH-target gene *Tbg* exhibited a different kinetic than positively regulated genes like *Dio1*, *Bcl3, Me1* and *Thrsp*. An explanation for this might be that gene repression is dependent on mRNA half-life, which varies from gene to gene (Sharova *et al.*, 2009). On the one hand, choosing a short time point for gene expression analysis would in some cases not allow detecting changes in mRNA content of negatively regulated genes. On the other hand, an extended time point would increase the detection of unwanted indirectly regulated genes. Thus, a time point of 6 h seemed to be appropriate for the detection of direct positively regulated genes with less interference of secondary ones, even though this would exclude the detection of slowly negatively regulated genes like *Tbg*.

Direct TH target gene expression is abolished on a genome-wide scale

The process of T3/TR regulated gene expression is highly complex. Direct induction of TRE-regulated genes, which encode for transcription factors other than TRs, might affect expression of several other TRE-independent genes, therefore referred to as indirectly regulated genes. Thus, chronic treatment of T3 cannot distinguish between direct and indirect regulated genes (Picou, Fauquier, Chatonnet, Richard, & Flamant, 2014). Moreover, non-canonical T3/TR-dependent activation of intracellular signaling cascades like the PI3K-Akt pathway might also result in expression of PI3K-Akt-dependent genes. Thus, it is possible that in the set of known TH-target genes some genes exist, which are not directly regulated via TR/TRE interaction rather than by non-canonical activation of intracellular signaling pathways.

To address this issue, a short time point of 6 h after a single T3 stimulation was chosen. Microarray analysis of mRNA isolated from livers of hypothyroid WT, $TR\beta^{-/-}$ and $TR\beta^{GS/GS}$ mice and the T3-treated corresponding genotypes, revealed a genome-wide abrogation of T3-response in $TR\beta^{-/-}$ and $TR\beta^{GS/GS}$ mice. The number of significantly regulated probe sets was absolutely different between WT and the two TRβ mutants. Moreover, the clustering algorithm could not distinguish between T3-treated $TR\beta^{-/-}$ and $TR\beta^{GS/GS}$ mice, confirming that the GS-mutation fully abolishes DNA binding, resembling a $TR\beta^{-/-}$ phenotype. Data analysis revealed two genes (*Adgrg3*, adhesion G protein-coupled receptor G3 and *Lrat*, lecithin-retinol acyltransferase), which were determined to be exclusively regulated in $TR\beta^{GS/GS}$ mice. Of note, this could be off-target effects that occur due to the mutated DBD in $TR\beta^{GS/GS}$ mice. *Adgrg3* was also regulated by T3 in WT and $TR\beta^{-/-}$ mice, but with fold changes of 1.82 and 1.92, respectively. Thus, these fold changes did not meet the statistical requirements used for generating the Venn diagrams (fold change >2), resulting in a false positive hit. Deeper data analysis revealed that *Lrat* was also regulated in WT and $TR\beta^{-/-}$ mice after T3 injection, but the variation in expression within the WT and $TR\beta^{-/-}$ individuals was higher compared to $TR\beta^{GS/GS}$ mice. Thus, this gene was excluded due to the step-up p-value which was above the threshold of *P<0.01*. In conclusion, introduction of the GS-mutation into the DBD of TR leads to a genome-wide loss of canonical TR signaling.

Grontved *et al.* performed ChIP-seq and reported that besides enrichment of the common DR4 also non-TRE motifs like HFN6 (ATTGAT) and FoxA (GT/CAAAT/CA) were found to be associated with TR-dependent gene regulation (Grontved *et al.*,

2015). Thus, one could suggest that these motifs are involved in non-canonical gene regulation of TRs. Furthermore, the FoxA motif is a target of forkhead transcription factors (Foxo) which are activated via the PI3K-Akt-pathway (Gomes, Zhao, & Lam, 2013). However, microarray analysis revealed no genes which were exclusively regulated via T3 in WT and TRβ$^{GS/GS}$ mice, in this study. Noteworthy, Grontved *et al.* treated mice with 10 µg/100 g BW T3 for 5 consecutive days. Thus, the reported enrichment of HNF6 and FoxA motifs might depend on secondary effects or FoxA-dependent gene regulation follows a different kinetic than that of TRE/TR. Hence, it should be considered that 6 h after a single injection of T3 could be too short to allow Foxo phosphorylation, nuclear export, Foxo ubiquitination and proteasomal degradation, steps which are necessary for Foxo/FoxA dependent gene regulation. Therefore, non-canonical TR-dependent gene regulation is supposed to follow a slower kinetic than canonical TR/TRE-dependent gene regulation.

T3 injection leads to T4 displacement from Tbg

Another interesting observation was, that a single injection of T3 (5 µg/ 100 g BW) led to a transient increase of FT4 serum concentration. It is well known that TH synthesis only takes place in the thyroid gland. Furthermore, formation of T4 requires coupling of two DIT molecules by TPO (Nussey & Whitehead, 2001). Additionally, T3 is a metabolite of T4 generated through deiodination and not *vice versa*. Hence, this rapid increase in FT4 serum concentration after a single injection of T3 was unexpected. A possible explanation for this phenomenon can be found in the context of *Tbg* expression and TH binding to serum proteins. The mice used for this experiment were rendered hypothyroid in the beginning. It was observed in this study, as well as independently by other researchers, that under hypothyroidism hepatic *Tbg* expression increases and Tbg is secreted into blood, resulting in higher Tbg serum concentration (Vranckx *et al.*, 1990). Higher concentration of TH-binding proteins in serum counteracts TH deprivation, hence helping to defend a euthyroid TH status. T3 and T4 bind to Tbg with different affinities due to diverse association constants (K_a, M^{-1}). K_a of T4 is about one decimal power greater that K_a of T3. Thus, more T4 is bound to Tbg than T3 (Hocman, 1981; Snyder, Cavalieri, Goldfine, Ingbar, & Jorgensen, 1976). Tbg exhibits only one TH binding site, accordingly T4 and T3 binding occurs in a competitive manner. Consequently, for every molecule T3 which binds to Tbg, one molecule of T4 must dissociate from Tbg. Under hypothyroid

circumstances a low residual fraction of T4 and T3 is bound to Tbg and a new steady-state is adjusted. A single injection of a supra-physiological dose of T3 will shift this steady-state and prefer T3 binding rather than T4 binding, hence T4 displacement is increased. This would result in an increased FT4 concentration, as observed in this study. Noteworthy, for a short period, in which processes of TH deiodination and clearance are negligible, the sum of FT3 and FT4 concentration should be approximately constant. The FT3 and FT4 measurement confirmed this hypothesis, as the sum of the FT4 and FT3 concentration (nM) is relatively stable over time and only slightly decreases.

Deciphering isoform-specific canonical and non-canonical TR action *in vivo*

The general approach of this thesis was based on the phenotypic comparison of WT mice TR^{KO} and TR^{GS} mice, as this should reveal which physiological TH effect is mediated by either canonical or non-canonical TR action. During the past years, phenotypic analysis of WT and corresponding TR^{KO} mice discovered several TR isoform-specific TH effects (Gauthier *et al.*, 1999; Gauthier *et al.*, 2001; Wikstrom *et al.*, 1998). In this study, this approach was extended to the two very different mechanism of TR signaling.

The use of TRα and TRβ isoform-specific mutants has the advantage that every physiological TH effect that is observed cannot only be attributed to canonical or non-canonical TR signaling, but also to TRα and TRβ. Therefore, known physiological TH effects were investigated in this study.

Isoform-specific physiological TH effects mediated by canonical TR action

Regulation of TH serum concentration in relation to *TSH* expression, linear growth and gain of body weight were unambiguously dedicated to canonical TR action. Serum TSH, as well as TT4 and TT3 concentrations were elevated in $TR\beta^{-/-}$ and $TR\beta^{GS/GS}$ mice but normal in $TR\alpha^{0/0}$ and $TR\alpha^{GS/GS}$ mice, whereas linear growth and gain of BW were only affected in TRα mutants. These results are in line with previous findings by Shibusawa *et al.* and Gauthier *et al.* (Gauthier *et al.*, 1999; Shibusawa, Hashimoto, *et al.*, 2003).

Interestingly, linear growth and gain of BW was delayed in TRα$^{GS/GS}$ mice to the same extent as in TRα$^{0/0}$ mice. Thus, indicating that DNA binding of TR was absolutely required for these TH effects. This novel finding suggests that developmental delays in growth and gain of BW caused by TRα mutations only result from disturbed TRα target gene expression and are not the cause of impaired non-canonical TRα action. Further, these results exclude the participation of several TRα isoforms in regulation of growth and gain of BW. In brief, while TRα$^{0/0}$ mice lack all isoforms encoded by *Thra* the TRα$^{GS/GS}$ mice express all isoforms including TRα p43, TRα p30, as well as the Δ-variants. Remarkably, these isoforms fail to rescue or affect the phenotype of delayed growth and gain of BW. Consequently, any involvement of these receptor isoforms in early *postnatal* development can be excluded. Studies on TRα p43$^{-/-}$ (isoform-specific p43 KO) mice confirm these results as TRα p43$^{-/-}$ show normal early *postnatal* development but are leaner in adulthood (Bertrand *et al.*, 2013). Here, TRα$^{0/0}$ and TRα$^{GS/GS}$ mice at the age of 4 month were slightly but not significantly thinner than WT mice. Of note, a group size of 14-31 used by Bertrand *et al.* can reveal smaller significant differences than a group size of 6-7 used in this study. Thus, if an increased group size revealed a significant difference in BW between TRα$^{GS/GS}$ and WT mice, one could conclude that canonical action of TRα p43 was essential for mitochondrial homeostasis, which then forms a link between mitochondrial energy expenditure and TH-regulated BW.

Impaired bone development is responsible for delayed postnatal linear growth

Skeletal abnormalities are known to be associated to RTHα in mice and man (Bassett *et al.*, 2014; Desjardin *et al.*, 2014; Moran & Chatterjee, 2015). THs are essentially required for juvenile bone development regarding longitudinal bone growth, mineralization, endochondral ossification and regulation of trabecular microarchitecture (Bassett & Williams, 2016). Whether non-canonical events play a role in juvenile bone development has not been investigated, yet.

Juvenile P21-old TRα$^{0/0}$ mice display a severe bone phenotype regarding impaired longitudinal growth clearly recognizable in reduced length of femurs, tibias and vertebrae. The smaller bone size of TRα$^{0/0}$ and TRα$^{GS/GS}$ mice correlates with tail lengths of the juvenile mice from these strains. As expected, the underlying cause of delayed linear growth, determined via tail length measurements, might be due to

impaired longitudinal bone growth. However, these results confirmed the requirement of canonical TRα signaling in longitudinal bone growth as bones from $TR\alpha^{GS/GS}$ mice were as short as bones from KO mice.

Growth of long bones relies on endochondral ossification and takes place in the epiphyseal growth plate which consists of a reserve, a proliferation and a hypertrophic zone. Under euthyroid conditions, chondrocytes progress from the reserve zone into the proliferation zone. After proliferation, chondrocytes undergo maturation and become hypertrophic chondrocytes. These hypertrophic chondrocytes synthesize a matrix of type X collagen and induce formation of calcified cartilage before becoming apoptotic (Bassett & Williams, 2016). Bassett *et al.* used $Pax8^{-/-}$ mice (a mouse model for congenital hypothyroidism, due to impaired thyroid development) to show that these processes are disturbed in hypothyroidism, resulting in a broader reserve zone and narrower hypertrophic zone. Additionally, growth plate width decreases with age, a process which is also altered under hypothyroidism (Bassett *et al.*, 2008). Similar findings were made in this study by analyzing the growth plate of tibias from $TR\alpha^{GS/GS}$ and $TR\alpha^{0/0}$ mice. Noteworthy, $TR\alpha^{GS/GS}$ and $TR\alpha^{0/0}$ mice are euthyroid regarding their TH serum concentration, but both resemble a hypothyroid bone phenotype with increased reserve zone width and decreased hypertrophic zone width and an overall larger growth plate width. Consequently, canonical action of TRα is required for chondrocyte maturation to become hypertrophic chondrocytes.

During *postnatal* bone development and proceeding linear growth, the trabecular structure beneath the growth plate is reduced by bone remodeling (Bassett *et al.*, 2007). Hence, an increased trabecular number and significant decrease in trabecular spacing, resembles delayed bone maturation in $TR\alpha^{GS/GS}$ and $TR\alpha^{0/0}$ mice, which is known to be associated with hypothyroidism. These results demonstrate that TRα acts via DNA binding and canonical signaling during *postnatal* bone development.

In 2014, Kalyanaraman *et al.* reported that the truncated TRα p30 isoform is expressed in primary human osteoblasts, as well as in the mouse osteoblast-like cell line MC3T3. Moreover, treatment of these cell lines with a physiological dose of 1 nM T3 rapidly increased intracellular Ca^{2+} and NO (nitric oxide) production and resulted in initiation of ERK- and PI3K-signaling (Kalyanaraman *et al.*, 2014). TRα p30 is a truncated TRα isoform generated through an alternative transcription start site at M^{150}. Thus, TRα p30 lack a DBD, accordingly all TH effects mediated by TRα p30

must be non-canonical. Kalyanaraman *et al.* proposed a TRα p30-NO-cGMP (cyclic guanosine monophosphate) dependent mechanism for maintaining osteoblast proliferation and activity. They could bypass TRα p30-NO signaling in hypothyroid mice and restore osteoblast survival and activity by using cinaciguat (a cGMP-enhancing agent). However, in their study they used 12-week-old C57BL/6J mice and rendered them hypothyroid by feeding a low-iodine diet with propylthiouracil for 4 weeks, hence mice were 16 weeks old when bones were analyzed. Bones from 16-week-old mice rather model the adult than the juvenile bone. In the adult bone, hypothyroidism leads to low bone turnover, resulting in osteosclerosis, caused by a low bone formation rate via decreased osteoblast activity (Bassett *et al.*, 2010; Mosekilde, Eriksen, & Charles, 1990). Taken together, non-canonical TRα p30-NO-cGMP is highly suspicious to maintain TH-dependent bone remodeling in the adult bone. TRα p30 is expressed in $TR\alpha^{GS/GS}$ mice but absent in $TR\alpha^{0/0}$ mice, hence comparison of bones from adult $TR\alpha^{GS/GS}$ with $TR\alpha^{0/0}$ should reveal whether TRα p30 plays a role in adult bone maintenance.

Non-canonical action of TRα contributes to the regulation of heart rate

As the predominant receptor in cardiac tissue (Bookout *et al.*, 2006), TRα plays a significant role in mediating TH effects to cardiac functions. Thus, thyroid dysfunction is associated with bradycardia in hypothyroidism and tachycardia in hyperthyroidism (Klein & Danzi, 2016). Determining heart rate (HR) in untreated WT, $TR\alpha^{GS/GS}$, $TR\alpha^{0/0}$, $TR\beta^{-/-}$ and $TR\beta^{GS/GS}$ mice confirmed TRα isoform dependency, that has been described before (Gloss *et al.*, 2001; Macchia *et al.*, 2001). While HR was reduced in $TR\alpha^{0/0}$ mice, $TR\beta^{-/-}$, as well as $TR\beta^{GS/GS}$ mice displayed an increased HR. RTHβ in $TR\beta^{-/-}$ and $TR\beta^{GS/GS}$ mice results in high TH serum concentration. In turn, overstimulation of cardiac TRα through high TH serum concentration in these animals leads to an increased HR, resembling a hyperthyroid cardiac phenotype. As opposed to this, elimination of TRα in $TR\alpha^{0/0}$ mice results in a decreased HR, while TH serum concentrations are within an euthyroid range. Strikingly, HR was not reduced in $TR\alpha^{GS/GS}$ mice resembling a WT phenotype, while lacking canonical TRα action. This result strongly suggests that TRα influences HR via non-canonical signaling. Of note, expression of two so-called pacemaker channel genes, *Hcn2* and *Hcn4*, associated with bradycardia in hypothyroidism and tachycardia in hyperthyroidism (Gloss *et al.*, 2001; Le Bouter *et al.*, 2003), was identically affected

in TRα$^{GS/GS}$ and TRα$^{0/0}$ mice and hence cannot explain why HR was normal in TRα$^{GS/GS}$ mice. Moreover, it was also shown in this study that expression of TH-dependent contractile proteins Myh6 and Myh7 was altered in TRα$^{GS/GS}$ mice to the same extent as in TRα$^{0/0}$ mice. Additionally, gene expression analysis of several ion channels involved in regulation of HR confirmed these observations. These data show for the first time, that TH-dependent regulation of HR is not only attributed to canonical TRα signaling.

Introduction of the GS-mutation into the *Thra* gene loci results in a global abrogation of canonical TRα action. Thus, it remains unclear whether this chronotropic effect of non-canonical TRα action is mediated directly in cardio myocytes or rather a result of restored sympathetic nervous stimulation. ECG was measured without anesthesia and mice were under mild stress. It is possible that the response to stress or the activity of the sympathetic nervous system (SNS) is reduced in TRα$^{0/0}$ mice, but preserved in TRα$^{GS/GS}$ mice. Clarifying this issue requires *ex vivo* HR measurements via *Langendorff* apparatus or abolishing sympathetic nervous stimuli via injection of β-blocker prior to ECG measurements.

Even though NO signaling in regulation of heart rate is still controversially discussed, there is evidence for interaction of NO with the SNS (Sartori, Lepori, & Scherrer, 2005). Thus, it is possible that the TRα p30-dependent NO-cGMP-signaling mechanism is transferable to the cardiac system. Hitherto, studies regarding TRα and cardiac function were either based on KO mouse models with ubiquitous isoform depletion or on dominant TRα-mutant mice incapable of T3 binding (Macchia *et al.*, 2001; Tinnikov *et al.*, 2002; Wikstrom *et al.*, 1998). By using these models, it is impossible to detect non-canonical TRα p30 action, because either this isoform is not expressed or it lacks T3 binding and thus it cannot respond on T3. Hence, the TRα$^{GS/GS}$ mouse serves as a good model to investigate these non-canonical actions *in vivo*, but also mechanistically in primary-cell culture experiments *in vitro*.

Non-canonical TRβ action functions in an insulin-like manner

Besides the clear demonstration that negative feedback regulation of the HPT axis requires DNA binding of TRβ, this study revealed that several TH/TRβ effects were independent of DNA binding. Regarding the rapid regulation of blood glucose, the phenotype of TRβ$^{GS/GS}$ mice was indistinguishable from that of WT mice. T3 injection

acutely decreased blood glucose concentration to the same extent in WT and TRβ$^{GS/GS}$ mice, but not in TRβ$^{-/-}$ mice. These results extend the findings by Lin and Sun (Y. Lin & Sun, 2011a). They could show that a moderate dose of T3 leads to a rapid decrease in blood glucose in obese leptin receptor KO mice, as well as in lean WT mice. Moreover, they reported that this rapid T3 effect acts via PI3K-Akt signaling as it was sensitive to a PI3K inhibitor. The results of this study clearly demonstrate that this rapid T3 effect is mediated via non-canonical TRβ signaling. Even though Lin and Sun proved *in vitro* that TRα is required in L-3T3 preadipocytes to induce T3 dependent glucose uptake (Y. Lin & Sun, 2011a, 2011b). However, here a clear TRβ dependency is described as TRα cannot compensate the lack of TRβ in TRβ$^{-/-}$ mice. Additionally, the insulin-like actions of TRβ have been confirmed by studies with selective TRβ agonists (Bryzgalova *et al.*, 2008).

Noteworthy, even in 1982 Levin *et al.* observed a beneficial effect on blood glucose by feeding Zucker fat rats with a thyroid powder supplemented diet (Levin, Triscari, & Sullivan, 1982). Moreover, the results of this study now provide a mechanism for the observations made by Segal and Ingbar in 1985. They found that T3 leads to a rapid uptake of glucose in rat thymocytes and additionally this effect was independent of protein synthesis (Segal & Ingbar, 1985). Here it was shown, that blood glucose decreases within 60 minutes, so that it is doubtful that canonical nuclear TH/TR action, requiring transcription and translation, is the underlying mechanism.

The task is now to verify whether T3 leads to an increased insulin secretion by β-cells or directly mediates glucose uptake in peripheral organs like adipose tissue and skeletal muscle. For this, organ-specific TRβ$^{GS/GS}$ mice would serve as a suitable tool.

Increase in body temperature depends on non-canonical TRβ action

Phenotyping of untreated WT, TRβ$^{GS/GS}$ and TRβ$^{-/-}$ mice revealed that at an ambient temperature of 22 °C, BT_c was approximately 1 °C higher in TRβ$^{GS/GS}$ mice than that in WT and TRβ$^{-/-}$ mice. It has been known for years, that TRα is involved in temperature regulation, as TRα$^{-/-}$, as well as TRα$^{0/0}$ mice are 0.5 °C colder than WT mice (Gauthier *et al.*, 2001; Marrif *et al.*, 2005; Wikstrom *et al.*, 1998). In addition to this, a simultaneous KO of all TRα and TRβ isoforms resulted in a severely decreased BT_c (reduction of 3.5 to 4 °C) (Gauthier *et al.*, 2001). Hence, participation

of TRβ in the TH-dependent processes of BT_c regulation is obvious. For excluding any compensatory or interfering effects of TRα the BT_c measurement was repeated in a $TR\alpha^{0/0}$ genetic background. The slight BT_c decrease in $TR\alpha^{0/0}$ mice, as well as the severe drop in BT_c in $TR\alpha^{0/0}$;$TR\beta^{-/-}$ mice could be confirmed in this study. Strikingly, again BT_c of $TR\alpha^{0/0}$;$TR\beta^{GS/GS}$ mice was about 1 °C than BT_c of their $TR\beta^{-/-}$ counterparts. These data suggest a TRα-independent contribution of non-canonical TRβ action to thermogenesis.

Noteworthy, on the first view it seems confusing that BT_c of $TR\beta^{-/-}$ is not different from WT mice but BT_c of $TR\beta^{GS/GS}$ is elevated in comparison to WT mice. An explanation for this can be found in the disruption of the negative feedback loop of the HPT axis observed for $TR\beta^{-/-}$ and $TR\beta^{GS/GS}$ mice. As described above, loss on canonical action of TRβ results in increased TH serum concentration in $TR\beta^{-/-}$ and $TR\beta^{GS/GS}$ mice. Thus, these genotypes exhibit a hyperthyroid TH serum status. Consequently, all TRα mediated effects in these mice appear like under hyperthyroidism e.g. increased HR. But of note, also all non-canonical TRβ actions in $TR\beta^{GS/GS}$ mice are enhanced, because even though the GS-mutation abrogates canonical action of TRβ, non-canonical action is unaffected. Thus, higher TH serum concentrations lead to amplified non-canonical actions in $TR\beta^{GS/GS}$ mice, which might explain the difference in BT_c between WT and $TR\beta^{GS/GS}$ mice.

Up to now, the complex processes of TH-induced thermogenesis are not fully understood. The classical idea of thyroid thermogenesis was that high TH serum concentrations increase the basal metabolic rate in peripheral tissues. It is suggested that T3 increases expression and activation of several proteins and enzymes like Na^+-K^+-ATPase, glycerol phosphate dehydrogenase in skeletal muscle and uncoupling protein 3 (UCP3) in skeletal muscle, resulting in an increase heat production (Cannon & Nedergaard, 2010). However, the mechanism behind this is still unknown and adding TH directly to cells has not resulted in an increased heat production. Hence, leading to the conclusion that the mechanisms behind TH-induced thermogenesis are complex and not restricted to direct TH action in peripheral tissue (reviewed in Silva, 2006).

In mammals, adaptive thermogenesis takes place in BAT (Cannon & Nedergaard, 2004; Oelkrug, Polymeropoulos, & Jastroch, 2015). Recently, Lopez *et al.* showed that they could activate BAT and induce browning of WAT by intraventricular cerebral injection of T3 into the ventromedial hypothalamus (Alvarez-Crespo *et al.*, 2016). A

general marker of BAT activation and browning of WAT is the increased expression of UCP1. UCP1 bypasses the oxidative phosphorylation by forming an ion channel for protons (H^+) to reenter the mitochondrial matrix directly and not via the ATPsynthase. The uncoupling of ATPsynthase leads to heat dissipation as energy is not stored as ATP anymore. It was shown that expression of UCP1 can occur in a TH-dependent manner. The beneficial effect of TH and TH analogous like GC-1 (a selective TRβ agonist, also known as sobetirome) on BAT activation and WAT browning doubtlessly demonstrate the close dependency between TH and activation of adipose tissue dependent thermogenesis (Krause *et al.*, 2015; J. Z. Lin *et al.*, 2015).

The challenge is now to determine whether non-canonical action of TRβ contributes to the thermogenic program directly in BAT or centrally in the hypothalamus. These possibilities are not mutually exclusive.

Triglyceride synthesis is increased in absence of non-canonical action of TRβ

In mice and humans, hypothyroidism and resistance to TH is associated with high TG serum concentration (Araki *et al.*, 2009; Petersson & Kjellstrom, 2001). Moreover, the hepatic lipid metabolism is a major physiological target of TH and has been studied profoundly (Elbers *et al.*, 2016; Gauthier *et al.*, 2010; Pramfalk *et al.*, 2011; Vatner *et al.*, 2013; Yao *et al.*, 2014; Zhu & Cheng, 2010). However, it remained unresolved, whether the underlying mechanism is canonical or non-canonical TRβ signaling.

It was not surprising to find increased TG concentration in $TR\beta^{-/-}$ mice; which are resistant to TH. But interestingly, $TR\beta^{GS/GS}$ mice are also resistant to TH on the pituitary level and, yet, serum and liver TG concentrations are normal like in WT mice. This phenotype similarity between $TR\beta^{GS/GS}$ and WT mice demonstrates that presence of non-canonical signaling alone suffices to produce a WT phenotype. Hence, this study provides evidence that TG synthesis is non-canonically regulated by T3 and TRβ, because TG concentrations were significantly elevated in the absence of TRβ, but not in WT and $TR\beta^{GS/GS}$ mice.

Expression analysis of genes encoding for lipogenic enzymes and proteins being involved in *de novo* fatty acid synthesis revealed a systemically altered expression in $TR\beta^{-/-}$ mice. Thus, gene expression correlates with TG concentration in serum and liver. Microarray analysis revealed that the GS-mutation abrogates DNA-binding

ability of TR on a genome-wide scale. Hence, a difference in gene expression between TRβ$^{-/-}$ and TRβ$^{GS/GS}$ mice was not expected. But it must be considered, that activation of second messenger signaling pathways in the cytoplasm might also end up with changes in gene expression. Of course, activation of the PI3K-Akt pathway also has genomic targets (Guertin *et al.*, 2006; Hemmings & Restuccia, 2012; Link *et al.*, 2009). Even though microarray analysis of short-term T3-treated mice (6 h) could not confirm non-canonical TH target genes in this study, Grontved *et al.* demonstrated the enrichment of regulatory DNA motifs different from TREs, in long-term T3-treated mice (Grontved *et al.*, 2015).

Spot14 (the gene product of *Thrsp*) is involved in regulating lipogenesis and expression of *Thrsp* is known to be regulated by TH and nutrients (Weiss *et al.*, 1998; J. Wu *et al.*, 2013). Depletion of TRβ results in loss of canonical TRE-dependent gene repression, which might explain the higher expression levels of *Thrsp* in livers of TRβ$^{-/-}$ mice. The GS-mutation abrogates DNA binding, thus one would expect higher expression levels of *Thrsp*, too. Interestingly, expression of *Thrsp* was lower in livers of TRβ$^{GS/GS}$ mice, which might contribute to the low TG concentration in liver and serum. For genes like *Fasn* and *Acc1* the presence of TREs has been proven previously (Joseph *et al.*, 2002; Xiong, 1998; Zhang, Yin, & Hillgartner, 2001). Hence, it is possible that TRβ deficiency in TRβ$^{-/-}$ mice leads to unoccupied and therefore unrepressed TREs, resulting in higher expression of these genes.

Interestingly, Hashimoto *et al.* could show that *Scd1* expression is negatively regulated by TRβ in a DNA-binding independent manner (Hashimoto *et al.*, 2013). These findings are supported as *Scd1* expression in TRβ$^{GS/GS}$ mice remained repressed like in WT mice. Noteworthy, Hashimoto *et al.* reported a strong decrease in *Scd1* expression in hyperthyroid mice compared to euthyroid mice. Thus, one would expect a decreased *Scd1* expression in TRβ$^{GS/GS}$ mice as they have 2.5-fold higher TH serum concentrations as WT mice. In contrast to this, *Scd1* expression in TRβ$^{GS/GS}$ mice did not differ from euthyroid WT mice. However, in the study of Hashimoto *et al.*, mice were i.p. injected with 10 µg/100 g BW, which resulted in free T3 serum concentrations which were three times higher than in untreated TRβ$^{GS/GS}$ mice. This might explain the difference between Hashimoto`s observations and the results presented here. However, *Scd1* plays an important role in the regulation of lipid metabolism and energy expenditure (Dobrzyn & Ntambi, 2005; Lee *et al.*, 2004). Low TG concentration was associated with a Scd1-KO genotype and a liver-specific

KO of Scd1 protected mice from a high-carbohydrate diet induced obesity (Miyazaki *et al.*, 2004; Miyazaki *et al.*, 2007). Therefore, it is possible that functional non-canonical TRβ signaling in $TR\beta^{GS/GS}$ mice could partly protect from a high-carbohydrate induced obesity, as expression of *Scd1* was decreased in livers of $TR\beta^{GS/GS}$ mice.

Even though this study demonstrates that loss of non-canonical action of TRβ is associated with an increase in liver and serum TG concentrations, the underlying cause remains unresolved. On the one hand, altered gene expression found in livers of $TR\beta^{-/-}$ mice can lead to higher TG concentrations but on the other hand, one cannot exclude that the origin of this ubiquitous metabolic phenotype could be found in other tissues, e.g. adipose tissue.

An evolutionary cause might link non-canonical TRβ action and thermogenesis

It was shown that non-canonical action of TRβ is involved in the regulation of body temperature and maintaining energy demand in parts of glucose utilization and regulation of TG concentrations. TRα was unable to compensate for these effects in $TR\beta^{-/-}$ mice suggesting a clear isoform-specific separation.

Support for this interpretation may be derived from evolution: TH stimulates thermogenesis in homeothermy, a feature of mammals. Interestingly, the tyrosine motifs in TRβ, that are required for non-canonical PI3K activation by TRβ, are found in all published mammalian TRβ ortholog sequences, but not in that of poikilothermic animals, such as alligator, clawed toad or zebrafish (Martin *et al.*, 2014). Hence, non-canonical TR signaling appears to be a newly acquired function in evolution that provides mammals with additional means for TH to regulate energy metabolism and thermogenesis. Moreover, as development of non-canonical TR signaling is found relatively late in evolution, long after TRs assumed their canonical role as ligand-dependent transcription factors, may also explain why canonical and non-canonical effects on physiology are so clearly separable from each other.

Possible tissue-specific mechanisms for negative regulation of gene expression

Still a matter of controversy is negative regulation of gene expression by TRs, especially whether binding of TRs to DNA is required or not. The fact that TSH is elevated in $TR\beta^{-/-}$ and $TR\beta^{GS/GS}$ mice clearly demonstrates that TSH suppression requires DNA binding, which is in agreement with previous reports (Shibusawa, Hashimoto, *et al.*, 2003). But results from $TR\beta^{GS/GS}$ mice suggest that additional, non-canonical mechanisms for negative regulation by TH may exist: TH represses *Scd1* expression (Hashimoto *et al.*, 2013; Waters, Miller, & Ntambi, 1997), which does not require DNA binding of TRβ (Hashimoto *et al.*, 2013). Hepatic *Scd1* expression was elevated only in $TR\beta^{-/-}$ mice, but not in WT and $TR\beta^{GS/GS}$ mice. Therefore, negative regulation of *Scd1* expression *in vivo* does not require DNA binding of TRβ. Interestingly, recent ChIP-seq analyses of TH-regulated genes revealed significant TRβ enrichment near positively regulated genes, but less or no enrichment of TRβ at negatively regulated genes, also suggesting that DNA binding of TRβ may not always be required (Ayers *et al.*, 2014; Grontved *et al.*, 2015; Ramadoss *et al.*, 2014). The possibility of several mechanisms for negative gene regulation by TRs, canonical (dependent on DNA binding; e.g. for *Tshb*) and non-canonical (independent of DNA binding; e.g. for *Scd1*), should be considered. Noteworthy, it was shown *in vivo* that expression of *Scd1*, *Fasn*, *Thrsp* and *Gpam* was increased in livers of mice expressing a liver-specific mutant of NCoR (L-NCoRΔID) which cannot interact with TR (Astapova *et al.*, 2008). The hepatic phenotypical accordance between $TR\beta^{-/-}$ mice and L-NCoRΔID mice and discordance to WT and $TR\beta^{GS/GS}$ mice suggest that NCoR/TR interaction is necessary for negative regulation, while DNA-binding ability of TR might only play a secondary role.

Limitations of the study

Generation of the two TR^{GS} mouse models was successful and fulfilled the requirements to study physiological non-canonical TH effects separately from canonical TR actions. However, these models have its limitations.

Experiments of this study do not yet allow determining the precise mechanism of non-canonical TR action in $TR\alpha^{GS/GS}$ and $TR\beta^{GS/GS}$ mice for each phenotype. The best studied non-canonical action of TRβ is rapid activation of PI3K (Cao *et al.*, 2005;

Martin *et al.*, 2014; Simoncini *et al.*, 2000; Storey *et al.*, 2006): cytosolic TRβ simultaneously binds p85α and another kinase, Lyn, which allows Lyn to activate p85α and consequently activates PI3K (Martin *et al.*, 2014). TRα also promotes signaling pathway activation (Cao *et al.*, 2009; Hiroi *et al.*, 2006), possibly as a short TRα p30 variant, activating ERK and PI3K after T3 binding (Kalyanaraman *et al.*, 2014). The underlying mechanism may not be the same for all physiological consequences of non-canonical TR action.

Theoretically, loss of canonical action of TRβ could be compensated by presence of the intact TRα and *vice versa*. This study demonstrated that this is not the case: the temperature difference between $TR\beta^{GS/GS}$ and $TR\beta^{-/-}$ mice is independent from the presence of TRα, HR is reduced in $TR\alpha^{0/0}$ mice despite presence of TRβ and glucose is not reduced by T3 in $TR\beta^{-/-}$ mice despite presence of TRα.

The regulation of physiological functions like thermogenesis and HR require a complex interaction between several different organs. Thus, a mouse model with a global KO or mutant TR will, for some reason, not suffice to determine the organ of origin of a certain TH-dependent phenotype. To do so, organ-specific KO and mutant KI-mouse models would be the model of choice.

Conclusion and Future Perspective

Since the discovery of TRs in the early 80´s, the field of TR research has dramatically evolved and gained substantial knowledge to the understanding of TH-mediated physiological functions, as well as diseases related to disorders in TH/TR signaling. The regulations of organ development, growth, body temperature, HR and metabolism have been attributed to TRα and TRβ isoforms. Throughout the years, transcriptional regulation by TRs has been established as the paradigm of TR signaling. Thus, the dogma of TR signaling was considered requiring transcription and translation. Hitherto, this paradigm is still valid, despite the fact that several TH effects are not compatible with the current paradigm of TR action. Even though it was proven that TRs could activate second messenger signaling cascades in the cytoplasm, evidence for a physiological relevance of this non-canonical TR signaling was still missing, mainly because suitable mouse models to study non-canonical TR action separately from canonical signaling did not exist.

The results of the present study indicate that the $TR\alpha^{GS}$ and the $TR\beta^{GS}$ mouse models serves as good tools for distinguishing between canonical and non-canonical TR action *in vivo.* Abrogation of DNA-binding ability via mutating the DBD of the receptors did not result in a full-functional-loss of TR action, as $TR\alpha^{GS/GS}$ and $TR\beta^{GS/GS}$ mice were phenotypically different from $TR\alpha^{0/0}$ and $TR\beta^{-/-}$ mice. By comparison of these mouse models, TH/TR mediated effects could be attributed to either canonical or non-canonical signaling and furthermore a distinct isoform-specific separation was possible.

While growth and bone development required DNA binding of TRα, regulation of HR did not. Similar results were obtained for TRβ. Loss of DNA binding resulted in disruption of the negative feedback loop of the HPT axis, whereas the rapid T3-dependent effect on lowering blood glucose and TG concentrations in serum and liver were preserved in $TR\beta^{GS/GS}$ mice (Figure 31). Although, determining the organs of origin, as well as the exact underlying molecular mechanisms could not be achieved in this study, *in vivo* evidence for physiological relevance of non-canonical TR signaling was clearly demonstrated. Non-canonical TR signaling mainly influences cardiometabolic functions as it promotes the conversion of energy into heat with increased body temperature, apparently increased glucose utilization, reduced storage of energy in form of TG and contributing to the regulation of HR.

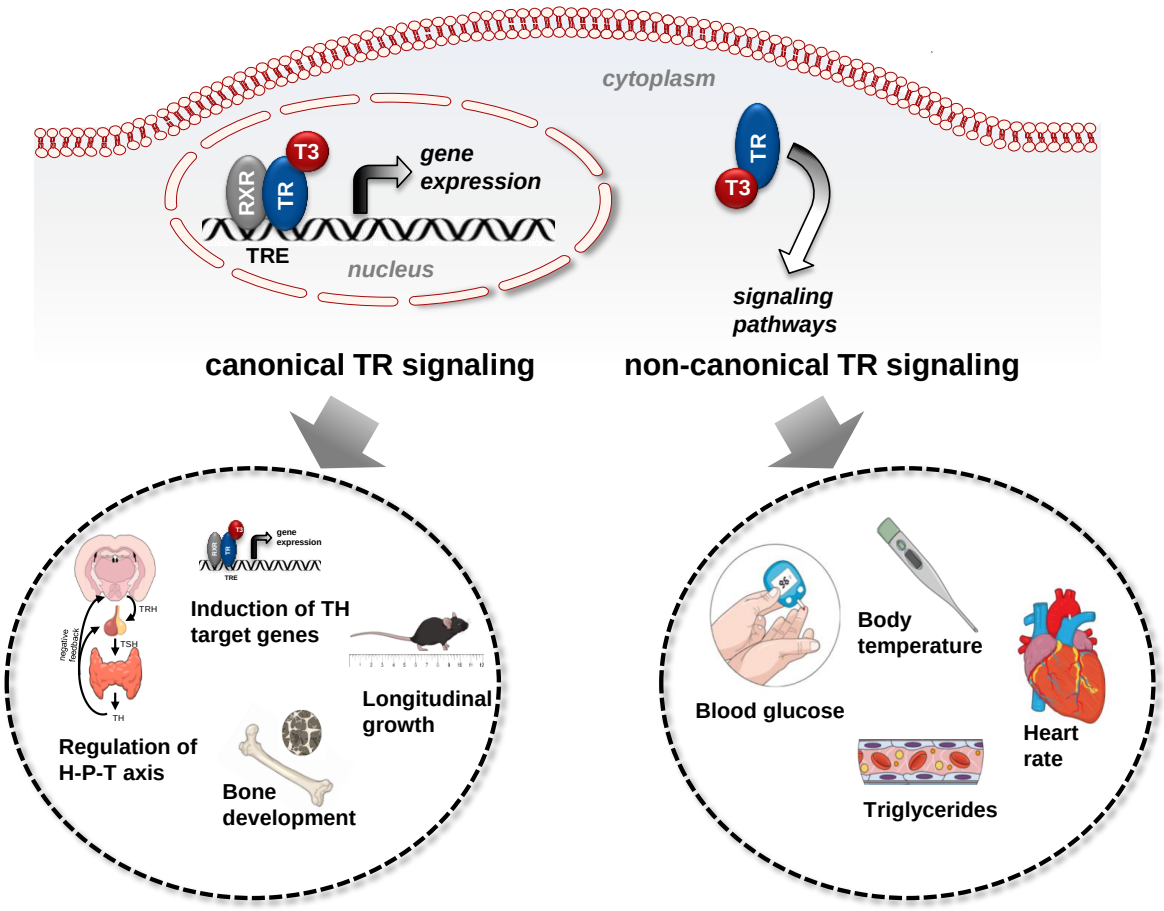

Figure 31: Shifting the current paradigm of TR action. *Non-canonical of action TRs is physiological relevant. For certain TH effects, there are clear separations between canonically and non-canonically mediated TR effects.*

In conclusion, this study provides evidence from TRα$^{GS/GS}$ and TRβ$^{GS/GS}$ mice that TRs mediate physiological effects without DNA binding, representing the first comprehensive demonstration of non-canonical action of TRα and TRβ *in vivo*. This expands the role of TRα and TRβ beyond the current paradigm with profound implications for their role in physiology and opens new possibilities for understanding and treating TH/TR related diseases more precisely.

References

Abel, E. D., Ahima, R. S., Boers, M. E., Elmquist, J. K., & Wondisford, F. E. (2001). Critical role for thyroid hormone receptor beta2 in the regulation of paraventricular thyrotropin-releasing hormone neurons. *The Journal of clinical investigation, 107*(8), 1017-1023. doi:10.1172/jci10858

Alvarez-Crespo, M., Csikasz, R. I., Martinez-Sanchez, N., Dieguez, C., Cannon, B., Nedergaard, J., & Lopez, M. (2016). Essential role of UCP1 modulating the central effects of thyroid hormones on energy balance. *Mol Metab, 5*(4), 271-282. doi:10.1016/j.molmet.2016.01.008

Apriletti, J. W., Ribeiro, R. C., Wagner, R. L., Feng, W., Webb, P., Kushner, P. J., Baxter, J. D. (1998). Molecular and structural biology of thyroid hormone receptors. *Clin Exp Pharmacol Physiol Suppl, 25*, S2-11.

Araki, O., Ying, H., Zhu, X. G., Willingham, M. C., & Cheng, S. Y. (2009). Distinct dysregulation of lipid metabolism by unliganded thyroid hormone receptor isoforms. *Mol Endocrinol, 23*(3), 308-315. doi:10.1210/me.2008-0311

Astapova, I., Lee, L. J., Morales, C., Tauber, S., Bilban, M., & Hollenberg, A. N. (2008). The nuclear corepressor, NCoR, regulates thyroid hormone action in vivo. *Proc Natl Acad Sci U S A, 105*(49), 19544-19549. doi:10.1073/pnas.0804604105

Ayers, S., Switnicki, M. P., Angajala, A., Lammel, J., Arumanayagam, A. S., & Webb, P. (2014). Genome-wide binding patterns of thyroid hormone receptor beta. *PLoS One, 9*(2), e81186. doi:10.1371/journal.pone.0081186

Bassett, J. H., Boyde, A., Howell, P. G., Bassett, R. H., Galliford, T. M., Archanco, M., Williams, G. R. (2010). Optimal bone strength and mineralization requires the type 2 iodothyronine deiodinase in osteoblasts. *Proc Natl Acad Sci U S A, 107*(16), 7604-7609. doi:10.1073/pnas.0911346107

Bassett, J. H., Boyde, A., Zikmund, T., Evans, H., Croucher, P. I., Zhu, X., Williams, G. R. (2014). Thyroid Hormone Receptor alpha Mutation Causes a Severe and Thyroxine-Resistant Skeletal Dysplasia in Female Mice. *Endocrinology, 155*(9), 3699-3712. doi:10.1210/en.2013-2156

Bassett, J. H., Harvey, C. B., & Williams, G. R. (2003). Mechanisms of thyroid hormone receptor-specific nuclear and extra nuclear actions. *Mol Cell Endocrinol, 213*(1), 1-11. doi:10.1016/j.mce.2003.10.033

Bassett, J. H., Nordstrom, K., Boyde, A., Howell, P. G., Kelly, S., Vennstrom, B., & Williams, G. R. (2007). Thyroid status during skeletal development determines adult bone structure and mineralization. *Mol Endocrinol, 21*(8), 1893-1904. doi:10.1210/me.2007-0157

Bassett, J. H., Williams, A. J., Murphy, E., Boyde, A., Howell, P. G., Swinhoe, R., Williams, G. R. (2008). A lack of thyroid hormones rather than excess thyrotropin causes abnormal skeletal development in hypothyroidism. *Mol Endocrinol, 22*(2), 501-512. doi:10.1210/me.2007-0221

Bassett, J. H., & Williams, G. R. (2016). Role of Thyroid Hormones in Skeletal Development and Bone Maintenance. *Endocr Rev, 37*(2), 135-187. doi:10.1210/er.2015-1106

Bates, J. M., St Germain, D. L., & Galton, V. A. (1999). Expression profiles of the three iodothyronine deiodinases, D1, D2, and D3, in the developing rat. *Endocrinology, 140*(2), 844-851. doi:10.1210/endo.140.2.6537

Baumann, C. T., Maruvada, P., Hager, G. L., & Yen, P. M. (2001). Nuclear cytoplasmic shuttling by thyroid hormone receptors. multiple protein interactions are required for nuclear retention. *The Journal of biological chemistry, 276*(14), 11237-11245. doi:10.1074/jbc.M011112200

Beato, M., Herrlich, P., & Schutz, G. (1995). Steroid hormone receptors: many actors in search of a plot. *Cell, 83*(6), 851-857.

Bertrand, C., Blanchet, E., Pessemesse, L., Annicotte, J. S., Feillet-Coudray, C., Chabi, B., Casas, F. (2013). Mice lacking the p43 mitochondrial T3 receptor become glucose intolerant and insulin resistant during aging. *PLoS One, 8*(9), e75111. doi:10.1371/journal.pone.0075111

Bianco, A. C., Anderson, G., Forrest, D., Galton, V. A. D., Gereben, B., Kim, B. W., Williams, G. (2013). American Thyroid Association Guide to Investigating Thyroid Hormone Economy and Action in Rodent and Cell Models. *Thyroid*. doi:10.1089/thy.2013.0109

Bianco, A. C., & Kim, B. W. (2006). Deiodinases: implications of the local control of thyroid hormone action. *The Journal of clinical investigation, 116*(10), 2571-2579. doi:10.1172/JCI29812

Bianco, A. C., Salvatore, D., Gereben, B., Berry, M. J., & Larsen, P. R. (2002). Biochemistry, cellular and molecular biology, and physiological roles of the iodothyronine selenodeiodinases. *Endocr Rev, 23*(1), 38-89. doi:10.1210/edrv.23.1.0455

Bochukova, E., Schoenmakers, N., Agostini, M., Schoenmakers, E., Rajanayagam, O., Keogh, J. M., Chatterjee, K. (2012). A mutation in the thyroid hormone receptor alpha gene. *The New England journal of medicine, 366*(3), 243-249. doi:10.1056/NEJMoa1110296

Bookout, A. L., Jeong, Y., Downes, M., Yu, R. T., Evans, R. M., & Mangelsdorf, D. J. (2006). Anatomical profiling of nuclear receptor expression reveals a hierarchical transcriptional network. *Cell, 126*(4), 789-799. doi:10.1016/j.cell.2006.06.049

Bryzgalova, G., Effendic, S., Khan, A., Rehnmark, S., Barbounis, P., Boulet, J., Grover, G. J. (2008). Anti-obesity, anti-diabetic, and lipid lowering effects of the thyroid receptor beta subtype selective agonist KB-141. *J Steroid Biochem Mol Biol, 111*(3-5), 262-267. doi:10.1016/j.jsbmb.2008.06.010

Bustin, S. A., Benes, V., Garson, J. A., Hellemans, J., Huggett, J., Kubista, M., Wittwer, C. T. (2009). The MIQE guidelines: minimum information for publication of quantitative real-time PCR experiments. *Clin Chem, 55*(4), 611-622. doi:10.1373/clinchem.2008.112797

Cannon, B., & Nedergaard, J. (2004). Brown adipose tissue: function and physiological significance. *Physiol Rev, 84*(1), 277-359. doi:10.1152/physrev.00015.2003

Cannon, B., & Nedergaard, J. (2010). Thyroid hormones: igniting brown fat via the brain. *Nat Med, 16*(9), 965-967. doi:10.1038/nm0910-965

Cao, X., Kambe, F., Moeller, L. C., Refetoff, S., & Seo, H. (2005). Thyroid hormone induces rapid activation of Akt/protein kinase B-mammalian target of rapamycin-p70S6K cascade through phosphatidylinositol 3-kinase in human fibroblasts. *Mol Endocrinol, 19*(1), 102-112. doi:10.1210/me.2004-0093

Cao, X., Kambe, F., Yamauchi, M., & Seo, H. (2009). Thyroid-hormone-dependent activation of the phosphoinositide 3-kinase/Akt cascade requires Src and enhances neuronal survival. *Biochem J, 424*(2), 201-209. doi:10.1042/BJ20090643

Carbery, I. D., Ji, D., Harrington, A., Brown, V., Weinstein, E. J., Liaw, L., & Cui, X. (2010). Targeted genome modification in mice using zinc-finger nucleases. *Genetics, 186*(2), 451-459. doi:10.1534/genetics.110.117002

Carvalho, D. P., & Dupuy, C. (2013). Role of the NADPH Oxidases DUOX and NOX4 in Thyroid Oxidative Stress. *Eur Thyroid J, 2*(3), 160-167. doi:10.1159/000354745

Chassande, O., Fraichard, A., Gauthier, K., Flamant, F., Legrand, C., Savatier, P., Samarut, J. (1997). Identification of transcripts initiated from an internal promoter in the c-erbA alpha locus that encode inhibitors of retinoic acid receptor-alpha and triiodothyronine receptor activities. *Mol Endocrinol, 11*(9), 1278-1290. doi:10.1210/mend.11.9.9972

Chatonnet, F., Guyot, R., Benoit, G., & Flamant, F. (2013). Genome-wide analysis of thyroid hormone receptors shared and specific functions in neural cells. *Proc Natl Acad Sci U S A, 110*(8), E766-775. doi:10.1073/pnas.1210626110

Chen, Y., & Young, M. A. (2010). Structure of a thyroid hormone receptor DNA-binding domain homodimer bound to an inverted palindrome DNA response element. *Mol Endocrinol, 24*(8), 1650-1664. doi:10.1210/me.2010-0129

Columbano, A., Simbula, M., Pibiri, M., Perra, A., Deidda, M., Locker, J., Pisanu, A., Uccheddu, A., Ledda-Columbano, G. M. (2008). Triiodothyronine stimulates hepatocyte proliferation in two models of impaired liver regeneration. *Cell Prolif, 41*(3), 521-531. doi:10.1111/j.1365-2184.2008.00532.x

Cui, X., Ji, D., Fisher, D. A., Wu, Y., Briner, D. M., & Weinstein, E. J. (2011). Targeted integration in rat and mouse embryos with zinc-finger nucleases. *Nat Biotechnol, 29*(1), 64-67. doi:10.1038/nbt.1731

Denver, R. J., Ouellet, L., Furling, D., Kobayashi, A., Fujii-Kuriyama, Y., & Puymirat, J. (1999). Basic transcription element-binding protein (BTEB) is a thyroid hormone-regulated gene in the developing central nervous system. Evidence for a role in neurite outgrowth. *The Journal of biological chemistry, 274*(33), 23128-23134.

Desjardin, C., Charles, C., Benoist-Lasselin, C., Riviere, J., Gilles, M., Chassande, O., Schibler, L. (2014). Chondrocytes play a major role in the stimulation of bone growth by thyroid hormone. *Endocrinology*, en20141109. doi:10.1210/en.2014-1109

Di Cosmo, C., Liao, X. H., Dumitrescu, A. M., Philp, N. J., Weiss, R. E., & Refetoff, S. (2010). Mice deficient in MCT8 reveal a mechanism regulating thyroid hormone secretion. *The Journal of clinical investigation, 120*(9), 3377-3388. doi:10.1172/JCI42113

Dobrzyn, A., & Ntambi, J. M. (2005). The role of stearoyl-CoA desaturase in the control of metabolism. *Prostaglandins Leukot Essent Fatty Acids, 73*(1), 35-41. doi:10.1016/j.plefa.2005.04.011

Dugas, J. C., Ibrahim, A., & Barres, B. A. (2012). The T3-induced gene KLF9 regulates oligodendrocyte differentiation and myelin regeneration. *Mol Cell Neurosci, 50*(1), 45-57. doi:10.1016/j.mcn.2012.03.007

Edwards, J. G., Bahl, J. J., Flink, I. L., Cheng, S. Y., & Morkin, E. (1994). Thyroid hormone influences beta myosin heavy chain (beta MHC) expression. *Biochemical and biophysical research communications, 199*(3), 1482-1488. doi:10.1006/bbrc.1994.1398

Elbers, L. P., Moran, C., Gerdes, V. E., van Zaane, B., Meijers, J., Endert, E., Fliers, E. (2016). The Hypercoagulable state in Hyperthyroidism is mediated via the Thyroid Hormone beta Receptor pathway. *Eur J Endocrinol*. doi:10.1530/eje-15-1249

Engels, K., Rakov, H., Zwanziger, D., Hones, G. S., Rehders, M., Brix, K., Fuhrer, D. (2016). Efficacy of protocols for induction of chronic hyperthyroidism in male and female mice. *Endocrine*. doi:10.1007/s12020-016-1020-8

Feng, X., Jiang, Y., Meltzer, P., & Yen, P. M. (2000). Thyroid hormone regulation of hepatic genes in vivo detected by complementary DNA microarray. *Mol Endocrinol, 14*(7), 947-955.

Flores-Morales, A., Gullberg, H., Fernandez, L., Stahlberg, N., Lee, N. H., Vennstrom, B., & Norstedt, G. (2002). Patterns of liver gene expression governed by TRbeta. *Mol Endocrinol, 16*(6), 1257-1268.

Forrest, D., Erway, L. C., Ng, L., Altschuler, R., & Curran, T. (1996). Thyroid hormone receptor beta is essential for development of auditory function. *Nat Genet, 13*(3), 354-357. doi:10.1038/ng0796-354

Forrest, D., Hanebuth, E., Smeyne, R. J., Everds, N., Stewart, C. L., Wehner, J. M., & Curran, T. (1996). Recessive resistance to thyroid hormone in mice lacking thyroid hormone receptor beta: evidence for tissue-specific modulation of receptor function. *EMBO J, 15*(12), 3006-3015.

Forrest, D., Sjoberg, M., & Vennstrom, B. (1990). Contrasting developmental and tissue-specific expression of alpha and beta thyroid hormone receptor genes. *EMBO J, 9*(5), 1519-1528.

Fraichard, A., Chassande, O., Plateroti, M., Roux, J. P., Trouillas, J., Dehay, C., Samarut, J. (1997). The T3R alpha gene encoding a thyroid hormone receptor is essential for post-natal development and thyroid hormone production. *EMBO J, 16*(14), 4412-4420. doi:10.1093/emboj/16.14.4412

Friedrichs, B., Tepel, C., Reinheckel, T., Deussing, J., von Figura, K., Herzog, V., Brix, K. (2003). Thyroid functions of mouse cathepsins B, K, and L. *The Journal of clinical investigation, 111*(11), 1733-1745. doi:10.1172/jci15990

Furuya, F., Lu, C., Willingham, M. C., & Cheng, S. Y. (2007). Inhibition of phosphatidylinositol 3-kinase delays tumor progression and blocks metastatic spread in a mouse model of thyroid cancer. *Carcinogenesis, 28*(12), 2451-2458. doi:10.1093/carcin/bgm174

Gauthier, K., Billon, C., Bissler, M., Beylot, M., Lobaccaro, J. M., Vanacker, J. M., & Samarut, J. (2010). Thyroid hormone receptor beta (TRbeta) and liver X receptor (LXR) regulate carbohydrate-response element-binding protein (ChREBP) expression in a tissue-selective manner. *The Journal of biological chemistry, 285*(36), 28156-28163. doi:10.1074/jbc.M110.146241

Gauthier, K., Chassande, O., Plateroti, M., Roux, J. P., Legrand, C., Pain, B., Samarut, J. (1999). Different functions for the thyroid hormone receptors TRalpha and TRbeta in the control of thyroid hormone production and post-natal development. *EMBO J, 18*(3), 623-631. doi:10.1093/emboj/18.3.623

Gauthier, K., Plateroti, M., Harvey, C. B., Williams, G. R., Weiss, R. E., Refetoff, S., Chassande, O. (2001). Genetic analysis reveals different functions for the products of the thyroid hormone receptor alpha locus. *Molecular and cellular biology, 21*(14), 4748-4760. doi:10.1128/MCB.21.14.4748-4760.2001

Gil-Ibanez, P., Bernal, J., & Morte, B. (2014). Thyroid hormone regulation of gene expression in primary cerebrocortical cells: role of thyroid hormone receptor subtypes and interactions with retinoic Acid and glucocorticoids. *PLoS One, 9*(3), e91692. doi:10.1371/journal.pone.0091692

Gil-Ibanez, P., Morte, B., & Bernal, J. (2013). Role of thyroid hormone receptor subtypes alpha and beta on gene expression in the cerebral cortex and striatum of postnatal mice. *Endocrinology, 154*(5), 1940-1947. doi:10.1210/en.2012-2189

Gloss, B., Trost, S., Bluhm, W., Swanson, E., Clark, R., Winkfein, R., Dillmann, W. (2001). Cardiac ion channel expression and contractile function in mice with deletion of thyroid hormone receptor alpha or beta. *Endocrinology, 142*(2), 544-550. doi:10.1210/endo.142.2.7935

Gomes, A. R., Zhao, F., & Lam, E. W. (2013). Role and regulation of the forkhead transcription factors FOXO3a and FOXM1 in carcinogenesis and drug resistance. *Chin J Cancer, 32*(7), 365-370. doi:10.5732/cjc.012.10277

Grontved, L., Waterfall, J. J., Kim, D. W., Baek, S., Sung, M. H., Zhao, L., Cheng, S. Y. (2015). Transcriptional activation by the thyroid hormone receptor through ligand-dependent receptor recruitment and chromatin remodelling. *Nat Commun, 6*, 7048. doi:10.1038/ncomms8048

Guertin, D. A., Stevens, D. M., Thoreen, C. C., Burds, A. A., Kalaany, N. Y., Moffat, J., Sabatini, D. M. (2006). Ablation in mice of the mTORC components raptor, rictor, or mLST8 reveals that mTORC2 is required for signaling to Akt-FOXO and PKCalpha, but not S6K1. *Dev Cell, 11*(6), 859-871. doi:10.1016/j.devcel.2006.10.007

Gullberg, H., Rudling, M., Forrest, D., Angelin, B., & Vennstrom, B. (2000). Thyroid hormone receptor beta-deficient mice show complete loss of the normal cholesterol 7alpha-hydroxylase (CYP7A) response to thyroid hormone but display enhanced resistance to dietary cholesterol. *Mol Endocrinol, 14*(11), 1739-1749.

Hard, T., Kellenbach, E., Boelens, R., Maler, B. A., Dahlman, K., Freedman, L. P., Kaptein, R. (1990). Solution structure of the glucocorticoid receptor DNA-binding domain. *Science, 249*(4965), 157-160.

Hashimoto, K., Ishida, E., Miura, A., Ozawa, A., Shibusawa, N., Satoh, T., Mori, M. (2013). Human stearoyl-CoA desaturase 1 (SCD-1) gene expression is negatively regulated by thyroid hormone without direct binding of thyroid hormone receptor to the gene promoter. *Endocrinology, 154*(1), 537-549. doi:10.1210/en.2012-1559

Hemmings, B. A., & Restuccia, D. F. (2012). PI3K-PKB/Akt pathway. *Cold Spring Harb Perspect Biol, 4*(9), a011189. doi:10.1101/cshperspect.a011189

Hiroi, Y., Kim, H. H., Ying, H., Furuya, F., Huang, Z., Simoncini, T., Liao, J. K. (2006). Rapid nongenomic actions of thyroid hormone. *Proc Natl Acad Sci U S A, 103*(38), 14104-14109. doi:10.1073/pnas.0601600103

Hocman, G. (1981). Human thyroxine binding globulin (TBG). *Rev Physiol Biochem Pharmacol, 91*, 45-89.

Hollenberg, A. N., Monden, T., & Wondisford, F. E. (1995). Ligand-independent and -dependent functions of thyroid hormone receptor isoforms depend upon their distinct amino termini. *The Journal of biological chemistry, 270*(24), 14274-14280.

Hunziker, E. B. (1994). Mechanism of longitudinal bone growth and its regulation by growth plate chondrocytes. *Microsc Res Tech, 28*(6), 505-519. doi:10.1002/jemt.1070280606

Iwaki, H., Sasaki, S., Matsushita, A., Ohba, K., Matsunaga, H., Misawa, H., Suda, T. (2014). Essential role of TEA domain transcription factors in the negative regulation of the MYH 7 gene by thyroid hormone and its receptors. *PLoS One, 9*(4), e88610. doi:10.1371/journal.pone.0088610

Izumo, S., & Mahdavi, V. (1988). Thyroid hormone receptor alpha isoforms generated by alternative splicing differentially activate myosin HC gene transcription. *Nature, 334*(6182), 539-542. doi:10.1038/334539a0

Jakacka, M. (2002). An Estrogen Receptor (ER)alpha Deoxyribonucleic Acid-Binding Domain Knock-In Mutation Provides Evidence for Nonclassical ER Pathway Signaling in Vivo. *Molecular Endocrinology, 16*(10), 2188-2201. doi:10.1210/me.2001-0174

Jakacka, M., Ito, M., Weiss, J., Chien, P. Y., Gehm, B. D., & Jameson, J. L. (2001). Estrogen receptor binding to DNA is not required for its activity through the nonclassical AP1 pathway. *The Journal of biological chemistry, 276*(17), 13615-13621. doi:10.1074/jbc.M008384200

Jansson, M., Philipson, L., Vennström, B. (1983). Isolation and characterization of multiple human genes homologous to the oncogenes of avian erythroblastosis virus. *EMBO J, 2*(4), 5.

Jones, I., Srinivas, M., Ng, L., & Forrest, D. (2003). The thyroid hormone receptor beta gene: structure and functions in the brain and sensory systems. *Thyroid, 13*(11), 1057-1068. doi:10.1089/105072503770867228

Jordans, S., Jenko-Kokalj, S., Kuhl, N. M., Tedelind, S., Sendt, W., Bromme, D., Brix, K. (2009). Monitoring compartment-specific substrate cleavage by cathepsins B, K, L, and S at physiological pH and redox conditions. *BMC Biochem, 10*, 23. doi:10.1186/1471-2091-10-23

Joseph, S. B., Laffitte, B. A., Patel, P. H., Watson, M. A., Matsukuma, K. E., Walczak, R., Tontonoz, P. (2002). Direct and indirect mechanisms for regulation of fatty acid synthase gene expression by liver X receptors. *The Journal of biological chemistry, 277*(13), 11019-11025. doi:10.1074/jbc.M111041200

Kalyanaraman, H., Schwappacher, R., Joshua, J., Zhuang, S., Scott, B. T., Klos, M., Pilz, R. B. (2014). Nongenomic thyroid hormone signaling occurs through a plasma membrane-localized receptor. *Sci Signal, 7*(326), ra48. doi:10.1126/scisignal.2004911

Katz, R. W., & Koenig, R. J. (1994). Specificity and mechanism of thyroid hormone induction from an octamer response element. *The Journal of biological chemistry, 269*(29), 18915-18920.

Kinne, A., Wittner, M., Wirth, E. K., Hinz, K. M., Schulein, R., Kohrle, J., & Krause, G. (2015). Involvement of the L-Type Amino Acid Transporter Lat2 in the Transport of 3,3'-Diiodothyronine across the Plasma Membrane. *Eur Thyroid J, 4*(Suppl 1), 42-50. doi:10.1159/000381542

Klein, I., & Danzi, S. (2016). Thyroid Disease and the Heart. *Curr Probl Cardiol, 41*(2), 65-92. doi:10.1016/j.cpcardiol.2015.04.002

Kowalik, M. A., Perra, A., Pibiri, M., Cocco, M. T., Samarut, J., Plateroti, M., Columbano, A. (2010). TRbeta is the critical thyroid hormone receptor isoform in T3-induced proliferation of hepatocytes and pancreatic acinar cells. *J Hepatol, 53*(4), 686-692. doi:10.1016/j.jhep.2010.04.028

Krause, K., Weiner, J., Hones, S., Kloting, N., Rijntjes, E., Heiker, J. T., Tonjes, A. (2015). The Effects of Thyroid Hormones on Gene Expression of Acyl-Coenzyme A Thioesterases in Adipose Tissue and Liver of Mice. *Eur Thyroid J, 4*(Suppl 1), 59-66. doi:10.1159/000437304

Krenning, E. P., Docter, R., Bernard, H. F., Visser, T. J., & Hennemann, G. (1978). Active transport of triiodothyronine (T3) into isolated rat liver cells. *FEBS Lett, 91*(1), 113-116.

Lazar, M. A. (1993). Thyroid hormone receptors: multiple forms, multiple possibilities. *Endocr Rev, 14*(2), 184-193. doi:10.1210/edrv-14-2-184

Le Bouter, S., Demolombe, S., Chambellan, A., Bellocq, C., Aimond, F., Toumaniantz, G., Charpentier, F. (2003). Microarray analysis reveals complex remodeling of cardiac ion channel expression with altered thyroid status: relation to cellular and integrated electrophysiology. *Circ Res, 92*(2), 234-242.

Ledda-Columbano, G. M., Perra, A., Pibiri, M., Molotzu, F., & Columbano, A. (2005). Induction of pancreatic acinar cell proliferation by thyroid hormone. *The Journal of Endocrinology, 185*(3), 393-399. doi:10.1677/joe.1.06110

Lee, S. H., Dobrzyn, A., Dobrzyn, P., Rahman, S. M., Miyazaki, M., & Ntambi, J. M. (2004). Lack of stearoyl-CoA desaturase 1 upregulates basal thermogenesis but causes hypothermia in a cold environment. *J Lipid Res, 45*(9), 1674-1682. doi:10.1194/jlr.M400039-JLR200

Levin, B. E., Triscari, J., & Sullivan, A. C. (1982). Sympathetic activity in thyroid-treated Zucker rats. *Am J Physiol, 243*(1), R170-178.

Lin, J. Z., Martagon, A. J., Cimini, S. L., Gonzalez, D. D., Tinkey, D. W., Biter, A., Phillips, K. J. (2015). Pharmacological Activation of Thyroid Hormone Receptors Elicits a Functional Conversion of White to Brown Fat. *Cell Rep*. doi:10.1016/j.celrep.2015.10.022

Lin, Y., & Sun, Z. (2011a). Thyroid hormone potentiates insulin signaling and attenuates hyperglycemia and insulin resistance in a mouse model of type 2 diabetes. *Br J Pharmacol, 162*(3), 597-610. doi:10.1111/j.1476-5381.2010.01056.x

Lin, Y., & Sun, Z. (2011b). Thyroid hormone promotes insulin-induced glucose uptake by enhancing Akt phosphorylation and VAMP2 translocation in 3T3-L1 adipocytes. *J Cell Physiol, 226*(10), 2625-2632. doi:10.1002/jcp.22613

Link, W., Oyarzabal, J., Serelde, B. G., Albarran, M. I., Rabal, O., Cebria, A., Bischoff, J. R. (2009). Chemical interrogation of FOXO3a nuclear translocation identifies potent and selective inhibitors of phosphoinositide 3-kinases. *The Journal of biological chemistry, 284*(41), 28392-28400. doi:10.1074/jbc.M109.038984

Lopez-Fontal, R., Zeini, M., Traves, P. G., Gomez-Ferreria, M., Aranda, A., Saez, G. T., Bosca, L. (2010). Mice lacking thyroid hormone receptor Beta show enhanced apoptosis and delayed liver commitment for proliferation after partial hepatectomy. *PLoS One, 5*(1), e8710. doi:10.1371/journal.pone.0008710

Macchia, P. E., Takeuchi, Y., Kawai, T., Cua, K., Gauthier, K., Chassande, O., Refetoff, S. (2001). Increased sensitivity to thyroid hormone in mice with complete deficiency of thyroid hormone receptor alpha. *Proc Natl Acad Sci U S A, 98*(1), 349-354. doi:10.1073/pnas.011306998

Makowski, A., Brzostek, S., Cohen, R. N., & Hollenberg, A. N. (2003). Determination of nuclear receptor corepressor interactions with the thyroid hormone receptor. *Mol Endocrinol, 17*(2), 273-286. doi:10.1210/me.2002-0310

Marrif, H., Schifman, A., Stepanyan, Z., Gillis, M. A., Calderone, A., Weiss, R. E., Silva, J. E. (2005). Temperature homeostasis in transgenic mice lacking thyroid hormone receptor-alpha gene products. *Endocrinology, 146*(7), 2872-2884. doi:10.1210/en.2004-1544

Martin, N. P., Marron Fernandez de Velasco, E., Mizuno, F., Scappini, E. L., Gloss, B., Erxleben, C., Armstrong, D. L. (2014). A rapid cytoplasmic mechanism for PI3 kinase regulation by the nuclear thyroid hormone receptor, TRbeta, and genetic evidence for its role in the maturation of mouse hippocampal synapses in vivo. *Endocrinology, 155*(9), 3713-3724. doi:10.1210/en.2013-2058

Maruvada, P., Baumann, C. T., Hager, G. L., & Yen, P. M. (2003). Dynamic shuttling and intranuclear mobility of nuclear hormone receptors. *The Journal of biological chemistry, 278*(14), 12425-12432. doi:10.1074/jbc.M202752200

Mavinakere, M. S., Powers, J. M., Subramanian, K. S., Roggero, V. R., & Allison, L. A. (2012). Multiple novel signals mediate thyroid hormone receptor nuclear import and export. *The Journal of biological chemistry, 287*(37), 31280-31297. doi:10.1074/jbc.M112.397745

McKenna, N. J., & O'Malley, B. W. (2002). Combinatorial control of gene expression by nuclear receptors and coregulators. *Cell, 108*(4), 465-474.

Miot, F., Dupuy, C., Dumont, J., & Rousset, B. (2000). Chapter 2 Thyroid Hormone Synthesis And Secretion. In L. J. De Groot, G. Chrousos, K. Dungan, K. R. Feingold, A. Grossman, J. M. Hershman, C. Koch, M. Korbonits, R. McLachlan, M. New, J. Purnell, R. Rebar, F. Singer, & A. Vinik (Eds.), *Endotext*. South Dartmouth (MA): MDText.com, Inc.

Miyazaki, M., Dobrzyn, A., Sampath, H., Lee, S. H., Man, W. C., Chu, K., Ntambi, J. M. (2004). Reduced adiposity and liver steatosis by stearoyl-CoA desaturase deficiency are independent of peroxisome proliferator-activated receptor-alpha. *The Journal of biological chemistry, 279*(33), 35017-35024. doi:10.1074/jbc.M405327200

Miyazaki, M., Flowers, M. T., Sampath, H., Chu, K., Otzelberger, C., Liu, X., & Ntambi, J. M. (2007). Hepatic stearoyl-CoA desaturase-1 deficiency protects mice from carbohydrate-induced adiposity and hepatic steatosis. *Cell Metab, 6*(6), 484-496. doi:10.1016/j.cmet.2007.10.014

Moeller, L. C., Dumitrescu, A. M., & Refetoff, S. (2005). Cytosolic action of thyroid hormone leads to induction of hypoxia-inducible factor-1alpha and glycolytic genes. *Mol Endocrinol, 19*(12), 2955-2963. doi:10.1210/me.2004-0542

Moeller, L. C., Dumitrescu, A. M., Walker, R. L., Meltzer, P. S., & Refetoff, S. (2005). Thyroid hormone responsive genes in cultured human fibroblasts. *J Clin Endocrinol Metab, 90*(2), 936-943. doi:10.1210/jc.2004-1768

Moeller, L. C., Wardrip, C., Niekrasz, M., Refetoff, S., & Weiss, R. E. (2009). Comparison of thyroidectomized calf serum and stripped serum for the study of thyroid hormone action in human skin fibroblasts in vitro. *Thyroid, 19*(6), 639-644. doi:10.1089/thy.2008.0293

Moran, C., & Chatterjee, K. (2015). Resistance to thyroid hormone due to defective thyroid receptor alpha. *Best practice & research. Clinical endocrinology & metabolism, 29*(4), 647-657. doi:10.1016/j.beem.2015.07.007

Moriya, H. (2015). Quantitative nature of overexpression experiments. *Mol Biol Cell, 26*(22), 3932-3939. doi:10.1091/mbc.E15-07-0512

Moriyama, K., Yamamoto, H., Futawaka, K., Atake, A., Kasahara, M., & Tagami, T. (2016). Molecular characterization of human thyroid hormone receptor beta isoform 4. *Endocr Res, 41*(1), 34-42. doi:10.3109/07435800.2015.1066801

Morkin, E. (1993). Regulation of myosin heavy chain genes in the heart. *Circulation, 87*(5), 1451-1460.

Mosekilde, L., Eriksen, E. F., & Charles, P. (1990). Effects of thyroid hormones on bone and mineral metabolism. *Endocrinol Metab Clin North Am, 19*(1), 35-63.

Nagy, L., Kao, H. Y., Love, J. D., Li, C., Banayo, E., Gooch, J. T., Schwabe, J. W. (1999). Mechanism of corepressor binding and release from nuclear hormone receptors. *Genes Dev, 13*(24), 3209-3216.

Nagy, L., & Schwabe, J. W. (2004). Mechanism of the nuclear receptor molecular switch. *Trends Biochem Sci, 29*(6), 317-324. doi:10.1016/j.tibs.2004.04.006

Nelson, C. C., Hendy, S. C., Faris, J. S., & Romaniuk, P. J. (1994). The effects of P-box substitutions in thyroid hormone receptor on DNA binding specificity. *Mol Endocrinol, 8*(7), 829-840. doi:10.1210/mend.8.7.7984145

Nolte, R. T., Wisely, G. B., Westin, S., Cobb, J. E., Lambert, M. H., Kurokawa, R., Milburn, M. V. (1998). Ligand binding and co-activator assembly of the peroxisome proliferator-activated receptor-gamma. *Nature, 395*(6698), 137-143. doi:10.1038/25931

Nussey, S., & Whitehead, S. (2001) *Endocrinology: An Integrated Approach*. Oxford: BIOS Scientific Publishers Limited.

Oelkrug, R., Polymeropoulos, E. T., & Jastroch, M. (2015). Brown adipose tissue: physiological function and evolutionary significance. *J Comp Physiol B, 185*(6), 587-606. doi:10.1007/s00360-015-0907-7

Ohguchi, H., Tanaka, T., Uchida, A., Magoori, K., Kudo, H., Kim, I., Sakai, J. (2008). Hepatocyte nuclear factor 4alpha contributes to thyroid hormone homeostasis by cooperatively regulating the type 1 iodothyronine deiodinase gene with GATA4 and Kruppel-like transcription factor 9. *Molecular and cellular biology, 28*(12), 3917-3931. doi:10.1128/mcb.02154-07

Ortiga-Carvalho, T. M., Chiamolera, M. I., Pazos-Moura, C. C., & Wondisford, F. E. (2016). Hypothalamus-Pituitary-Thyroid Axis. *Compr Physiol, 6*(3), 1387-1428. doi:10.1002/cphy.c150027

Pantos, C., & Mourouzis, I. (2014). The Emerging Role of TR1 in Cardiac Repair: Potential Therapeutic Implications. *Oxid Med Cell Longev, 2014*, 481482. doi:10.1155/2014/481482

Pantos, C., Mourouzis, I., Saranteas, T., Brozou, V., Galanopoulos, G., Kostopanagiotou, G., & Cokkinos, D. V. (2011). Acute T3 treatment protects the heart against ischemia-reperfusion injury via TRalpha1 receptor. *Mol Cell Biochem, 353*(1-2), 235-241. doi:10.1007/s11010-011-0791-8

Pawlak, M., Lefebvre, P., & Staels, B. (2012). General molecular biology and architecture of nuclear receptors. *Curr Top Med Chem, 12*(6), 486-504.

Perra, A., Simbula, G., Simbula, M., Pibiri, M., Kowalik, M. A., Sulas, P., Columbano, A. (2008). Thyroid hormone (T3) and TRbeta agonist GC-1 inhibit/reverse nonalcoholic fatty liver in rats. *FASEB J, 22*(8), 2981-2989. doi:10.1096/fj.08-108464

Petersson, U., & Kjellstrom, T. (2001). Thyroid function tests, serum lipids and gender interrelations in a middle-aged population. *Scand J Prim Health Care, 19*(3), 183-185.

Pfaffl, M. W. (2001). A new mathematical model for relative quantification in real-time qRT-PCR. *Nucleic Acids Res, 29*(9), e45.

Picou, F., Fauquier, T., Chatonnet, F., Richard, S., & Flamant, F. (2014). Minireview: Deciphering direct and indirect influence of thyroid hormone with mouse genetics. *Mol Endocrinol*, me20131414. doi:10.1210/me.2013-1414

Pizzagalli, F., Hagenbuch, B., Stieger, B., Klenk, U., Folkers, G., & Meier, P. J. (2002). Identification of a novel human organic anion transporting polypeptide as a high affinity thyroxine transporter. *Mol Endocrinol, 16*(10), 2283-2296. doi:10.1210/me.2001-0309

Plateroti, M., Gauthier, K., Domon-Dell, C., Freund, J. N., Samarut, J., & Chassande, O. (2001). Functional interference between thyroid hormone receptor alpha

(TRalpha) and natural truncated TRDeltaalpha isoforms in the control of intestine development. *Molecular and cellular biology, 21*(14), 4761-4772. doi:10.1128/mcb.21.14.4761-4772.2001

Pohlenz, J., Maqueem, A., Cua, K., Weiss, R. E., Van Sande, J., & Refetoff, S. (1999). Improved radioimmunoassay for measurement of mouse thyrotropin in serum: strain differences in thyrotropin concentration and thyrotroph sensitivity to thyroid hormone. *Thyroid, 9*(12), 1265-1271.

Pramfalk, C., Pedrelli, M., & Parini, P. (2011). Role of thyroid receptor beta in lipid metabolism. *Biochim Biophys Acta, 1812*(8), 929-937. doi:10.1016/j.bbadis.2010.12.019

Ramadoss, P., Abraham, B. J., Tsai, L., Zhou, Y., Costa-e-Sousa, R. H., Ye, F., Hollenberg, A. N. (2014). Novel mechanism of positive versus negative regulation by thyroid hormone receptor beta1 (TRbeta1) identified by genome-wide profiling of binding sites in mouse liver. *The Journal of biological chemistry, 289*(3), 1313-1328. doi:10.1074/jbc.M113.521450

Rao, G. S., Eckel, J., Rao, M. L., & Breuer, H. (1976). Uptake of thyroid hormone by isolated rat liver cells. *Biochemical and biophysical research communications, 73*(1), 98-104.

Rastinejad, F., Huang, P., Chandra, V., & Khorasanizadeh, S. (2013). Understanding nuclear receptor form and function using structural biology. *J Mol Endocrinol, 51*(3), T1-T21. doi:10.1530/JME-13-0173

Robbins, J., & Rall, J. E. (1960). Proteins associated with the thyroid hormones. *Physiol Rev, 40*, 415-489.

Robson, H., Siebler, T., Stevens, D. A., Shalet, S. M., & Williams, G. R. (2000). Thyroid hormone acts directly on growth plate chondrocytes to promote hypertrophic differentiation and inhibit clonal expansion and cell proliferation. *Endocrinology, 141*(10), 3887-3897. doi:10.1210/endo.141.10.7733

Samuels, H. H., Stanley, F., & Casanova, J. (1979). Depletion of L-3,5,3'-triiodothyronine and L-thyroxine in euthyroid calf serum for use in cell culture studies of the action of thyroid hormone. *Endocrinology, 105*(1), 80-85. doi:10.1210/endo-105-1-80

Sap, J., Munoz, A., Damm, K., Goldberg, Y., Ghysdael, J., Leutz, A., Vennstrom, B. (1986). The c-erb-A protein is a high-affinity receptor for thyroid hormone. *Nature, 324*(6098), 635-640. doi:10.1038/324635a0

Sarne, D. R., S. (1988). Normal Cellular Uptake of Thyroxine From Serum of Patients With Familial Dysalbuminemic Hyperthyroxinemia or Elevated Thyroxine-binding Globulin. *JCEM, 67*(6), 1166-1170.

Sartori, C., Lepori, M., & Scherrer, U. (2005). Interaction between nitric oxide and the cholinergic and sympathetic nervous system in cardiovascular control in humans. *Pharmacol Ther, 106*(2), 209-220. doi:10.1016/j.pharmthera.2004.11.009

Schimmel, M., & Utiger, R. D. (1977). Thyroidal and peripheral production of thyroid hormones. Review of recent findings and their clinical implications. *Ann Intern Med, 87*(6), 760-768.

Schwabe, J. W., Chapman, L., Finch, J. T., & Rhodes, D. (1993). The crystal structure of the estrogen receptor DNA-binding domain bound to DNA: how receptors discriminate between their response elements. *Cell, 75*(3), 567-578.

Schwartz, H. L., Lazar, M. A., & Oppenheimer, J. H. (1994). Widespread distribution of immunoreactive thyroid hormone beta 2 receptor (TR beta 2) in the nuclei of extrapituitary rat tissues. *The Journal of biological chemistry, 269*(40), 24777-24782.

Segal, J., Buckley, C., & Ingbar, S. H. (1985). Stimulation of adenylate cyclase activity in rat thymocytes in vitro by 3,5,3'-triiodothyronine. *Endocrinology, 116*(5), 2036-2043. doi:10.1210/endo-116-5-2036

Segal, J., & Ingbar, S. H. (1981). Studies of the mechanism by which 3,5,3'-triiodothyronine stimulates 2-deoxyglucose uptake in rat thymocytes in vitro. Role of calcium and adenosine 3',5'-monophosphate. *The Journal of clinical investigation, 68*(1), 103-110.

Segal, J., & Ingbar, S. H. (1985). In vivo stimulation of sugar uptake in rat thymocytes. An extranuclear action of 3,5,3'-triiodothyronine. *The Journal of clinical investigation, 76*(4), 1575-1580. doi:10.1172/jci112139

Sharova, L. V., Sharov, A. A., Nedorezov, T., Piao, Y., Shaik, N., & Ko, M. S. (2009). Database for mRNA half-life of 19 977 genes obtained by DNA microarray analysis of pluripotent and differentiating mouse embryonic stem cells. *DNA Res, 16*(1), 45-58. doi:10.1093/dnares/dsn030

Shibusawa, N., Hashimoto, K., Nikrodhanond, A. A., Liberman, C. M., Applebury, M. L., Liao, X. H., Robbins, J. T., Refetoff, S., Cohen, R. N., Wondisford, F. E. (2003). Thyroid hormone action in the absence of thyroid hormone receptor DNA-binding in vivo. *Journal of Clinical Investigation, 112*(4), 588-597. doi:10.1172/jci200318377

Shibusawa, N., Hollenberg, A. N., & Wondisford, F. E. (2003). Thyroid hormone receptor DNA binding is required for both positive and negative gene regulation. *The Journal of biological chemistry, 278*(2), 732-738. doi:10.1074/jbc.M207264200

Silva, J. E. (2006). Thermogenic mechanisms and their hormonal regulation. *Physiol Rev, 86*(2), 435-464. doi:10.1152/physrev.00009.2005

Silveira, J. C., & Kopp, P. A. (2015). Pendrin and anoctamin as mediators of apical iodide efflux in thyroid cells. *Current opinion in endocrinology, diabetes, and obesity, 22*(5), 374-380. doi:10.1097/med.0000000000000188

Simoncini, T., Hafezi-Moghadam, A., Brazil, D. P., Ley, K., Chin, W. W., & Liao, J. K. (2000). Interaction of oestrogen receptor with the regulatory subunit of phosphatidylinositol-3-OH kinase. *Nature, 407*(6803), 538-541. doi:10.1038/35035131

Snyder, S. M., Cavalieri, R. R., Goldfine, I. D., Ingbar, S. H., & Jorgensen, E. C. (1976). Binding of thyroid hormones and their analogues to thyroxine-binding globulin in human serum. *The Journal of biological chemistry, 251*(21), 6489-6494.

Storey, N. M., Gentile, S., Ullah, H., Russo, A., Muessel, M., Erxleben, C., & Armstrong, D. L. (2006). Rapid signaling at the plasma membrane by a

nuclear receptor for thyroid hormone. *Proc Natl Acad Sci U S A, 103*(13), 5197-5201. doi:10.1073/pnas.0600089103

Storey, N. M., O'Bryan, J. P., & Armstrong, D. L. (2002). Rac and Rho mediate opposing hormonal regulation of the ether-a-go-go-related potassium channel. *Curr Biol, 12*(1), 27-33.

Tagami, T., Yamamoto, H., Moriyama, K., Sawai, K., Usui, T., Shimatsu, A., & Naruse, M. (2010). Identification of a novel human thyroid hormone receptor beta isoform as a transcriptional modulator. *Biochemical and biophysical research communications, 396*(4), 983-988. doi:10.1016/j.bbrc.2010.05.038

Tata, J. R., Ernster, L., Lindberg, O., Arrhenius, E., Pedersen, S., & Hedman, R. (1963). The action of thyroid hormones at the cell level. *Biochem J, 86*, 408-428.

Tata, J. R., & Widnell, C. C. (1966). Ribonucleic acid synthesis during the early action of thyroid hormones. *Biochem J, 98*(2), 604-620.

Tinnikov, A., Nordstrom, K., Thoren, P., Kindblom, J. M., Malin, S., Rozell, B., Vennstrom, B. (2002). Retardation of post-natal development caused by a negatively acting thyroid hormone receptor alpha1. *EMBO J, 21*(19), 5079-5087.

Tokuyama, T., Yoshinari, M., Rawitch, A. B., & Taurog, A. (1987). Digestion of thyroglobulin with purified thyroid lysosomes: preferential release of iodoamino acids. *Endocrinology, 121*(2), 714-721. doi:10.1210/endo-121-2-714

Toyoda, N., Zavacki, A. M., Maia, A. L., Harney, J. W., & Larsen, P. R. (1995). A novel retinoid X receptor-independent thyroid hormone response element is present in the human type 1 deiodinase gene. *Molecular and cellular biology, 15*(9), 5100-5112.

Trajkovic-Arsic, M., Muller, J., Darras, V. M., Groba, C., Lee, S., Weih, D., Heuer, H. (2010). Impact of monocarboxylate transporter-8 deficiency on the hypothalamus-pituitary-thyroid axis in mice. *Endocrinology, 151*(10), 5053-5062. doi:10.1210/en.2010-0593

Twyffels, L., Strickaert, A., Virreira, M., Massart, C., Van Sande, J., Wauquier, C., Kruys, V. (2014). Anoctamin-1/TMEM16A is the major apical iodide channel of the thyrocyte. *American journal of physiology. Cell physiology, 307*(12), C1102-1112. doi:10.1152/ajpcell.00126.2014

van Mullem, A. A., Chrysis, D., Eythimiadou, A., Chroni, E., Tsatsoulis, A., de Rijke, Y. B., Peeters, R. P. (2013). Clinical phenotype of a new type of thyroid hormone resistance caused by a mutation of the TRalpha1 receptor: consequences of LT4 treatment. *J Clin Endocrinol Metab, 98*(7), 3029-3038. doi:10.1210/jc.2013-1050

Vatner, D. F., Weismann, D., Beddow, S. A., Kumashiro, N., Erion, D. M., Liao, X. H., Samuel, V. T. (2013). Thyroid hormone receptor-beta agonists prevent hepatic steatosis in fat-fed rats but impair insulin sensitivity via discrete pathways. *Am J Physiol Endocrinol Metab, 305*(1), E89-100. doi:10.1152/ajpendo.00573.2012

Vella, K. R., Ramadoss, P., Costa, E. S. R. H., Astapova, I., Ye, F. D., Holtz, K. A., Hollenberg, A. N. (2014). Thyroid hormone signaling in vivo requires a balance

between coactivators and corepressors. *Molecular and cellular biology, 34*(9), 1564-1575. doi:10.1128/mcb.00129-14

Vennstrom, B., & Bishop, J. M. (1982). Isolation and characterization of chicken DNA homologous to the two putative oncogenes of avian erythroblastosis virus. *Cell, 28*(1), 135-143.

Vranckx, R., Savu, L., Maya, M., & Nunez, E. A. (1990). Characterization of a major development-regulated serum thyroxine-binding globulin in the euthyroid mouse. *Biochem J, 271*(2), 373-379.

Waters, K. M., Miller, C. W., & Ntambi, J. M. (1997). Localization of a negative thyroid hormone-response region in hepatic stearoyl-CoA desaturase gene 1. *Biochemical and biophysical research communications, 233*(3), 838-843. doi:10.1006/bbrc.1997.6550

Weinberger, C., Thompson, C. C., Ong, E. S., Lebo, R., Gruol, D. J., & Evans, R. M. (1986). The c-erb-A gene encodes a thyroid hormone receptor. *Nature, 324*(6098), 641-646. doi:10.1038/324641a0

Weiss, R. E., Forrest, D., Pohlenz, J., Cua, K., Curran, T., & Refetoff, S. (1997). Thyrotropin regulation by thyroid hormone in thyroid hormone receptor beta-deficient mice. *Endocrinology, 138*(9), 3624-3629. doi:10.1210/endo.138.9.5412

Weiss, R. E., Murata, Y., Cua, K., Hayashi, Y., Seo, H., & Refetoff, S. (1998). Thyroid hormone action on liver, heart, and energy expenditure in thyroid hormone receptor beta-deficient mice. *Endocrinology, 139*(12), 4945-4952.

Wikstrom, L., Johansson, C., Salto, C., Barlow, C., Campos Barros, A., Baas, F., Vennstrom, B. (1998). Abnormal heart rate and body temperature in mice lacking thyroid hormone receptor alpha 1. *EMBO J, 17*(2), 455-461. doi:10.1093/emboj/17.2.455

Williams, G. R. (2000). Cloning and characterization of two novel thyroid hormone receptor beta isoforms. *Molecular and cellular biology, 20*(22), 8329-8342.

Williams, G. R., Zavacki, A. M., Harney, J. W., & Brent, G. A. (1994). Thyroid hormone receptor binds with unique properties to response elements that contain hexamer domains in an inverted palindrome arrangement. *Endocrinology, 134*(4), 1888-1896. doi:10.1210/endo.134.4.8137757

Wrutniak-Cabello, C., Casas, F., & Cabello, G. (2001). Thyroid hormone action in mitochondria. *J Mol Endocrinol, 26*(1), 67-77.

Wu, J., Wang, C., Li, S., Li, S., Wang, W., Li, J., Guan, Y. (2013). Thyroid hormone-responsive SPOT 14 homolog promotes hepatic lipogenesis, and its expression is regulated by liver X receptor alpha through a sterol regulatory element-binding protein 1c-dependent mechanism in mice. *Hepatology, 58*(2), 617-628. doi:10.1002/hep.26272

Wu, Y., Yang, Y. Z., & Koenig, R. J. (1998). Protein-protein interaction domains and the heterodimerization of thyroid hormone receptor variant alpha2 with retinoid X receptors. *Mol Endocrinol, 12*(10), 1542-1550. doi:10.1210/mend.12.10.0178

Xiao, S., Dorris, M. L., Rawitch, A. B., & Taurog, A. (1996). Selectivity in tyrosyl iodination sites in human thyroglobulin. *Arch Biochem Biophys, 334*(2), 284-294. doi:10.1006/abbi.1996.0457

Xiong, S., Chirala, S. S., Hsu, M. H., Wakil, S. J. (1998). Identification of thyroid hormone response elements in the human fatty acid synthase promoter. *PNAS, 95*, 6.

Yao, X., Hou, S., Zhang, D., Xia, H., Wang, Y. C., Jiang, J., Ying, H. (2014). Regulation of fatty acid composition and lipid storage by thyroid hormone in mouse liver. *Cell Biosci, 4*, 38. doi:10.1186/2045-3701-4-38

Yen, P. M. (2001). Physiological and molecular basis of thyroid hormone action. *Physiol Rev, 81*(3), 1097-1142.

Yen, P. M. (2015). Classical nuclear hormone receptor activity as a mediator of complex biological responses: A look at health and disease. *Best practice & research. Clinical endocrinology & metabolism, 29*(4), 517-528. doi:10.1016/j.beem.2015.07.005

Yoshida, A., Taniguchi, S., Hisatome, I., Royaux, I. E., Green, E. D., Kohn, L. D., & Suzuki, K. (2002). Pendrin is an iodide-specific apical porter responsible for iodide efflux from thyroid cells. *J Clin Endocrinol Metab, 87*(7), 3356-3361. doi:10.1210/jcem.87.7.8679

Zavacki, A. M., & Larsen, P. R. (2013). RTHalpha, a newly recognized phenotype of the resistance to thyroid hormone (RTH) syndrome in patients with THRA gene mutations. *J Clin Endocrinol Metab, 98*(7), 2684-2686. doi:10.1210/jc.2013-2475

Zhang, Y., Yin, L., & Hillgartner, F. B. (2001). Thyroid hormone stimulates acetyl-coA carboxylase-alpha transcription in hepatocytes by modulating the composition of nuclear receptor complexes bound to a thyroid hormone response element. *The Journal of biological chemistry, 276*(2), 974-983. doi:10.1074/jbc.M005894200

Zhu, X., & Cheng, S. Y. (2010). New insights into regulation of lipid metabolism by thyroid hormone. *Current opinion in endocrinology, diabetes, and obesity, 17*(5), 408-413. doi:10.1097/MED.0b013e32833d6d46

Abbreviations and Acronyms

Ac	Acetyl residue
acetyl-CoA	Acetyl-coenzyme A
AF1	Activator function 1
AF2	Activator function 2
Akt/PKB	Protein kinase B
ANOVA	Analysis of variance
ATP	Adenosine triphosphate
BAT	Brown adipose tissue
BMD	Bone mineral density
BSA	Bovine serum albumin
BT_c	Body core temperature
BW	Body weight
cGMP	Cyclic guanosine monophosphate
ChIP-seq	Chromatin immunoprecipitation sequencing
CNS	Central nervous system
CoA	Coactivator
CoR	Corepressor
CT	Computer tomography
Ct.Ar	Cortical area
Ct.Th	Cortical thickness
DBD	DNA-binding domain
DIO 1/2/3	Deiodinase 1/2/3
DIT	Diiodotyrosine
DMEM	Dulbecco´s modified Eagle`s medium
DMSO	Dimethyl sulfoxide
DNA	Deoxyribonucleic acid
DR	Direct repeat
DRIPs	Vitamin D receptor-interacting protein
DTT	Dithiothreitol
DUOX 1/2	Dual oxidase 1/2
E	Glutamic acid
E2	Estradiol
ECG	Electrocardiography
EDTA	Ethylenediaminetetraacetic acid
EG	Glutamic acid and glycine
eNOS	Endothelial nitic oxide synthase
ERα	Estrogen receptor α
EtOH	Ethanol
EV	Empty vector
FCS	Fetal calf serum
Foxo	Forkhead transcription factor
FT3	Free thyronine
FT4	Free thyroxine
G	Glycine
Gapdh	Glycerin aldehyde phosphate dehydrogenase
GC-1	Sobetirome
GS	Glycine and serine
GSV	Gycine, serine and valine
H_2O_2	Hydrogen peroxide
HAT	Histone acetylase
HDAC	Histone deacetylase
HIF-1α	Hypoxia inducible factor 1α
HPT	Hypothalamic-pituitary-thyroid
HR	Heart rate
HZ	Hypertrophic zone
I^-	Iodide ion
IP	Inverted repeat
IVC	Individually ventilated cages
K_a	Association constant
KO	Knockout
LBD	Ligand-binding domain
LID	Low-iodine diet
L-NCoRΔID	Liver-specific NCoR mutant
Lyn	Lyn-Kinase
MCT8/10	Monocarboxylate transporter 8/10
Met^x	Methionine at position x
MIS	Microinjection solution

MIT	Monoiodotyrosine
MMI	Methimazole
mRNA	Messenger RNA
NaF	Sodium fluoride
NaOH	Sodium hydroxide
$NaVO_4$	Sodium orthovanadate
NCoR	Nuclear corepressor
NES	Nuclear export sequence
NIS	Sodium iodine symporter
NLS	Nuclear localization sequence
NO	Nitic oxide
PAL	Palindrome
PBS	Phosphate buffered saline
PCR	Polymerase chain reaction
PI3K	Phosphatidylinositol 3 kinase
PIP_2	Phosphatidylinositol 2 phosphate
PIP_3	Phosphatidylinositol 3 phosphate
PZ	Proliferation zone
qRT-PCR	Quantitative reverse transcriptase PCR
RAR	Retinoid acid receptor
RFLP-PCR	Restriction fragment length polymorphism PCR
RIN	RNA integrity number
RNA	Ribonucleic acid
rT3	Reverse thyronine
RTH	Resistance to thyroid hormone
RXR	Retinoic x receptor
RZ	Reserve zone
S	Serine
SD	Standard deviation
SDS	Sodium dodecyl sulfate
SEM	Standard error of the mean
SMRT	silencing mediator for retinoid and thyroid receptors
SNS	Sympathetic nervous system
SRC-1	Steroid receptor coactivator-1
T2	Diiodothyronine
T3	Thyronine
T4	Thyroxine
Tb.N	Trabecular number
Tb.Sp	Trabecular spacing
Tb.Th	Trabecular thickness
TBG	Thyroxine-binding globulin
Tg	Thyroglobulin
TG	Triglycerides
TH	Thyroid hormone
TPO	Thyroid peroxidase
TR	Thyroid hormone receptor
TRAPs	Thyroid hormone receptor associated proteins
TRE	Thyroid hormone response element
TRH	Thyrotropin releasing hormone
TRα/β	Thyroid hormone receptor α/β
TSH	Thyroid stimulating hormone (thyrotropin)
TSHR	Thyrotropin receptor
TT3	Total thyronine
TT4	Total thyroxine
Tyr	Tyrosine residue
UCP 1/3	Uncoupling protein 1/3
VDR	Vitamin D receptor
WT	Wildtype
ZFN	Zinc finger nuclease

List of Figures

List of Tables

Acknowledgements

Foremost, I would like to express my deepest gratitude to my supervisor PD Dr. Lars C. Möller. Thank you for providing this fantastic topic for me, for confiding in my work, for discussions at eye level and for introducing me to the scientific field of endocrinology. Your infectious scientific enthusiasm, as well as your advices helped me a lot. You have always found the right words and quotations to encourage me and keep me focused:

"The brick walls are there for a reason. The brick walls are not there to keep us out. The brick walls are there to give us a chance to show how badly we want something. Because the brick walls are there to stop the people who don't want it badly enough. They're there to stop the other people."

— Randy Pausch

and

"Don't complain; just work harder."

— Randy Pausch

You have been an excellent mentor and I hope you did benefit as much from our teamwork as I did. It was a pleasure being your *first* Ph.D. student. Thank you for the great time and I am looking forward to the scientific journey of the next years.

I also would like to highly appreciate the supervision and support by Prof. Dr. Dr. Dagmar Führer-Sakel, who always had a sympathetic ear for every, howsoever small, issue. Your patient leadership, even in difficult situations, has been an inspiring example.

I am also grateful to our cooperation partners within the SPP1629 consortium, as well as our external partners, who provided substantially to this study:

Prof. Dr. Samuel Refetoff and Xiao Hui-Liao (University of Chicago)

Prof. Dr. Graham Williams, Prof. Dr. Duncan Bassett, Dr. John Logan and Andrea Pollard (Imperial College London)

Prof. Dr. Josef Köhrle and Dr. Eddy Rijntjes (Charité Universitätsmedizin Berlin)

Dr. Ralph Waldschütz and Wojciech Wegrzyn (Transgene Unit, Animal laboratory of the University Hospital Essen)

PD Dr. Ludger Klein-Hitpass (BioChip Laboratory, University Hospital Essen)

Special thanks to Denise for managing the lab and always taking care of the team spirit and the friendly atmosphere within the group. Further, I want to acknowledge your efforts into

proofreading my manuscripts and my thesis (*twice*). My work did always benefit from your comments and recommendations.

I would like to take the opportunity to thank every past and present member of our lab. I am thankful to our technicians, especially Andrea, Steffi and Julius for their technical support and for making it possible to handle the whole workload. Thanks to Vera, Denise, Kathrin, Helena and Sören for organizing the unforgettable after work events during business travel and for having fruitful controversies with *Mr. Hendrick* and *Mr. Thomas Henry*. I very much appreciate the in passing but intensive discussions with Helena, Sören, Daniela and my sister Judith. This helped me to evaluate my work from a different point of view and often these discussions triggered the solutions for many problems.

I must acknowledge the work of the employees of the animal laboratory at the MFZ. Without the tremendous help from Ina and her great team many things wouldn´t have been possible.

Last but not least, I would like to express my gratitude to my family, especially my parents, who always backed my decisions and advanced my interests. Thanks to my *little* sister Judith, for cross-cutting discussions, advices and proofreading of my thesis ("*After scarifying mice with CO_2…"*)

A special thank goes to my significant other, Anna. Your permanent support, your energy and your motivational advices contributed essentially to reaching my aims. I really appreciate our after-work discussions during cooking, reconsidering the day and sharing everyday problems true to the motto: *"A problem shared is a problem halved."*

Curriculum Vitae

Der Lebenslauf ist in der Online-Version aus Gründen des Datenschutzes nicht enthalten.

Grants and Awards:

05/2016 ***Von Basedow-Preis 2016*** *(DGE)*
"TRαGS and TRβGS knock-in mice demonstrate physiological relevance of non-classical thyroid hormone action"

12/2015 ***Best Oral Presentation****, "Effect of non-classical action of TRβ on blood glucose and triglyceride metabolism", 30. AESF, Berlin*

12/2014 ***Best Oral Presentation,*** *"Protocols to induce hypothyroidism validated by gene expression in liver and heart", 29. AESF, Berlin*

09/2016 ***Travel Grant of the European Thyroid Association*** *(ETA) for the 12th International Workshop on Resistance to Thyroid Hormone, Colorado Springs, USA*

10/2015 ***Travel Grant of the European Thyroid Association*** *(ETA) for the 15th International Thyroid Conference, Orlando, USA*

Publications and Congress Contributions

Publications:

1. *Hönes GS, Rakov H, Logan J, Liao X-H, Werbenko E, Pollard AS, Rijntjes E, Latteyer S, Engels K, Strucksberg K-H, Zwanziger D, Klein-Hitpass L, Köhrle J, Bassett JHD, Williams GR, Refetoff S, Führer D, Moeller LC,* ***Non-canonical thyroid hormone signaling mediates cardiometabolic effects in vivo****, PNAS, in revision*

2. *Hönes GS, Loeffler J, Rakov H, Armstrong DL, Zwanziger D, Führer D, Moeller LC,* ***Triglyceride metabolism in liver is regulated by non-canonical action of TRβ****, in preparation*

3. *Rakov H, Engels K, Hönes GS, Brix K., Köhrle J, Moeller LC, Zwanziger D, Führer D.,* ***Influence of age on sex-specific phenotypes of thyroid dysfunction in mice****, Biol Sex Differ., submitted*

4. *Rakov H, Hönes GS, Moeller LC, Führer D., Zwanziger D,* ***Bile acid homeostasis in hypothyroid mice is exerted via water transport and tightening proteins****, The Journal of Lipid Research, submitted*

5. *Engels K., Rakov H., Zwanziger D., Hönes S., Rehders M., Brix K., Köhrle J., Moeller L.C., Führer D.,* ***Efficacy of protocols for induction of chronic hyperthyroidism in male and female mice****, Endocrine, 2016 Oct;54(1):47-54*

6. *Rakov H, Engels K, Hönes GS, Strucksberg KH, Moeller LC, Köhrle J, Zwanziger D, Führer D.,* ***Sex-specific phenotypes of hyperthyroidism and hypothyroidism in mice****, Biol Sex Differ. 2016 Aug 24;7(1):36. doi: 10.1186/s13293-016-0089-3.*

7. *Krause K., Weiner J., Hönes S., Klöting N., Rijntjes E., Gebhardt C., Heiker J.T., Köhrle J., Führer D., Steinhoff K., Hesse S., Moeller L.C., Tönjes A.,* ***The effects of thyroid hormones on gene expression of acyl-coenzyme A thioesterases in adipose tissue and liver of mice****, European Thyroid Journal 2015 Sep;4(Suppl 1):59-66*

Oral presentations:

03/2017 Hönes S., ***Non-classical thyroid hormone signaling – a paradigm shift in thyroid hormone action***, *60. Deutscher Kongress für Endokrinologie (DGE), Würzburg*

11/2016 Hönes S., ***Effect of non-classical action of TR-beta on blood glucose and triglyceride metabolism***, *Tagung der Sektion Schilddrüse, Heidelberg*

09/2016 Hönes S., Moeller L.C., ***Non-classical TH action mediated by TRα and TRβ***, *12th International Workshop on Resistance to Thyroid Hormone, Colorado Springs, USA*

12/2015 Hönes S., Löffler J., Hui-Liao X., Rijntjes E., Köhrle J., Strucksberg K.-H., Zwanziger D., Refetoff S., Führer D., Moeller L.C., ***Effect of non-classical action of TRβ on blood glucose and triglyceride metabolism***, *30. Arbeitstagung Experimentelle Schilddrüsenforschung, Berlin*

10/2015 Hönes S., Latteyer S., Hui-Liao X., Werbenko E., Engels K., Rakov H., Rijntjes E., Köhrle J., Zwanziger D., Bassett D., Williams G.R., Refetoff S., Führer D., Moeller L.C., ***TRαGS and TRβGS knock-in mice demonstrate physiological relevance of non-classical thyroid hormone action***, *15th International Thyroid Conference, Orlando, USA (Highlighted Oral Presentation)*

12/2014 Hönes S., Latteyer S., Engels K., Rakov H., Rijntjes E., Köhrle J., Zwanziger D., Führer D., ***Non-classical action of thyroid hormone receptors***, *1st Thyroid Trans Act International Conference, Bremen*

12/2014 Hönes S., Boelen A., Horn S., Rijntjes E., Köhrle J., Führer D., Heuer H., Moeller L.C., ***Protocols to induce hypothyroidism validated by gene expression in liver and heart***, *29. Arbeitstagung Experimentelle Schilddrüsenforschung, Essen*

12/2013 Hönes S., Moeller L.C., ***Non-classical thyroid hormone signaling mediated by thyroid hormone receptor β***; *28. Arbeitstagung Experimentelle Schilddrüsenforschung, Berlin*

Poster presentations

03/2017 *Groeben M., Hönes G.S., Auer R., Zwanziger D., Führer D., Moeller L.C.,* ***TRαΔ1 is not an inhibitor of nuclear TRα signaling,*** *60. Symposium der Deutschen Gesellschaft für Endokrinologie, Würzburg*

01/2017 *Groeben M., Hönes S., Zwanziger D., Führer D., Möller C.L.,* ***Molekularbiologische Untersuchungen zur physiologischen Rolle des TRαΔ1****, 22. Jahrestagung der NRW-Gesellschaft Endokrinologie und Diabetologie, Bochum (Posterpreis)*

11/2016 *Daniela Geist, Sebastian Hönes, Denise Zwanziger, Dagmar Führer, Lars C. Moeller,* ***Non-canonical thyroid hormone action in vascular smooth muscle cells****, 15. Tag der Forschung der Medizinischen Fakultät, University Hospital Essen, Essen*

11/2016 *Auer R., Hönes S., Zwanziger D., Führer D., Moeller L.C.,* ***FLAG-Tag gestützter Nachweis der zytoplasmatischen Lokalisation der TRαp30 Variante des Schilddrüsenhormonrezeptors α****, 15. Tag der Forschung der Medizinischen Fakultät, University Hospital Essen, Essen (Posterpreis)*

11/2015 *Hönes S, Loeffler J, Strucksberg K-H, Rijntjes E, Köhrle J, Führer D, Moeller LC,* ***Effect of non-classical action of TRβ on blood glucose and triglyceride metabolism****, 14. Tag der Forschung der Medizinischen Fakultät, University Hospital Essen, Essen*

11/2015 *Hannah Kohler, Sebastian Hönes, Sarah Synoracki, Kurt-Werner Schmid, Dagmar Führer, Lars C. Moeller,* ***Generation of a mouse model for the ALK-positive anaplastic thyroid carcinoma****, 14. Tag der Forschung der Medizinischen Fakultät, University Hospital Essen, Essen*

08/2015 *Hönes S, Loeffler J, Strucksberg K-H, Rijntjes E, Köhrle J, Führer D, Moeller LC,* ***Effect of non-classical action of TRβ on triglyceride metabolism****, ESE (European Society of Endocrinology) Bregenz Summer School 2015, Bregenz, Austria*

03/2015 *Hönes S, Latteyer S, Engels K, Rakov H, Zwanziger D, Führer D, Moeller LC,* ***TRα^{GS} and TRβ^{GS} knock-in mice demonstrate physiological relevance of non-classical thyroid hormone action****, 58. Symposium der Deutschen Gesellschaft für Endokrinologie, Lübeck*

12/2014 *Sebastian Hönes, Kathrin Engels, Helena Rakov, Andrea Jaeger,Stefanie Rehn, Denise Zwanziger, Ralph Waldschütz, Dagmar Führer, Lars Möller,* ***TRα^{GS} knock-in mice demonstrate relevance of non-classical thyroid hormone action****, 1st Thyroid Trans Act International Conference, Bremen*

11/2014 *Sebastian Hönes, Kathrin Engels, Helena Rakov, Andrea Jaeger,Stefanie Rehn, Denise Zwanziger, Ralph Waldschütz, Dagmar Führer, Lars Möller,* ***TRα^{GS} knock-in mice demonstrate relevance of non-classical thyroid hormone action****, 13. Tag der Forschung der Medizinischen Fakultät, University Hospital Essen, Essen*

09/2014 *Hönes S, Boelen A, Horn S, Rijntjes E, Köhrle J, Zwanziger D, Führer D, Heuer H, Moeller LC,* ***Protocols for induction of hypothyroidism in mice validated by gene expression in liver and heart****, 38th Annual Meeting European Thyroid Association, Santiago de Compostella, Spain*

03/2014 *Hönes S, Boelen A, Horn S, Rijntjes E, Köhrle J, Zwanziger D, Führer D, Heuer H, Moeller LC,* ***Protocols for induction of hypothyroidism in mice validated by gene expression in liver and heart****, 57. Symposium der Deutschen Gesellschaft für Endokrinologie, Dresden*

11/2013 *Sebastian Hönes, Andrea Jaeger, Ralph Waldschütz, Dagmar Führer, Lars Möller,* ***Generation of novel mouse models to study non-classical action of thyroid hormone****, 12. Tag der Forschung der Medizinischen Fakultät, University Hospital Essen, Essen*

Eidesstattliche Erklärungen

Erklärung I:

Hiermit erkläre ich, gem. § 7 Abs. (2) d) + f) der Promotionsordnung der Fakultät für Biologie zur Erlangung des Dr. rer. nat., dass ich die vorliegende Dissertation selbständig verfasst und mich keiner anderen als der angegebenen Hilfsmittel bedient, bei der Abfassung der Dissertation nur die angegebenen Hilfsmittel benutzt und alle wörtlich oder inhaltlich übernommenen Stellen als solche gekennzeichnet habe.

Essen, den _____ _____

Georg Sebastian Hönes

Erklärung II:

Hiermit erkläre ich, gem. § 7 Abs. (2) e) + g) der Promotionsordnung der Fakultät für Biologie zur Erlangung des Dr. rer. nat., dass ich keine anderen Promotionen bzw. Promotionsversuche in der Vergangenheit durchgeführt habe und dass diese Arbeit von keiner anderen Fakultät/Fachbereich abgelehnt worden ist.

Essen, den _____ _____

Georg Sebastian Hönes

Erklärung III:

Hiermit erkläre ich, gem. § 6 Abs. (2) g) der Promotionsordnung der Fakultät für Biologie zur Erlangung des Dr. rer. nat., dass ich das Arbeitsgebiet, dem das Thema ***„Non-canonical action of thyroid hormone receptors α and β“*** zuzuordnen ist, in Forschung und Lehre vertrete und den Antrag von **Georg Sebastian Hönes** befürworte.

Essen, den _____ _____

PD Dr. Lars C. Möller